UNIVERSIDAD COMPLUTENSE DE MADRID

FACULTAD DE CIENCIAS FÍSICAS
Departamento de Física de la Tierra, Astronomía y Astrofísica I
(Geofísica y Meteorología) (Astronomía y Geodesia)

TESIS DOCTORAL

A comprehensive assessment of precipitation at Sierra de Guadarrama through observation and modeling

Evaluación integral de la precipitación en la Sierra de Guadarrama mediante observación y modelización

MEMORIA PARA OPTAR AL GRADO DE DOCTOR

PRESENTADA POR

Luis Durán Montejano

Directores

Enrique Sánchez Sánchez
Carlos Yagüe Anguis

Madrid, 2016

A Comprehensive Assessment of Precipitation at Sierra de Guadarrama Through Observation and Modeling

Evaluación integral de la precipitación en la Sierra de Guadarrama mediante observación y modelización

MEMORIA DE TESIS PRESENTADA PARA OPTAR AL GRADO DE DOCTOR

Departamento de Física de la Tierra, Astronomía y Astrofísica I

Universidad Complutense de Madrid

Dirigida por: Dr. Enrique Sánchez Sánchez y Dr. Carlos Yagüe Anguis

Luis Durán Montejano

Madrid 2015

Quiero dedicar esta Tesis a Belen,
a mis hijos y a mis padres.

Agradecimientos

En primer lugar me gustaría agradecer a mis padres la oportunidad que me han dado de existir. Supongo que tener el séptimo hijo en Rascafría un día gris de noviembre en 1970 no seria una situación fácil, así que les agradezco no haberme dado cuenta de esa dificultad hasta hace muy pocos años. Les agradezco los esfuerzos realizados para que todos en casa tuviéramos acceso a la educación en un clima de tolerancia y libertad. Soy consciente de los sacrificios que han tenido que hacer, especialmente mi madre, la cual habría aprovechado mucho mejor que yo la oportunidad que yo he tenido gracias a su esfuerzo. Les agradezco enormemente haber elegido ese pueblo para construir su familia, ya que no concibo un lugar mejor donde disfrutar de una infancia donde la mayor preocupación era la longitud del día. Un pueblo ligado a lugares, personas, sensaciones y recuerdos que me han servido, y aún me sirven, para seguir creciendo.

Agradezco a mis hermanos y cuñados su ayuda y protección para salir adelante cuando las cosas se pusieron difíciles, pero también su respeto y consideración conforme me hice mayor.

Agradezco a mis amigos de la facultad los años que pasamos juntos durante la carrera. Les agradezco tanto las horas de cachondeo como su ayuda para sacar adelante alguna de las asignaturas para las que, obviamente, no había nacido. Con los que aún conservo el contacto, les agradezco a ellos y a sus parejas su cariño y decirles que son como hermanos.

Agradezco a mi familia "postiza" su buena acogida y generosidad. Gracias a todos por hacerme sentir tan cómodo desde el primer día. Sois una familia estupenda.

Agradezco a los directores de los departamentos de la Universidad Europea y de la Facultad de Física de la UCM para los que he trabajado por apoyar mi investigación, por su interés y respecto sobre mi forma de trabajar. También agradezco al programa NILS la financiación necesaria para culminar la última fase de esta Tesis, y en particular a Idar, por su tiempo, conocimientos e implicación.

Agradezco a todo el personal del Parque Natural de Peñalara y del E.A. una ayuda sin la que este trabajo no habría sido posible. Siempre tan dispuestos a ayudar y con tanta alegría, lo que demuestra que la falta de oxígeno alegra el alma. Me gustaría agradecer a Juan la gran confianza depositada en mí desde el primer momento con esta aventura.

Agradezco a mis compañeros de trabajo su paciencia y su gran apoyo en estos últimos años. Sin ellos esta tesis tampoco habría sido posible debido a mis ausencias físicas y mentales que ellos han sabido solventar incluso mejor que yo. Gracias por vuestra disposición y ánimo en los momentos duros, cuando sale lo peor y lo mejor de las personas.

Agradezco a mis directores su esfuerzo y empuje para sacar adelante esta Tesis, su gran profesionalidad, respeto y delicadeza a la hora de expresar sus diferencias. Agradezco

enormemente que hayan podido dedicar parte de su valioso tiempo, conocimiento y experiencia a dirigir y mejorar esta Tesis.

Me gustaría agradecer a mis hijos, Pablo y Javier, por no haberme reprochado nunca el tiempo que he perdido de estar con ellos. Les agradezco su felicidad y vitalidad contagiosas. Finalmente, me cuesta encontrar las palabras para agradecer a Belén su apoyo, sacrificio, inteligencia, conocimientos y cariño que me han permitido haber podido llegar a este punto hoy. Sin ella esta tesis no habría sido posible y me consta que la siente como la suya propia. Gracias Belén.

INDEX

SUMMARY

Introduction

Mountains are of crucial importance for many environmental, social and economical reasons. Water demanding agriculture, some renewable energies, the industry and population depend on mountains, and specially on its precipitation.

From a climatic point of view, they also play a crucial role in the climate system at very different time and spatial scales and they are unique areas for the detection of climate change and the assessment of climate-related impacts. Sierra de Guadarrama, in the central system of the Iberian Peninsula, is not an exception. Understanding the phenomenology of precipitation at this excellent laboratory will not only help to understand its local impact, but will also help to solve unresolved planetary questions.

Objective

The main objective of this PhD Thesis is to make a high resolution assessment of the climatological behavior and variability of precipitation at Guadarrama based on measurement and modeling.

Methods

In order to achieve this, the following methods have being used:

- design, installation and operation of a mountain meteorological network;
- climatological analysis of the historical precipitation observations available in Sierra de Guadarrama;

- analysis of the relationships between synoptic forcing and precipitation in Sierra de Guadarrama using Principal Component Analysis and k-means for weather typing;

- physical modeling of the precipitation processes using a orographic precipitation model with very high resolution.

Results and Conclusions

During the last 15 years, motivated by the need of filling the gap of observations at this area, observations have been made at one of the more complex areas of Guadarrama, the massif of Peñalara. This data set has helped to have a first estimation of the climate of this region and has given support to other scientific activities that demanded local meteorological observations. This action has given an unique opportunity to acquire knowhow on meteorological observing techniques and operational practices at mountains. Sharing of this knowhow will help the mountain meteorology observing community but it will also help for future improvements and to extend the number of sites to the rest of Guadarrama.

The limitation on having reliable measurements of precipitation at this mountain area, led to perform technical improvements of the methods of measurement but also to perform a classical analysis of the historical records of observations made at three AEMET observatories for the period 1989-2012 (Duran et al., 2013). This data set showed to be very homogeneous and valuable to understand precipitation at this area. No previous research of this kind had ever been made and published for this specific mountain area despite its relevance. Some of the features of precipitation found are shared with northern and southern plateau observatories like the pronounced summer drought, the high inter-annual variability and the strong connection with the advection of humidity from the Atlantic Ocean. Nevertheless, some others features are more specific to this area like the strong altitudinal

gradient, the complexity of the spatial patterns and some differences between observatories on the start time and duration of the summer drought.

The strong connection found between the advection of humidity from the Atlantic and local precipitation led to perform an analysis of the connections between the advection of humidity and precipitation at Guadarrama using weather typing methodologies (Duran et al., 2015). This analysis has given relevant knowledge about the strong relationship between the direction of the humidity flux and the orography. Also interesting information that could be used for operational prediction specific to Guadarrama, climate change downscaling or precipitation assessment. This analysis also stressed the importance of orographic precipitation as the phenomena explaining the altitudinal gradient. Normally, two main mechanisms are cited as responsible of air lifting and precipitation: large scale synoptic systems and convective instability. Here, orographic precipitation seemed to be another essential contributor.

In order to confirm this hypothesis an orographic precipitation model was applied (Duran and Barstad, 2015). Here, the Linear Model of Orographic Precipitation (Smith and Barstad, 2004) was applied for simulating precipitation at Guadarrama from 1990 to 2013 with 200 m resolution and a time step of 6 hours. For this application, some new phenomena have been included to the original version of the model, like a sub-saturated condition and a topographic mesoscale flow blocking. Also recoding of the model from FORTRAN to Matlab(R) was made. Results show a good agreement with observations at all scales, specially at monthly scale. Some disagreement has been found for winter months and also in May and October. While the winter overestimation can be attributable to under catching in the measuring process, the May and October under estimation has been related with convective origin precipitation.

Thanks to the application of this model to Guadarrama, a comprehensive assessment of precipitation through observation and modeling is now available for the community. It also has helped to confirm that orographic precipitation is the leading precipitation phenomena at this area. The gridded data base of precipitation now available going from 1990 to 2013, with 200 m spatial resolution and daily temporal resolution opens new possibilities for research at this area. It also complements the observations available, since it considers precipitation that is still difficult to account for using only measurement techniques.

RESUMEN

Introducción

Los sistemas montañosos son cruciales desde muchos puntos de vista tanto medioambientales, sociales y económicos. La agricultura, algunas energías renovables, gran parte de la industria y una gran cantidad de la población dependen de las montañas, especialmente de la precipitación que ocurre en su seno.

Desde el punto de vista climático, las montañas juegan un papel fundamental en el sistema climático a escalas temporales y espaciales muy diferentes y son excelentes indicadores del cambio climático. La Sierra de Guadarrama, situada en el Sistema Central de la Península Ibérica, no es una excepción. Entender mejor los fenómenos que dan lugar a la precipitación en este excelente laboratorio natural es crucial, no sólo por conocer su impacto a nivel local, sino también porque permitirá ayudar a responder preguntas a nivel planetario.

Objetivo

El objetivo principal de esta tesis es realizar un análisis climatológico exhaustivo y una evaluación integral de la precipitación en Guadarrama utilizando observaciones y modelización.

Metodología

Para alcanzar este objetivo se ha hecho uso de los siguientes métodos::

- Diseño, instalación y operación de una red meteorológica de montaña.

- Análisis de los históricos de precipitación observados disponibles en Guadarrama.

- Análisis de las relaciones existentes entre el forzamiento sinóptico y la precipitación en Guadarrama.

- Simulación numérica de los procesos físicos que dan lugar a la precipitación utilizando un modelo de precipitación orográfica.

Resultados y conclusiones

Con el objeto de paliar el gran déficit existente de medidas meteorológicas en zonas montañosas, y más concretamente, en Guadarrama, se ha procedido a la instalación de una red meteorológica en una de las zonas más complejas de esta sierra, el Macizo de Peñalara. El resultado ha sido, por un lado disponer de una base de datos de los últimos 15 años que permitan conocer y evaluar de forma más precisa la climatología de la zona. También se ha satisfecho la demanda de datos meteorológicos por parte de los numerosos estudios científicos que tienen lugar en esta área. Finalmente, ha permitido construir un conocimiento valioso sobre la medida meteorológica en alta montaña, útil para la comunidad científica, pero también útil con vistas a mejorar la red en el futuro, extenderla a otras áreas de Guadarrama o incluso a otras zonas montañosas.

A pesar de las grandes dificultades encontradas, la completitud de datos y calidad de los mismos ha sido aceptable. No obstante, la dificultad ha sido mucho mayor para la obtención de medidas fiables de la precipitación lo que sugiere cambios en las técnicas automáticas de medida pero, sobre todo, la necesidad de contemplar el análisis de otras fuentes de datos.

Se ha realizado un análisis de las observaciones realizadas por la Agencia Estatal de Meteorología (AEMET) en los observatorios manuales cercanos de Puerto de Navacerrada, Segovia y Colmenar Viejo (Durán et al., 2013). Este conjunto de datos se ha mostrado muy homogéneo y tremendamente útil para evaluar la climatología pluviométrica de esta zona. Algunas de las características encontradas son comunes a las de las zonas mesetarias limítrofes tales como la pronunciada sequía estival, la gran variabilidad interanual y la fuerte conexión de la precipitación con la advección de aire húmedo procedente del Atlántico. Sin embargo, han aparecido otros aspectos propios, como el gran gradiente altitudinal, la complejidad espacial de los patrones de precipitación y algunas diferencias relativas a la duración, comienzo y final de la sequía estival entre observatorios.

Esta fuerte conexión entre la advección de humedad procedente del Atlántico y la precipitación observada condujo a la realización de un análisis en mayor profundidad entre los flujos totales de vapor de agua de origen sinóptico y la precipitación observada (Duran et al., 2015). Este análisis ha permitido mejorar el conocimiento sobre la interacción entre advección de humedad y orografía y ha permitido la obtención de una serie de patrones de comportamiento muy útiles para predicción operativa, ejercicios de regionalización, estudios de cambio climático y evaluaciones de la precipitación. Pero sobre todo, ha servido para enfatizar la importancia que tiene la precipitación orográfica en esta región. La precipitación está asociada generalmente a dos fenómenos que producen ascensos de aire: los asociados a sistemas sinópticos de gran escala y los ascensos provocados por inestabilidad convectiva de origen térmico. Estos dos fenómenos, que explican la mayoría de la precipitación en ambas mesetas, no bastarían para explicar la variabilidad espacial encontrada en esta zona.

Esta hipótesis ha podido ser confirmada realizando un conjunto de simulaciones con un Modelo Lineal de Precipitación Orográfica (Smith and Barstad, 2004) para el periodo 1990-2013 (Durán and Barstad, 2015). Se hicieron algunas mejoras respecto al modelo inicial, desde su re-programación en lenguaje Matlab$^{(R)}$ hasta la incorporación de una formulación para reflejar condiciones de sub-saturación y fenómenos de bloqueo mesoescalar. Los resultados muestran como es capaz de simular con gran eficacia la sequía estival, aunque se encuentran ciertas discrepancias durante algunos meses de invierno y en mayo y octubre. La sobre-estimación de los meses de invierno puede asociarse a una infravaloración de la precipitación en el proceso de observación debido al propio método de observación, mientras que la infravaloración de primavera y otoño se ha relacionado con procesos convectivos de origen térmico que este modelo no es capaz de simular. Aunque la simulación de la variabilidad interanual es satisfactoria, se apunta la necesidad de mejorar la metodología para ciertos episodios prolongados de sequía.

Finalmente, este ejercicio ha hecho posible disponer de la primera base de datos de precipitación en malla de alta resolución en la Sierra de Guadarrama. Esto abre la posibilidad de avanzar significativamente en el conocimiento de la fenomenología meteorológica, pero también en otras disciplinas que requieran bases de datos de precipitación en mallas regulares. Por otro lado se resuelve de forma eficaz las dificultades encontradas en la observación de este parámetro. Finalmente sirve para confirmar el papel crucial que juega la precipitación de origen orográfico en la Sierra de Guadarrama, y por extensión, en otras regiones montañosas del planeta.

Photograph of the skyline of Madrid against Sierra de Guadarrama with Jarama river meadows in the front.

Chapter 1. Introduction

1.1 Motivation

This Ph.D project aims at describing the main precipitation features and meteorological processes over Sierra de Guadarrama (Guadarrama hereafter), a mountainous region in the center of the Iberian Peninsula (IP hereafter). This Thesis faces multiple aspects and scales, ranging from observational field work, statistical analysis, synoptic meteorology and physical modeling of the precipitation processes.

From a scientific point of view, this Thesis is specially challenging since the area of study is a mountain area, precipitation at these areas are much less known due to their intrinsic difficulties for field work and the added complexity of the meteorological processes. Focusing on the region of interest, not much is known about the overall climatology, and specifically about precipitation, at Guadarrama even though this massif has been giving sustainability during centuries to a precious ecosystem with a great biodiversity and providing fresh water to millions of inhabitants, including Madrid city, the capital of Spain.

During the last decades there has been a growing scientific interest on this region and many disciplines have found in Guadarrama an excellent area to conduct research studies that try to answer some still open questions, not only at a local scale, but also global. These researches demand reliable meteorological information in order to conduct their assessments. Try to satisfy this demand in the most honest way and also the hope of bringing some light into the knowledge of the climate and meteorology of such an important region (which has also been recently (2013) included in the list of National Parks in Spain, which means the highest degree of protection and environmental interest for a natural area. There are only 15 for the whole country), are the motivation of the work done during all these years and shown here.

Dug by glaciers, Peñalara Massif still hides pristine and secret bowls

1.2. Mountainous Environments. Sierra de Guadarrama

Finding a simple and automatic definition of what is a mountainous region is more difficult than expected. It seems clear in the case of high summits, but discrepancies are found when trying to differentiate between hills and mountains and also to decide how far down from a well defined massif is feasible to extend the mountainous area to lower lands. The irruption of detailed global digital elevation models from satellite and airplanes helped to the development of purely orographically based algorithms (Gesch et al., 1999). But a combination of elevation an other topographic characteristics along with climatic issues have found to be as the more convenient procedure. A nice example of such classification is the work done by Hazeau et al. (2010), who found a total of 4.231.683 km^2 of the European Union to be classified as

mountainous regions, representing about a 29% of the total area (Figure 1.1). Specifically for Spain, they found an area of 505.964 km^2, which represents a 54% of total area. Following this classification, Spain is, after Slovenia, Austria, Greece and Italy, the sixth more mountainous country of the European Union out of 28 countries.

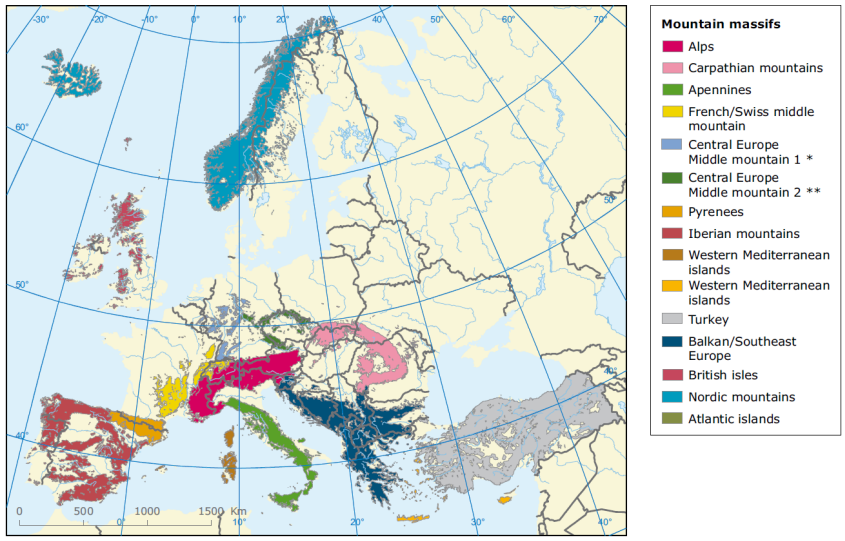

Figure 1.1. Mountain massifs in Europe from Hazen et al. (2010)

Mountains are of crucial importance for many economical, environmental and social reasons. Just to cite some:

- Agriculture: many water-intensive crops depend on rivers that originate in mountains.
- Biodiversity: the peculiar and variety of micro-climates at mountains host a big amount of species that are not able to survive at lower lands.

- Energy: hydro power and wind power resources at mountains is often higher than lower lands.
- Industry: Forestry, timberland and tourism.
- Population: many cities sustainability depends on fresh water that comes from mountains.

From a hydrological point of view, mountains are crucial in regulating fresh water systems which are vital for the sustenance of all kind of life. They are also called "water towers" since they represent an elevated area of land that supplies much higher runoff in comparison to the adjacent lowland regions (de Jong et al., 2009; Hazeau et al., 2010). From the hydrological point of view mountains show some advantages as sources of fresh water: with altitude precipitation is higher, there is more snow than rain, and this makes storage more efficient, better water quality, lower evapotranspiration and the fact that snow melts gradually, delays the runoff. One illustrating case of the importance of mountains for hydrology is the case of snow melt on the Pyrenees which has found to be crucial for ecological and socio-economic development of the semi-arid Ebro valley (López-Moreno and García-Ruiz, 2004; López-Moreno et al., 2009; López and Justribó, 2010). These works also show how the Ebro River receives 50–60 % of its discharge from the Pyrenees, although only 30 % of its catchment is in the mountains.

i. Mountains, Meteorology and Climate

The climate system is usually defined as a global system of complex interactions between its components, which are the atmosphere, the hydrosphere, the cryosphere, the lithosphere and the biosphere (Peixoto and Oort, 1992). All of these neighboring systems

interchange fluxes of mass, energy and momentum following non-linear interactions and making their full understanding very difficult. Mountains play a crucial role in the climatic system at very different time and spatial scales.

From a strictly meteorological point of view, attending to different scales, mountains have three basics effects on climate:

1. Mountains are a key factor in the climatic system since can change considerably the flow of the air masses due to dynamical and thermodynamical effects. These perturbations can reach the higher vertical levels of the troposphere and extend to broader horizontal areas influencing the climate of large areas of the Earth and in mid-latitudes. It is also known how mountains can act as a trigger of cyclogenesis (Buzzi and Tibaldi, 1978; Broccoli and Manabe, 1992; Frei et al., 2003; Yasunari et al., 2006).

2. Trough interactions with the atmosphere, mountains generate specific and recurrent meteorological conditions on their immediate environment and areas of influence. These conditions conform what is known as alpine or mountain climate (James, 1922; Jungo and Beniston, 2001; Rolland, 2001; Schotterer et al., 2003; Richter and Mechoso, 2006; AEMET, 2011).

3. At a local scale, mountains show a great variety of micro-climates due to their complex orography (Jungo and Beniston, 2001; Schotterer et al., 2003; Barry, 2013). They show a marked high spatial variability and in some cases

different topo-climates[1] that host great biodiversity (Sancho et al., 2007; Moeslund et al., 2013).

Mountains are remote from human activity and, due to altitude, almost immersed on the free atmosphere (Pepin and Seidel, 2005). This means that they are not perturbed by urbanization changes, local human activity and other factors that could strongly affect the homogeneity of meteorological observations made on them. For these reasons, mountains are unique areas for the detection of climatic change and the assessment of climate-related impacts (Beniston, 2003, 2006; Wang et al., 2013).

Even though not much direct observations are available at mountain regions, the available ones and proxy records indicate that, both, historical and recent climatic changes in mountains are comparable, and may be greater, than those observed at lower lands, as found by Beniston (2006) for the Alps. Other works like López-Moreno et al. (2008, 2009), for the case of the Pyrenees or Bosch et al. (2007) for the case of Guadarrama show this behavior.

Mountain ecosystems are specially fragile to climate variations whether or not they are due to internal causes of the system, or antropogenically induced (Jungo and Beniston, 2001; Rolland, 2003; Huber et al., 2005; Lurgi et al., 2012). At the same time, the very specific conditions of mountain environments can make their ecosystems excellent indicators of climate change (Gottfried et al., 2012; Ruiz-Labourdette et al., 2013).

[1] *Topo-climate is understood here as a characteristic climate of a very small portion of terrain due to its slope orientation, angle, curvature, sky view, shelter, terrain, albedo, exposure to wind. Usually, mountains regions show a great variety of topoclimates that host many different species in some hundred of meters.*

ii. Mountains and Observation

Despite the importance of mountains in climate, meteorological observations at mountains were not intensively made until the mid nineteenth century. Since then, and mostly in the last decades, progress to conduct continuous observations has been made according to the generalization of standardized methods for observing the atmosphere, but not without serious difficulties (Auer et al., 2007; Böhm et al., 2009).

Meteorological observation at mountains has shown to be a very challenging issue, not only from the metrological point of view, but also for humans conducting the observations. It is generally accepted that a better understanding of the climatic characteristics of mountain regions is limited by a lack of observations adequately distributed in time and space. Also not enough theoretical attention has been given to the complex interaction of spatial scales in weather and climate phenomena in mountains (Smiatek et al., 2005).

As done at similar situations with high deficit of observations, some climatic information for mountains could be retrieved remotely trough the use of satellite information, radiosonde or observations obtained at closer lower lands observatories. But in this case, differences between these observations and ground observations are significant due to decoupling of the boundary layer from the free troposphere, showing different climatic and meteorological behavior (Seidel and Free, 2003; Schär and Frei, 2005; Hazeau et al., 2010; Barry, 2013). Thus, more in-situ mountain observatories are necessary.

There are several reasons that explain this lack of reliable and long meteorological observations at mountains. Among these, one could

mention remoteness, extreme environmental conditions and difficulties on having powerful energy sources and good communications. On the other hand, due to higher spatial variability, one observatory might be representative of a very small area, requiring a higher density of stations than in lower lands.

iii. Mountains and Numerical Modeling

In the last decades, thanks to the fast evolution of the computing techniques (software and hardware) a better characterization of meteorological phenomena and climate has been reached trough the use of numerical models (Chang, 2012). These tools can not substitute the observations of course, but can be very helpful when they are scarce or unreliable.

Numerical models try to simulate the always complex real phenomena with simplifications. The so called 'conceptual models' provide a very direct way of interpreting the results by a very simplified formulation of the complete equations that describe the atmospheric system (Browning, 1986). Other models are developed to consider as less simplifications as possible in an attempt to be as close as possible to reality, trying to accurately solve the full system of differential equations that define the atmospheric fluid in motion, both dynamical and thermodynamically (IPCC, 2013).

In the last decades a considerable amount of models are available for simulating atmospheric processes, but a common limitation for all of them is how they deal with space. Space can't be treated as a continuum due to computational limitations, and it is discretized in grid cells. These grids have a spatial resolution, that could be defined as the minimum distance that the model is able to resolve the equations numerically. Any decrease in this minimum distance, means a considerable increase in the number of points to solve the

equations, what means an increment in the time for the model to perform the simulations if computing time is limited.

Mountains are characterized for having very complex orography, so height can vary hundreds of meters for short horizontal distances. As a matter of fact, mountain climate is mainly the response to altitude and complex orography (Whiteman, 2000; Barry, 2013). If a model wants to be used for simulating mountain weather phenomena, then, higher resolution than lower lands needs to be considered (Giorgi and Mearns, 1991).

Overtaking this resolution issue along with other added difficulties of modeling mountains (like higher expected climate variability or other local phenomena) make the application of models to mountains very challenging.

One clear example of this issue is the relation between global climate models (GCMs, Chang, 2012) and regional climate models (RCMs, Giorgi and Mearns, 1991; Arribas et al., 2003; Castro et al., 2007; Jacob et al., 2007). In the past decades, RCMs have been developed and it has been proved that they are able to enhance the regional description of the climatic features given by Gems (IPCC, 2013; Flato et al., 2013). This is due to fact that RCMs increase the spatial resolution, considering that they are forced in their outer limits by the GCM or the reanalysis. Several examples of the better regional description of RCMs when dealing with mountainous regions can be found in the literature, mainly over the Alps in Europe (Frei et al., 2003; Rauscher et al., 2010; Isotta et al., 2015).

iv. Sierra de Guadarrama: an Excellent Laboratory for Mountain Meteorology and Climate Research

Guadarrama is located in the central part of the Central System of the IP. This massif is located around 400 km away from the Atlantic coast on the North and West and also about 400 km to the East and South to the Mediteranean Sea. IP is located at midlatitudes in the Northern Hemisphere between 44ºN and 36ºN.

This region is exposed to the General Circulation of the Atmosphere (GCA), defined as the total amount of atmospheric motions that take place as a result of the radiative imbalance between tropical and polar regions. Due to the rotation of the Earth, 3 different circulations are then developed and, in the mid latitudes (where the IP is located) a thermally indirect cell appears, being determined by the presence of extratropical cyclones which appear to preserve the angular momentum of the rotating Earth. Thus, this mountain range, contrary to others located in polar and in tropical regions, is exposed to this kind of circulation, in which a variety different weather regimes can be operating.

Guadarrama mountain range runs from SW to NE and has considerable elevations like Pico de Peñalara: 2428 masl or Cabeza de Hierro Mayor: 2383 masl. An approximate mean elevation of the massif would be of around 1600 masl and it settles over an extensive plateau with a mean elevation for the northern plateau of about 900 masl and around 600 masl for the southern plateau. Following Hedberg (1964) definition of mountains, Guadarrama is like an “island” rising above the surrounding plains (Figure 1.2).

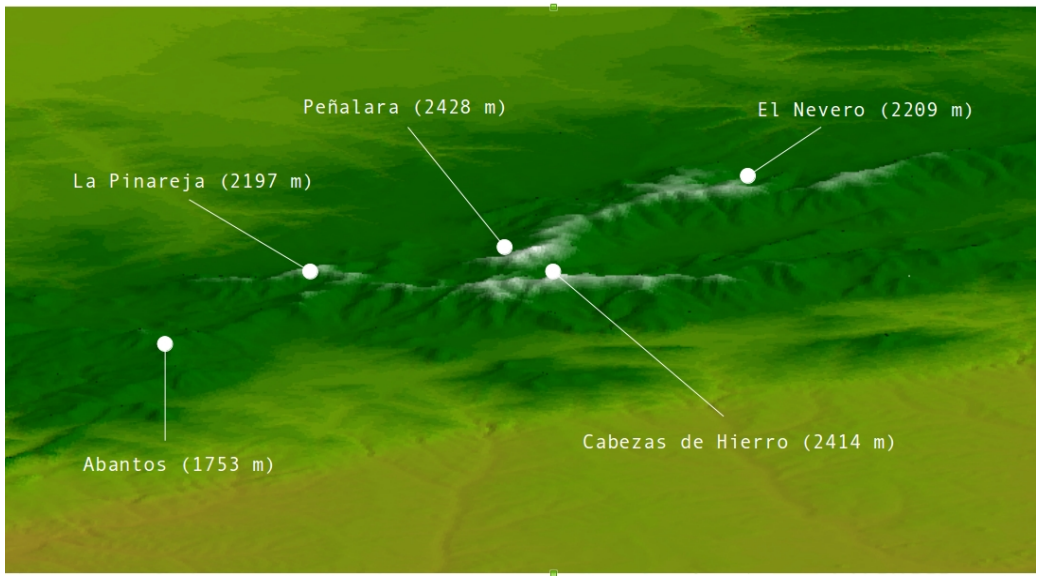

Figure 1.2. Massif of Guadarrama with names and altitudes of the main peaks.

The presence of this mountain range has being crucial for the development of the different civilizations that have settled down on its vicinities, in particular, Madrid, the capital of Spain (Martinez de Pisón, 2006). Thanks to the precipitation that falls as rain or snow at these mountains, fresh water is given to the tributaries of two of the main rivers of the IP, Tagus on the southern side and Douro on the northern side.

This mountain range also hosts a great biodiversity due to the amount of micro-climates found from the first hills to the highest summits. A set of circumstances has kept this area almost as it was centuries ago. First, some areas where environmentally protected like the former Parque Natural de Peñalara or Parque Natural Alto Valle del Manzanares. Since 2013, this range has been included in

the Network of National Parks as "Parque Nacional Sierra de Guadarrama" (BOE, 2013).

This mountainous region can be climatologically defined as an Alpine climate immersed into a Mediterranean continentalized climate (García-Romero et al., 2010). Alpine climates are known to have significant amounts of solid precipitation, low temperatures with small diurnal temperature amplitude, accused large scale but also synoptic forcing due to the high altitude and strong winds locally influenced by the generalized complex orography. This mountain range has some own features due to be under the continental influence of the extensive and surrounding Castillian plateau which causes high contrast in temperatures between summer and winter and low precipitation during summer. This continental behavior is in some way softened by the remaining influence of the Atlantic Ocean and the Mediterranean Sea. These Mediterranean and semi-arid mountain environments behave as humidity islands (López-Moreno et al., 2008).

Precipitation in the center of the IP has been related to advection of moist air masses and storms coming from the Atlantic Ocean which are dried in their way from the North and West to the East and South, losing gradually their water content as they go through the orography zones (Font-Tullot, 1983). In spring, summer and fall, convective precipitation due to thermal instability is also responsible for some precipitation, but it is very scarce and regionalized compared to total precipitation.

Although Guadarrama is located at a relatively long distance from the Atlantic Ocean, there is an oceanic influence related with the advection of humid air masses from this ocean (Muñoz-Díaz and Rodrigo, 2004). On the other hand, due to its altitude, this sierra is often under conditions of almost free atmosphere, a feature that

simplifies relatively some of its phenomenology since many soil processes are not dominant (Pepin and Seidel, 2005).

From a scientific point of view, this mountain range is a valuable natural laboratory that has been kept partly undisturbed and pristine through the centuries. This area is under a set of complex geological, biological, meteorological and climatic processes that have conformed what it is at present. Understanding all these processes will help not only to understand the past, but also can help to understand the future. Answering to the open questions will not only help to understand Guadarrama but also to understand global phenomena.

Considering this, it is understandable how this area has being subject of numerous scientific and multidisciplinary studies in the past. Just to cite some of them, there are works on:

- Geomorphology: Palacios and Sánchez-Colomer (1997), Palacios et al. (2003), Álvarez and Sierra (2011), Palacios et al. (2012).
- Limnology: Granados et al. (2006), Granados (2007), Toro et al. (2006), Granados (2011), Sanchez López et al. (2015).
- Ecology: Baonza and Montouto, (2001), Wilson et al. (2005); García-Romero et al. (2010).
- Zoology: Juez (2001), Bosch and Martínez-Solano (2006), Bosch et al. (2007), Merrill et al. (2008), Ortiz-Santaliestra et al. (2011), Horcajada (2011), Pérez (2011).
- Botanics: Schroeter et al. (1999), Montouto-González (2000), Sanz-Elorza et al. (2003), Sancho et al. (2007), Gómez-González et al. (2009), García-Romero et al. (2010),

Gutiérrez-Girón and Gavilán, (2010), Schwaiger and Bird (2010), Moreno (2011), García-Camacho et al. (2012), Mera et al. (2012), Amat et al. (2013), García-Fernández et al. (2013), Ruiz-Labourdette et al. (2013).

- Air pollution: Inclán et al. (2007, 2010, 2011).
- Climate: Durán (2003), Palacios et al.(2003), Bosch et al. (2007), Durán (2007), Durán and Sánchez (2009), Ruiz Zapata et al. (2009), Granados (2011), Ruiz-Labourdette et al. (2013), Palacios et al., (2012), Génova (2012), Durán et al (2012a, 2012b), Durán et al. (2013), Durán et al. (2014), Durán et al (2015), Durán and Rodríguez-Muñoz (2015a), Durán and Rodríguez-Muñoz (2015b), Durán and Barstad (2015).

Many of these and future works need meteorological input data for feeding their models or for establishing reliable relationships. Any mountain range of this size shows a high spatial variability so specific measurements or assessments are needed on the area. Having reliable and long enough records of the main meteorological variables is always welcomed by the scientific community and other potential users like the industry, the administration or even general public.

There are another features that makes this range an excellent laboratory for environmental research. This area is relatively close to many research centers and institutions, most of them located in Madrid. For field work this is very valuable since it is a relatively close area in terms of logistics and costs associated with deployment of instrumentation and development of measurement field campaign programs. Another added value is the always cooperative attitude from the institutions responsible of the area

under study. First from the Natural Park Cumbre Circo y Lagunas de Peñalara, and now from the National Park Sierra de Guadarrama. This support has helped with resources, optimization of logistics, expertise advisement in terms of instruments security, samples and personal safety. Without this support, the work presented here would have not been possible.

Areal view of Sierra de Guadarrama early morning August 16th of 2003. A Foehn formed in the northern side of the range. Valley locals call this event "olla hirviendo" since it reminds a boiling pot when looked from the ground.

1.3. State-of-the-art

The observation, measurement and numerical description of precipitation is a complex and challenging issue within many fields of atmospheric science research, due to its irregular nature in space and time, and the diversity of atmospheric scales and processes involved on its description. When the influence of the orography is included on the analysis of precipitation, the problem becomes even more complex.

Many rainfall analysis from rain gauges measured data and observational campaigns have been carried on in the past years over the main mountainous regions in Western Europe: Frei and Schär (1998), or Bougeault et al. (2001) over the Alps, López-Moreno et al. (2008) for the Pyrenees, Romero et al. (1999a, 1999b) over Mediterranean Spain. The studies focused over the IP concluded that precipitation over the IP presents a wide and complex range of different features: from the Atlantic climate on the northern and north-west region, with annual amounts up to 2500 mm yr^{-1}, to the Mediterranean area on the east and south coast of the IP. At the south-east coast, there is even a region with semiarid conditions, with less than 100 mm yr^{-1}. The inner part of the IP exhibits a remarkable pattern in terms of precipitation, as it is divided by the Central System mountain range. Both southern and northern plateaus present annual precipitations around 500 mm, but mountains show more than 1000 mm (Font-Tullot, 1983). Some studies have analyzed precipitation climatic features from different perspectives (Martin-Vide, 2004), showing the large spread on the regimes shown in the IP.

Superimposed to these climatic features, climate variability determines the presence of anomalous years in which the rainfall behavior is separated from its climatological mean. In this sense, many literature has been produced relating the anomalous precipitation at IP with large scale patterns of atmospheric variability. Zorita et al. (1992) showed how IP precipitation is connected with a "high-index" of the North Atlantic Sea Level Pressure (MSLP), confirming that the dominant process responsible for the variability of rainfall over the IP was the intensity of the westerly winds and the frequency of storms embedded in this flow. The North Atlantic Oscillation pattern (NAO) ended to be the main teleconnection pattern in relation with precipitation

(Rodriguez-Puebla et al., 1998; Serrano et al., 1999; Goodess and Jones, 2002; Rodriguez-Fonseca and Serrano, 2002; Muñoz-Díaz and Rodrigo, 2004; Trigo et al., 2004; Gallego et al., 2005) showing seasonal and interannual dependency. Also climate variability and its relationship with fauna in the area has being documented (Bosh et al., 2007).

It has been shown by several authors (Zorita et al., 1992; Trigo and Palutikov, 2001; Rodríguez-Fonseca and Castro, 2002; Trigo et al., 2004; Rodriguez-Fonseca et al., 2006) the strong influence of the Atlantic Ocean on Iberian climate, and specifically on precipitation on the central area of the IP. They indicate how humid air masses from the Atlantic are advected into the Peninsula and transported by storms, fronts and the general synoptic western circulation through this mountain range.

Recent studies, like the one conducted by Gimeno et al. (2010) using a dynamic 3D back-tracking algorithm, have shown how the origin of the moist that precipitates at the IP in winter is in the tropical–subtropical North Atlantic corridor stretching between the Gulf of Mexico and the IP. The contribution of the surrounding Mediterranean Area in winter is negligible while turns important in summer. This work makes a strong emphasis in two main mechanisms that force the moist air to rise and precipitation to occur: moisture supply and instability due to large scale dynamics in winter, and moisture supply and convective instability due to thermodynamic structure and soil factors in summer. But not mention is made, since this is a not specific work on mountains, that there might be an extra leading phenomena that should be taken into account in a mountain region: orographic forcing.

Despite the numerous works available for other regions, there are not works dealing specifically with relationships between the synoptic scale and Guadarrama.

One way of analyzing such interaction between scales has been historically performed through the analysis of weather regimes or circulation types (Mo and Ghil, 1988; Michelangeli et al., 1995; Panziera et al., 2015). This methodology has been applied over the IP for different applications such as snowfall (Esteban et al., 2005), extreme events (Fernández-Montes et al., 2013) and other climatological variables for specific seasons and areas (Corte-Real et al., 1998; Romero et al., 1999; Trigo and DaCamara, 2000; Rodríguez-Puebla et al., 2001; Santos et al., 2005; Paredes et al., 2006; Ortíz-Beviá et al., 2011; García-Valero et al., 2012; Cortesi et al., 2013) and some of them analyze how these weather regimes are projected to change along the twenty-first century (Rojas et al., 2013). But none of these studies have ever had specifically Guadarrama as the region of interest.

At the same time, not much is known about precipitation observations in Guadarrama. There are several scientific works dealing with different disciplines directed related but nothing specifically done about temporal and spatial variability of precipitation on the area. Hydrological records and other studies point out how precipitation is much higher at higher lands, with isoyets following elevation contour lines (Gavilán et al., 1998; AEMET, 2011; Herrera et al., 2012). But the lack of long rain time series with enough spatial coverage have made difficult to keep a reliable assessment of rain fields with enough resolution.

In fact, most of those previous works on precipitation in the IP usually do not include observations from mountain sites (Rodriguez-Puebla et al., 1998; Serrano et al., 1999; Andres et al.,

2000; Gonzalez-Rouco et al., 2001; Martin-Vide, 2004), probably because of their peculiar behavior and the lack of enough surrounding observations.

Fernandez-Mills (2005), using principal component analysis (PCA) performed a regionalization of the Spanish precipitation data into ten main clusters. Navacerrada mountain station located at Guadarrama was included, along with many other stations from all over the IP. One of the clusters found in the analysis was the North-Western Coast of the Peninsula, which included surprisingly an isolated island in the middle of the plateau, right where this mountain station was located. A similar behavior was found by Beranova and Huth (2008) who identified five modes of variability in winter monthly precipitation using stations all over Europe. They used eleven stations in the IP, including Navacerrada station, which ended to be included in the central European cluster, very far away from the immediate Iberian stations which were included in the south-European cluster as expected.

Meteorological research has tended to focus on the upstream and downstream influences of barriers to flow and on orographic effects on weather systems (Smith, 1979) rather than on micro-climates within the mountain environments themselves. Climatic features relevant to mountain environments include microscale features of the atmosphere that are superimposed on larger scales of motion and the influence of elements of the surface, such as vegetation and geomorphologic features, which can create micro-climatic contrasts in surface heating, soil moisture, or snow-cover duration (Geiger, 1965).

Regarding observations in Spain, the main institution taking care of standardized WMO (World Meteorological Organization) compliant observations is the Agencia Estatal de Meteorología

(AEMET hereafter). This agency has several observation networks with different measuring strategies and objectives like the SYNOP, aeronautic, automatic, climatological networks and more recently the mountain climate network with most of the sites at the Pyrenees and Sierra Nevada. Fortunately, AEMET have been running an observatory (Navacerrada,) at a location in the heart of Guadarrama, since 1946. It is located at 1894 m and shows excellent records in terms of data completion, following acceptable measuring standards and data quality procedures. Apart from Navacerrada observatory there are other two high quality observatories in the area of influence of Guadarrama: Colmenar Viejo observatory operative since 1978 and Segovia observatory operative since 1989.

For hydrology, limnology and many other applications, point observations conducted at a limited number of sites might not be enough. These disciplines often need to integrate spatially precipitation in a territory, basin or grid. How well an observation represents the whole domain of integration will depend on the complexity of the precipitation spatial patterns, which are known to be high at mountains (Buytaert et al., 2006).

Gridded precipitation databases are regularly spaced estimations of precipitation in a region that tried to solve the spatial variability of the precipitation fields. There are several of these available worldwide which are widely used for climate models validation, hydrology impact assessment, ecology studies and others. Some widely used ones are CRU (New et al., 1999) with 0.5º resolution or E-OBS (Haylock et al., 2008) for Europe. Spain02 (Herrera et al., 2012) with a 0.2º resolution covering the IP is another example with higher resolution but for a smaller domain. Most of these databases are based on observations and have considerable uncertainty on mountainous areas as a consequence of their low

resolution and the lack of mountain observatories. There are some exceptions like is shown by Brugnara et al. (2012) for the central part of the European Alps.

An usual approach when dealing with spatial interpolation of rainfall and the effects of complex terrain is the use of digital elevation models along with different statistical procedures, usually multivariate linear regression through different krigging approaches. The basic assumption here is a linear relation with elevation of measured precipitation at the available rain gauge stations (Daly et al., 1994; Goovaerts, 2000; Kyriakydis et al., 2001; Marquinez et al., 2003; Guan et al., 2005).

Normally, all these gridded databases have a too coarse resolution for giving a reliable picture of spatial precipitation variability on a mountain area. Another weakness of these approaches is that they are based on measurements, and normally, there are not enough mountain observatories in the area capturing the real spatial variability. On the other hand, it is commonly accepted that precipitation observations underestimate real precipitation, specially in the case of snow, so extra corrections are necessary (Groisman and Legates, 1994; Sevruk, 1996; Goodison et al., 1989; Adam and Lettenmaier, 2003; Cheval et al., 2011).

In order to assess precipitation at mountain regions that do not have enough density of stations with long records, the use of physical models needs to explored. A combination of available measurements and physical modeling might produce a more accurate assessment.

Nowadays there are some physical modeling tools available for simulating precipitation at a mesoscale level like MM5 (Grell et al., 1995; Zängl, 2007), RAMS (Pielke et al., 1992), MC2 (Benoit et

al., 1997), COAMPS (Hodur, 1997), WRF (Michalakes et al., 2001; Soares et al., 2012). These models are able, in principle, to simulate fairly well the complex phenomena that generate precipitation at mountains but are computationally expensive, especially when high spatial resolutions, and long time periods want to be simulated.

On the other hand there are some numerical models that have been developed to deal with the physical description of how precipitation is affected by the existence of a mountain barrier (Barros and Lettenmaieret, 1993; Smith, 2003; Kunz and Kottmeier, 2006). Their idea is to answer, from a physical point of view, to the question of how the mountains interact with the air flow extracting its humidity in form of precipitation. These orographic precipitation models give more realistic results over very complex terrain focusing on small domains but do not take into account other phenomena difficult to study like convection. This reduction on the physics presents two important advantages: they are easy to understand and it is possible to make many simulations at very high resolution with a reasonable computational cost.

Linear Model of Orographic Precipitation (LMOP hereafter) is based in the linear, steady-state theory of orographic precipitation proposed by Smith and Barstad in 2004 (Smith and Barstad, 2004; Barstad and Smith 2005; Smith et al., 2005; Smith, 2006). This model has shown to perform fairly well at other mountainous regions of the world with high orographic complexity like Andes, Norwegian Alps or Icelandic mountains (Smith et al., 2005; Barstad et al., 2007; Crochet et al., 2007; Smith and Evans 2007).

However, previous LMOP experiments have been conducted at coastal areas with oceanic climates. Never before mountain range located in the middle of the IP, between two extensive plateaus and immersed into a Continentalized Mediterranean climate has been

subject of such kind of modeling. It seems to be necessary to perform a study that validates the usefulnesses of this tool for assessing precipitation at Guadarrama and check if it is able to simulate correctly the precipitation amplitudes at a selected number of observatories, but also to simulate correctly the summer drought and the high inter-annual variability. Only after this is confirmed, it can be used to assess precipitation at Guadarrrama and obtain high resolution daily gridded databases with some hundred of meters of horizontal resolution.

Defiant snow flaps challenging gravity near Pico de Peñalara

Chapter 2. Hypothesis and objectives

As it has been pointed out, researching at mountains implies many intrinsic difficulties. In order to reach reasonable objectives it is necessary to establish certain working hypothesis that will reduce the degrees of freedom of the problem under study.

Taking into account the multidisciplinary approach followed at this work, the next hypothesis and objectives belong to different areas of meteorology: instrumental, statistical and modeling.

2.1 Hypothesis

1. From a observational point of view, the best way of dealing with the high spatial variability of meteorological fields at mountains is to design a high density meteorological network based on automatic methods.

2. Massif of Peñalara, and its area of influence, is an excellent area for experimenting the operational and metrological difficulties of conducting automatic meteorological observations in an alpine area.

3. Observations made at Navacerrada observatory are representative of the higher elevations of Guadarrama. Observations made at Segovia and Colmenar Viejo are representative of the transition area between the northern and southern plateau and this mountain range.

4. Total precipitation observed at Guadarrama is the sum of the following contributions: large-scale precipitation, thermally driven convective precipitation and orographic precipitation.

5. A model that is able to reproduce precipitation amplitude at different temporal scales, the summer drought and the interannual variability at Navacerrada, Segovia and Colmenar Viejo, is then valid for assessing precipitation at the whole domain of Guadarrama.

2.2 Objectives

The objectives of this work could be grouped into four categories. Objectives related with meteorological observation techniques at mountains, climatological analysis of historical precipitation observations, relationships between synoptic scale and local precipitation and modeling and assessing precipitation at Guadarrama.

1. To define a methodology for conducting meteorological observations at mountains that will serve as a first evaluation of climate at Guadarrama using in-situ measurements.

2. To have a climatology of precipitation at Guadarrama using historical observations available on the area in terms of annual cycle, interannual variability and spatial differences within Guadarrama.

3. To progress on the understanding of the influence of the synoptic scale flows of humidity and precipitation at Guadarrama.

4. To understand the contribution of the different types of precipitation attending to their phenomenology: large scale, convective and orographic.

5. To progress on the understanding the role of orographic precipitation at Guadarrama and the interaction between orography and precipitation.

6. To analyze the performance of a Linear Orographic Precipitation Model at Guadarrama and the feasibility to build a high resolution grid data base on its results. Evaluate the possibility that this data base, along with the in-situ observations, will serve to have a comprehensive assessment of precipitation at Guadarrama.

Humid air mases coming from the northwest form orographic clouds over Malagosto watering the higher lands. Convective activity shown by cumulus behind them reminds that reality is always more complex.

Chapter 3. Method and Data

The next sections show the different methods applied for achieving the objectives expresses in Sec. 2.2. These methods correspond to the four different phases followed in this work, which are:

- Design and Operation of a Mountain Meteorological Network (Sec. 3.1).
- Analysis of Long Time Series of Observed Precipitation (Sec. 3.2).

- Analysis of the Relationships Between Synoptic Flows and Precipitation (Sec. 3.3).

- High Resolution Physical modeling and Assessessment of Precipitation (Sec 3.4).

Cabeza Mediana monitoring site looks after Peñalara Massif in a perfect day for maintenance.

3.1 Design and Operation of a Mountain Meteorological Network[2]

Peñalara Massif is located in Sierra de Guadarrama, which is part of the Iberian Central System (Pedraza et al., 2004). This mountain range lies over two extensive plateaus in the center part

[2] This section follows closely the publication: Durán, L. and Rodríguez-Muñoz, I. (2015b). "Automatic Monitoring of Weather and Climate at Mountain Areas. The Case of Peñalara Meteorological Network 1999-2014 " Submitted.

of the Iberian Peninsula and shows excellent conditions for conducting weather and climate observations. It has been kept unaltered for centuries, even though it is relatively close to the city of Madrid. This area shows some particular conditions due to its complex orography and a strategic location that exposes the mountain to the advection of the humid air masses coming from the Atlantic (Durán et al., 2014). This range has an Alpine climate immersed in a Continentalized Mediterranean climate. This means temperature and precipitation mean values are comparable to other mountain areas in southern Europe, but with a strong summer drought and high inter-annual variability (Durán et al., 2013).

In the last years, this area has been subject of numerous scientific and multidisciplinary studies. This increasing scientific interest during the last decade made necessary to have local meteorological observations of scientific quality in order to be used by the scientific community working on the area. The first step was taken in 1998 with the installation of one of the first fully automatic meteorological stations above the 2000 masl of scientific quality and with a long term horizon in the Iberian Peninsula. Since then, other four automatic meteorological stations have been installed along with other measurement points and becoming a fully operative mountain meteorological network (the Red Meteorológica del Parque Natural de Peñalara, RMPNP hereafter).

The next sections outlines some concepts taken into account during its design, installation and operation. Some results and discussions about the representativeness of the data is also included. Technical and operational procedures that are described can be helpful to the mountain meteorology observing community and future mountain networks (Rath, 2012; Rath et al., 2014; Santolaria-Canales et al., 2015). This works pretends also to be a reference document for future users of the RMPNP data users.

Since 1998 the number of observatories in the area has increased in order to take into account the complexity of the area and the new resources available. The process has been sequential following a measuring strategy, in terms of siting criteria of new sites at macro and micro scale levels. Nowadays, the network consist of 5 automatic weather stations, one manual observatory and some fixed sites for ancillary measurements and prototype testing (Figure 3.1).

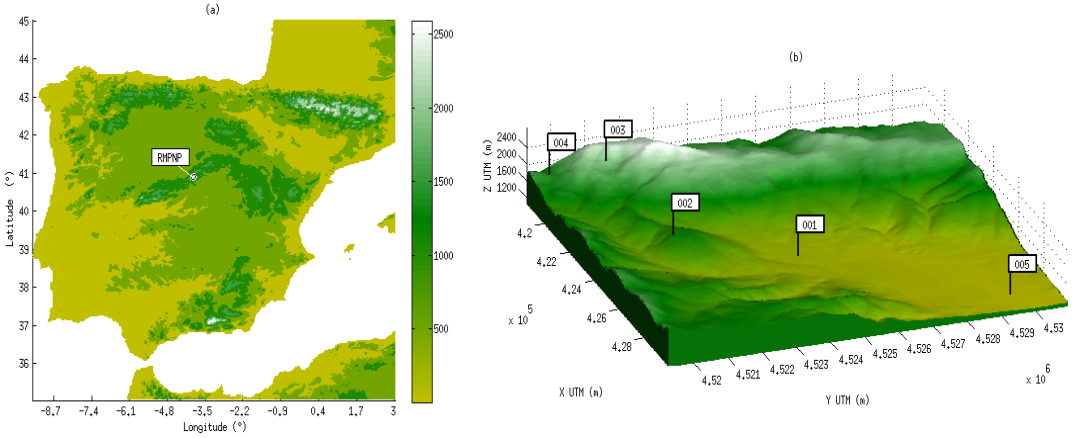

Figure 3.1: (a) Location of the Peñalara Natural Park Meteorological Network in Sierra de Guadarrama. (b) Location of the automatic monitoring stations.

3.1.1 Measuring Objective

The objective of a meteorological network determines its design and configuration. Depending on the potential use of the data, different network designs are possible (Frei et al., 2003). For this

network, the main objective was to obtain representative meteorological data at the Park of Peñalara and upper valley of Lozoya for scientific applications.

The representativeness of an observation is the degree to which it accurately describes the value of the variable needed for a specific purpose (WMO, 2008). Thus it depends on the measuring objective and also on other factors like the measuring technique, instrumentation used (quality of the sensors, calibration procedures, long term drift, configuration), measurement interval, exposure (sitting criteria), and even maintenance protocols (data handling, collection intervals, post-processing and storage).

3.1.2 Specific Difficulties to Overcome at Mountains

All of the technical and human issues that affect the performance of a meteorological network can be applied also at mountain networks (WMO, 2008). Nevertheless, the following specific difficulties to overcome at a mountain environment have been identified:

i) Remoteness. This is one of the most added values of mountains from a meteorological and climatological point of view, but for an automatic meteorological network, it is the main source of errors. Difficulties start during the installation process, since it complicates logistics and reduces the options of materials and structures to be potentially used. It also affects negatively the frequency of the maintenance procedures and increases the vulnerability of the instruments to animals or vandalism acts. It also reduces the telecommunication options, something that turns crucial for these kind of unattended networks. Remote sites usually do not have power available for powering the

electronic systems or for heating the sensors. Remoteness has the highest impact on the final cost of these kind of networks.

ii) Extreme environmental conditions. Low temperatures last for many days at these areas. This seriously compromises the correct functioning of powering systems. Scientific quality electronics are able to handle these low temperatures, but batteries drop their efficiency drastically at low temperatures. A power loss affects directly completeness of data. Persistent low clouds or fog is also more frequent that at lower altitudes, so the solar power resource is also lower. Frequent saturating conditions also affect temperature measurements when drops form over sensors evaporate. Most of the conventional sensors are designed and calibrated for regular ambient temperatures and accuracy decreases when reaching their limits of operation which might be normal at mountains. In summer, solar radiation is very high, specially short wave radiation, accelerating the degradation of plastics and paints. This combined with rain and snow accelerates corrosion of structures. In winter high radiation during a sunny day with snow covering the ground, can affect temperature measurements, due to reflection when using regular solar radiation shields, and giving higher readings than real. Snow and rime are also a special issue since the first can affect the readings after deposing over sensors like pyrometers, temperature radiation shields, typing bucket rain gauges and solar panels. Rime icing has a devastating effect on mountain meteorological networks. It forms when supercooled water drops transported by the wind make contact with an obstacle and freeze immediately. Data from

a sensor covered with rime is useless and sometimes it is hard to find a method to detect when rime starts and ends to affect the measurements. Rime is also responsible, in combination with high wind, of tearing down towers, breaking supporting cables and sensors. Other factors that are specially enhanced at mountains and also affect reliability are strong winds and lightning.

iii) Micro-climate. Orography causes that a great variety of micro climates can be found in a small area of a mountain. This makes mountains very valuable but has a direct impact on representativeness. At mountains it is difficult to find a location that is not too influenced by local conditions or perturbed by obstacles, projected shades, stagnation, cold pools, and other local effects. Thus, a mountain weather station is usually representative of a very small area compared with stations at lower lands and for a correct assessment, a higher density of stations is necessary.

iv) Security and Environment. Mountains can be very dangerous and maintenance personnel need to increase their security protocols, specially in winter. Also, greater precautions need to be taken in order to minimize the environmental impact of towers, sensors and equipment. This is specially important for highly environmentally protected areas like Peñalara.

3.1.3 Measuring Strategy

Once established the measuring objective, considered the difficulties of conducting observations at mountains and with the resources available, the following measuring strategy was defined:

i) Measuring Technique. Automatic measurements are the base of this network. Additional manual measurements for calibration and data quality control are performed at a small number of sites.

ii) Density of stations. Considering the size and orographic complexity of the area, five sites are considered enough to cover the elevation range going from 1102 masl to 2079 masl. Since highest point of the area is 2414 masl, this makes an average of one site per 260 m of altitude. Density of stations is higher at higher altitudes.

iii) Sitting criteria. Recommendations from the World Meteorological Organization (WMO, 2008) will be followed when possible. Additional criteria applied are: the site needs to be representative of a broader area of similar elevation, environmental impact will have to be minimized during installation and operation; the site needs to be relatively accessible most of the year in save conditions for personnel. And good signal coverage from public telecommunication networks is desirable.

3.1.4 Quality Assurance and Quality Control

Quality assurance and control (QA/QC) of meteorological networks deserves even more resources and attention than installation itself (Shafer et al., 2000). The lack of a clear, continuous and realistic QA/QC program is probably the main reason for the frequent data gaps found in mountain networks data series. Even the best infrastructures, sensors and powering systems will not last much without a proper QA/QC program. There is an extended and

wrong thought that automatic networks are fully automatic, and consequently, not enough human resources are normally planned.

Quality of data does not only depend on quality of sensors. It also depends on the quality of every aspect that intervenes in the measuring chain (Brock and Richardson, 2001). This chain starts at the installation, it continues during the maintenance and finishes with the data management, storage and reporting. Considering only the measurement process, the accuracy of a measurement depends on a sum of factors that accumulate one after the other. The first one is the sensor itself, which needs to have a valid calibration. Another common source of errors at mountains is a wrong exposure, difficult to guarantee that the sensor will be correctly exposed to the measurand all over the year, specially in winter. Distance to ground changes due to snow height, structures can project rain shadows. Wind can also affect rain catchment due to aerodynamic effects (underestimation) or turbulence can hurry the tipping bucket process (overestimating). Snow can settle on top of pyrometers and collapse non heated rain gauges. Snow can melt afterwards and give spurious precipitation under clear sky. These errors could be acceptable if they were random like, but they are weather dependent and can lead to wrong climatic conclusions if this bias is not corrected.

The quality assurance program has evolved through the years of operation of this network since there has been a progressive building of knowhow. During the first years of operation most of the resources available were invested in the installation and instrumental consolidation of the network. In the last years, once the number of sites reached the optimum number, a higher effort was given to define and apply the following QA/QC program:

i) Preventive maintenance. Consisting of regular visits to the sites before any problem is detected. The expected frequency of this visits has been between one to two months, depending on the weather conditions. Works done include: cleaning panels and sensors, structures checking, parallel measurement for checks of performance and extension of calibration times given by manufacturer. On site rain gauge calibration once a year using a rain gauge calibrator. Electrical and telecommunications checks are also performed. All these tasks are recorded in a control chart.

ii) Corrective maintenance. Reparation of a malfunctioning part of the automatic station. Sometimes it requires a previous visit for diagnostic and evaluation of damages. The correction should be made as soon as possible in order to minimize data loss, but it depends on availability of spare parts and weather conditions.

iii) Data validation. This is the process that decides whether or not an observation is valid and becomes part of the variable time series (Salvati and Brambilla, 2008). This process is done following a two phase protocol. A first level validation is done almost at real-time in order to detect outliers and clear malfunctions. The purpose of this phase is to trigger alarms for maintenance and to filter data that will be reported online to general public in graph form or special users. Climatological site specific thresholds are used and internal consistency checks are made. A second level validation process is performed once a year and can be repeated indefinitely when more information or knowhow is increased. Spatial coherence checks using information from neighbor stations and data from other networks or reanalysis are made. After this phase is concluded, data is individually tagged with the following codes: V: valid data, D: not valid data, C: corrected data and T: temporal not validated data. Once validated, data is ready for exchanging with scientists and other users of the data.

iv) Storage and Reporting. As long as the volume of data increases with new data and new sites, the storage technology becomes more important. This has been evolving from individual ASCII files to spreadsheets to finally a PostgreSQL (Momjian, 2001; PostgreSQL Global Development Group, 1996-2014) data base with a PHP (Achour et al., 2006) graphical user interface accessible remotely through the web for data storage, validation and reporting to users, general public and organizations. Validation and graphics routines are programed with Python (Van Rossum and Drake, 1995). Last evolutions of this software is relying to Python most of the work along with newer versions of PosgreSQL (Figure 3.2).

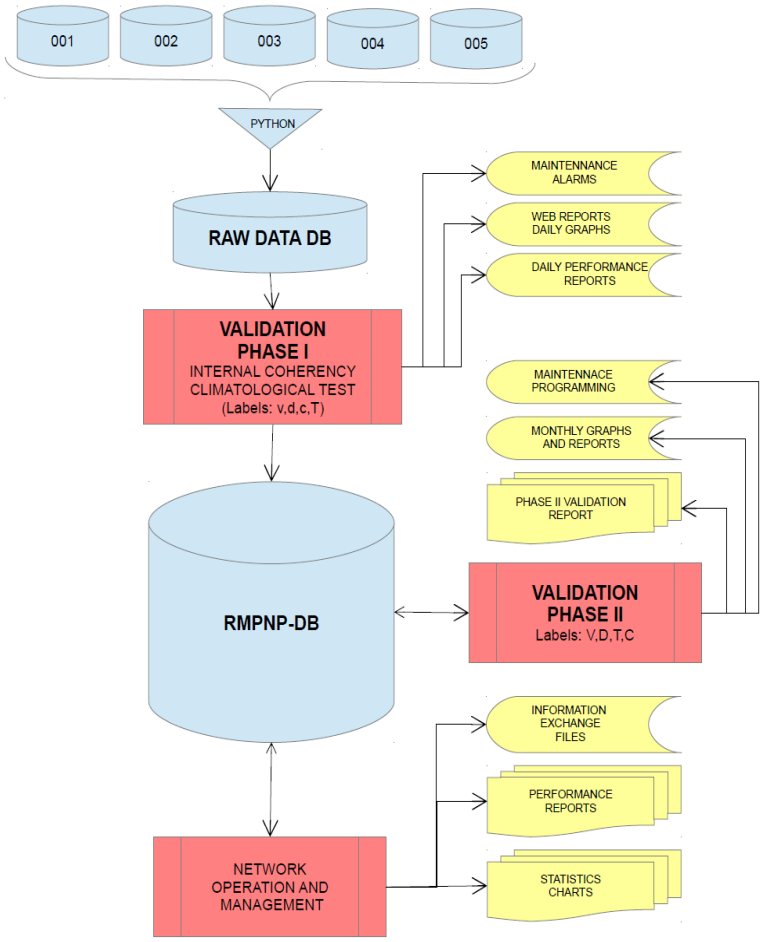

Figure 3.2.Flow chart of RMPNP data management and QA/QC system

Different cloud layers developed over Sierra de la Morcuera as seen from Los Cascajales, Rascafría.

3.2 Analysis of the Historical Records of Observed Precipitation

3.2.1 Observed Precipitation Data

In order to conduct a climatological analysis of precipitation at Guadarrama a data set of good quality and some decades is necessary. There are some automatic networks data sets, like Peñalara Natural Park Network and others like those belonging to

water confederations at both sides of Guadarrama, but these are too recent or use automatic tipping bucket techniques. Conducting meteorological measurements at mountains implies many difficulties, specially for observing precipitation (see Sec. 1.2; Sec. 4.1; Duran, 2003; Lo et al., 2011; Durán and Rodríguez-Muñoz, 2015b).

Fortunately, the Spanish Meteorological Agency (AEMET) have been running the mountain observatory Puerto de Navacerrada (N hereafter) located in the heart of Sierra de Guadarrama since 1946 (Figure 3.3.a and Figure 3.3.b). During this period, manual observations of the main meteorological variables have been collected by the Agency staff following World Meteorological Organization (WMO) standards every 6 h. There are some other observatories with historical records and good measurement practises in Madrid (since 1920, M hereafter), Colmenar Viejo (since 1978, C hereafter), Segovia (since 1989, S hereafter) and Avila (since 1985, A hereafter). Only N observatory can be considered a mountain observatory. C and S are located at the southern and northern side of the mountain range, and A and M are located at the northern and southern plateau, at a considerable distance. Geographical location of the observatories is shown in Figure 3.3.b.

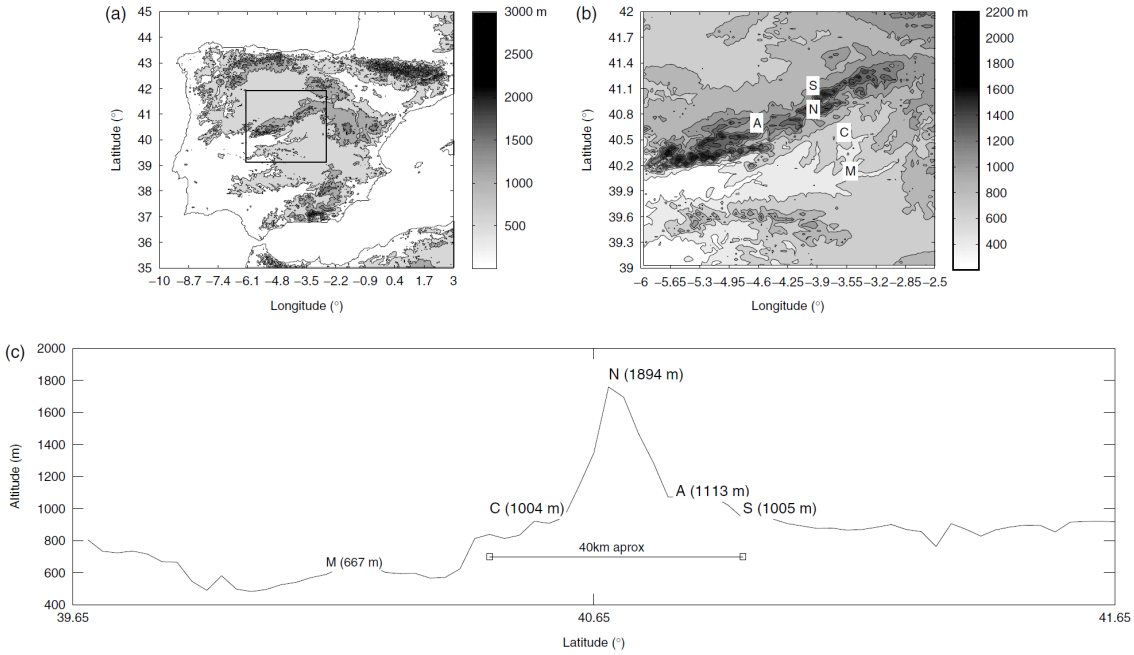

Figure 3.3. Elevations of Iberian Peninsula (a) and Central System (b) with locations of rain observatories used in this study: Madrid (M), Colmenar Viejo (C), Navacerrada (N), Segovia (S) and Avila (A). An approximate cross section from a trajectory south to north passing close to observatories is also shown (c).

3.2.2 ERA-Interim Reanalysis Data

In order to describe and analyze the synoptic conditions and their relationship with precipitation at the three sites, the ECMWF ERAinterim reanalisys has been used (Uppala et al., 2008). The same time period as for the stations is chosen, with a 1.5º horizontal resolution. Surface variables used are: 2 meters air temperature and sea level pressure; and 23 atmospheric levels from surface up to 200 hPa: U and V components of wind, geopotential

height, specific humidity. The domain of study for the reanalysis is taken from 48ºN to 33ºN in latitude and 15ºW to 1.5ºE in longitude.

3.2.3 Method

The method used for building this basic information about Guadarrama precipitation climatology was:

i. Analysis of the Time Series.

Very often long term time series suffer from changes in position, measuring method or change in the micro-environment (Giovannini et al., 2011). For this reason, as a first step, an Alexandersson homogeneity test (Alexandersson, 1986) has been performed using Madrid Retiro (AEMET) observatory as the reference station concluding that the observations at the three observatories are fairly homogeneous. Then, the mean, median, standard deviation, maximum, minimum for the whole year and for winter (December, January, February; DJF hereafter), spring (March, April, May; MAM hereafter), summer (June, July, August; JJA hereafter) and fall (September, October, November; SON hereafter) was calculated for the period 1989-2010. Also precipitation anomalies, related to the annual climatology, at each of the three observatories was calculated in order to extract conclusions about inter-annual variability. The mean altitudinal precipitation gradient for both sides and for every month was calculated using two observatories for each side of Guadarrama and sharing *N* at the top. A comparison two-by-two of the three stations was performed in order to check if populations behave statistically different; and finally, the frequency of eight spatial patterns have defined going from very spatially extended patterns with precipitation at the

three sites to very local precipitation events with precipitation at only one site.

ii. Analysis of the Relationship Between Precipitation and humid air masses reaching Guadarrama.

Advection of humid air masses over Guadarrama was done analyzing the flux of total column of water vapor flux in the atmosphere (TCWVF hereafter) following Rasmuson (1968). For this calculation, specific humidity (q) and wind velocity (u and v) was integrated from surface to 200 hPa levels using Equation 3.1, 3.2 and 3.3.

$$\overline{Q_u} = \frac{1}{g}\int_{p_u}^{p_s} qudp \qquad (3.1)$$

$$\overline{Q_v} = \frac{1}{g}\int_{p_u}^{p_s} qvdp \qquad (3.2)$$

$$\overline{Q} = \overline{Q_u}i + \overline{Q_v}j \qquad (3.3)$$

Where p_s is surface pressure and p_u is 200 hPa, thus Q is total column of water vapor flux at each grid.

Then, the Pearson linear correlation coefficients between the monthly precipitation anomalies, at the three observatories, and monthly TCWVF anomalies for each grid point was calculated. This was performed in order to analyze the relationships between moisture advection and precipitation at Guadarrama. Not significant correlations are neglected after applying a t-student test with 95% confidence level. The anomalies are computed subtracting to the monthly value at each particular year, the climatological monthly mean, dividing the result by the climatological standard deviation (These are known as standardized anomalies).

iii. Average Conditions of the Air Masses that Lead to Precipitation at Guadarrama.

The following variables are analyzed upwind the mountain range: TCWVF, surface temperature, relative humidity at 950 hPa and wind speed and wind direction sector. The level of 950 hPa has been chosen since it is the average pressure level of the plateau. Box plot diagrams are a common tool for detecting different populations in a sample using null hypothesis contrast from the median and the interquartile values since both parameters are robust towards the presence of outliers. Two groups of data have been considered per site and season: wet (W) and dry (D). Then, the extremes, the upper and lower hinges (quartiles), and the median have been calculated and used for the box plot. On each box, the central mark is the median, the edges of the box are the 25^{th} (q_1) and 75^{th} (q_3) percentiles, the whiskers extend to the most extreme data points not considered outliers, and outliers are plotted individually. Points are drawn as outliers if they are larger than $q_3 + 1.5(q_3 - q_1)$ or smaller than $q_1 - 1.5(q_3 - q_1)$. The value of 1.5 corresponds to approximately $+ 2.7\sigma$ (being σ the standard deviation) and 99.3% data coverage if the data are normally

distributed. The plotted whisker extends to the adjacent value, which is the most extreme data value that is not an outlier. The two medians, corresponding wet and dry day populations, are considered significantly different at the 5% significance level if their intervals, defined by the notches, do not overlap. In that case, true medians do differ with 95% confidence. Applying the notches comparison graphically is like applying a t test with the upper and lower limits that fulfill the frequency distribution for the significance level (Mc Gill et al., 1978).

Local saying: "Cuando Peñalara se enoja, Rascafría se moja".

3.3 Analysis of the Relationships Between Synoptic Flows and Precipitation

3.3.1 Observed Precipitation Data

Again observatories *S*, *N* and *C* from AEMET are used for this analysis (Figure 3.3.b). This data set is very valuable thanks to its homogeneity and long records, and it has been shown to be very suitable for characterizing the climatology of precipitation at this mountain range and its vicinities (see Durán et al., 2013 for more details). The period from 1989 to 2011 has been chosen in order to maximize overlapping with ERA-Interim reanalysis fields (Uppala et al., 2008) and simultaneous data availability at the three observatories.

3.3.2 ERA-Interim Reanalysis Data

Here, the ECMWF ERA-Interim reanalysis for the period 1989-2011, with a 1.5º horizontal resolution is chosen, and zonal and meridional components of wind and specific humidity at 23 atmospheric levels (from surface up to 200 hPa) have been used. Also geopotential height of 850 hPa and mean sea level pressure have been used.

To account for synoptic scale air masses flows, TCWVF Patterns have been calculated (WVFP hereafter) for a small domain going from 48ºN to 33ºN in latitude and from 15ºW to 1.5ºE in longitude. This domain covers the whole IP, and the surrounding oceanic areas. This relatively small area is chosen due to the high spatial variability of water vapor fluxes when precipitation occurs.

On the other hand, in order to have some indications about the synoptic configuration that is originating the water vapor fluxes and their sources, composite maps of Mean Sea Level Pressure (MSLP) and 500 hPa geopotential height anomalies (Z500) have been calculated for a much larger domain, going from 20ºN to 80ºN in latitude and 60ºW to 20ºE in longitude.

The methodology of the study is as follows: first, the total column water vapor flux advected over the IP is calculated from ERA-Interim reanalysis in a very constrained domain and for winter (DJF), spring (MAM), summer (JJA) and fall (SON). Second, a principal component analysis of the TCWVF anomalies is performed in order to build a subspace of empirical orthogonal functions (EOFs) that will be used for applying a k-means clustering and a cost function that uses local precipitation in order to determine a set of WVFPs for every season. Anomalies are calculated from climatology, in a way that the mean of seasonal

mean along the period of study is subtracted to the seasonal mean of each particular year. These patterns are supposed to summarize the main forcings of orographic precipitation at Sierra de Guadarrama and became valuable scenarios for further high resolution modeling that will help to understand the precipitation phenomenology at this area. Finally a composite map of MSLP and 500hPa height geopotential anomalies with broader domain are calculated for each WVFP in order to have some indications about the synoptic weather pattern associated with it. Then, an analysis in terms of frequency, persistence, contribution to total precipitation, precipitation intensity and probability of precipitation for each WVFP is calculated. Finally an analysis about transitions between WVFP is performed. This methodology is similar to other previous works over IP (Santos et al., 2005; Garcia-Valero, 2012) but there are some significant differences: TCWVF is used instead of geopotential height as predictor field; all seasons are included in the analysis; a slight variation of the cost function is made averaging for all the sites and precipitation observations at Guadarrama.

3.3.3 Total Column Water Vapor Flux Anomalies Calculation

The transport of moist air masses can be studied through the integrated flux of water vapor in the lower layers of the atmosphere (Rasmuson, 1968). Relating this transport with precipitation is very useful since it takes into account both the water vapor content of the air and its velocity. Both aspects are necessary when orographic precipitation is expected. Here, specific humidity and wind velocity, integrated from surface to 200 hPa level have been used to calculate the TCWVF following Eq. (3.1), Eq. (3.2) and Eq. (3.3).

TCWVF daily anomalies have been calculated as the deviations of the daily value from its seasonal climatological value (calculated for the 1989-2011 period). These have shown to be strongly correlated with precipitation anomalies in this region (Durán et al., 2013), so they have been computed for every day and for the whole domain. Days have been assigned to their corresponding season following: winter (DJF), spring (MAM), summer (JJA) and fall (SON).

3.3.4 Principal Components Analysis

For every season, the Empirical Orthogonal Functions (EOFs) of the daily TCWVF anomaly are calculated in Durán et al. (2014). EOF (von Storch and Zwiers, 2001) is a discriminant analysis methodology used to determine the principal directions of variability followed by a particular variable. This methodology, also named as Principal Component Analysis (PCA) diagonalizes the covariance matrix of a variable. The eigenvectors (EOFs) are the spatial maps in which the variability is comprissed explaining more variance; and the principal components (PCs) are the weights of these maps along the time period of analysis.

Thus, the problem to be solved is to find an ortonormal base in a new vectorial space $\{\mathbf{e}_m\}_{m=1,\ldots,M}$, in a way that each vector $\mathbf{e_m}$ is a linear combination of the vectors $\left\{\vec{f}_{ny}\right\}_{n_y=1,\ldots N}$, being M<N (Figure 3.4). Thus, the new set of vectors $\{\vec{e}_1, \vec{e}_2, \ldots, \vec{e}_M\}$, called EOFs, can be used to represent the original set of vectors $\{\vec{f}_1, \vec{f}_2, \ldots, \vec{f}_N\}$. Consequently, the value of Y in a n_y point and for the time n_t is given by:

$$Y_{ny}(t) = \sum_{j=1,M} P_j(nt)\, e_{ny,j} \qquad (3.4)$$

being $e_{ny,j}$ the ny-component of vector e_j and $P_j(nt)$ the corresponding principal component. In this way, the field Y can be expressed as a linear combination of the M-modes selected.

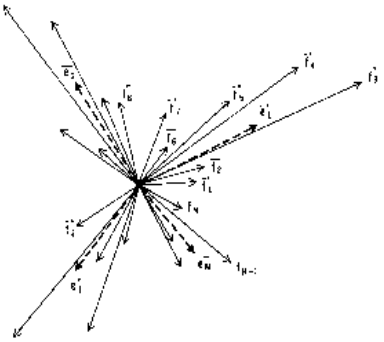

Figure 3.4. Scheme of Principal Component Analysis. The original base is f_i and the new base is formed by the EOFs or vectors e_i. From Peixoto and Oort (1992)

In this case the EOFs of TCWVF are calculated diagonalizing the covariance matrix of the daily TCWVF anomalies. The resultant elements of the diagonal matrix (or eigenvalues) are weighted to obtain the fractions of variance given by each of the PCs. The PC, EOF and the corresponding percentage of explained variance represent a mode, being the leading mode the group of EOF and

PC associated with the higher eigenvalue (von Storch and Zwiers, 2002; Wilks, 2011).

In this work, the number of modes is chosen following the criteria established by North et al. (1982). These modes build up a new orthogonal base in which the data is oriented explaining a percentage of variance given by the sum of the fraction of variances of the selected modes. The projection of each of the EOFs onto the original TCWVF data gives a time series in which each of the scores indicates the weight of each EOF in each of the days analyzed.

3.3.5 K-means Clustering

The selected principal components (PCs) are used as input variables for the clustering analysis using the k-means two-phase iterative algorithm (Hartigan and Wong, 1979). This methodology has been widely used for weather typing, and very often in relation with precipitation (Michelangeli et al., 1995; Corte Real et al., 1998; Corte Real et al., 1999; Cassou et al., 2004; Santos et al., 2005; Moron et al., 2008; Polo et al., 2011). Days are disposed in a N dimension space, where N is the number of PCs. First, a random selection of k centroids is made, reassigning days to their nearest cluster centroid and recalculating the new resultant centroid. In the second phase, days are individually reassigned, if this new assignation reduces the sum of distances, then cluster centroids are recomputed after each reassignment. This second phase will converge to a local minimum, although there may be other local minimum with lower total sum of distances. In order to solve this problem and find the global minimum, 15 runs with random starting points have been made.

An always-interesting point when using k-means clustering is the selection of optimum number of clusters. Since any grouping is valid because they are all very close in the PCs space, a criterion is needed in order to find an optimum number of centroids small enough to comply the simplification objective. There are some methodologies that relay only on the value of the PCs (Riddle et al., 2012). For this case, an information criterion formula, or cost function, based on observed precipitation is used Eq. (3.5). This method is very similar to the ones used by other authors (Corte Real et al., 1998; Santos et al., 2005; Moron et al., 2008).

$$IC(thr,K)=\frac{\sum_{o=1}^{N}\sum_{i=1}^{K}\left|n_{r_{io}}(thr)-p_{ro}\,n_i\right|}{\mathrm{N}} \qquad (3.5)$$

where N is the number of observatories, K is the number of clusters, nr_{io} is the number of rainy days within the ith cluster with a rainfall amount beyond the threshold thr at observatory o; n_i is the total number of days within the same cluster; p_{ro} is the probability of a rainfall total above the specified threshold (0.1 mm in this case) at observatory o in all time realizations of the full series.

This function gives higher values when dry clusters are differentiated from wet clusters. Since here three observatories are used, an average of the value obtained for each observatory is made Eq. (3.5). After establishing a fixed precipitation threshold (thr) of 0.1 mm for considering a rainy day, this formula gives higher values

when the grouping is made in a way that separates wet from dry water vapor flux patterns.

The use of this kind of information criterion formula is very useful when having enough observed precipitation data, which is the case. The resulting classification is then optimum for Guadarrama.

Finally, once the optimum number of clusters is selected, the centroids of each cluster have been used as a weighting factor of each PC in order to obtain a TCWVF field associated for each WVFP. Also, composite maps of MSLP and Z500 anomalies fields over the North Atlantic for each WVFP are calculated in order to give more insights about the large-scale patterns associated with each cluster and its phenomenology.

3.3.6 Analysis of the Relationship Between Advection of Humidity and Local Precipitation

For every season the frequency of occurrence of each WVFP and its mean persistence are calculated. Also, for every observatory and season, total precipitation fallen under each WVFP, the probability of precipitation as the rate between wet days (having a precipitation higher than *thr*) and dry days, the contribution of each WVFP to total seasonal precipitation and the mean precipitation rate as total precipitation under each flux pattern divided by the number of wet days for that WVFP are evaluated. Finally, the transitions between WVFP are calculated as the ratio between intra WVFP transitions relative to total transitions for that season.

Composite maps of MSLP and 500hPa height geopotential (Z500) anomalies are calculated for each WVFP in order to have indications about the synoptic weather pattern associated with it.

A nice curtain of rain hiding the southern entrance of Sierra de Guadarrama near Navacerrada.

3.4 Physical Modeling and Assessment of Precipitation at Guadarrama[3]

3.4.1 Area of Study and Background Information

Figure 3.5b and Figure 3.5b show the location of the three observatories that will be used for evaluating the performance of LMOP. A detailed description of these observatories can be found at Durán et al. (2013).

[3] *This section follows closely the publication: Durán, L. and Barstad, I. (2015). "Multi-scale validation of a Linear Model of Orographic Precipitation over Sierra de Guadarrama". To be submitted.*

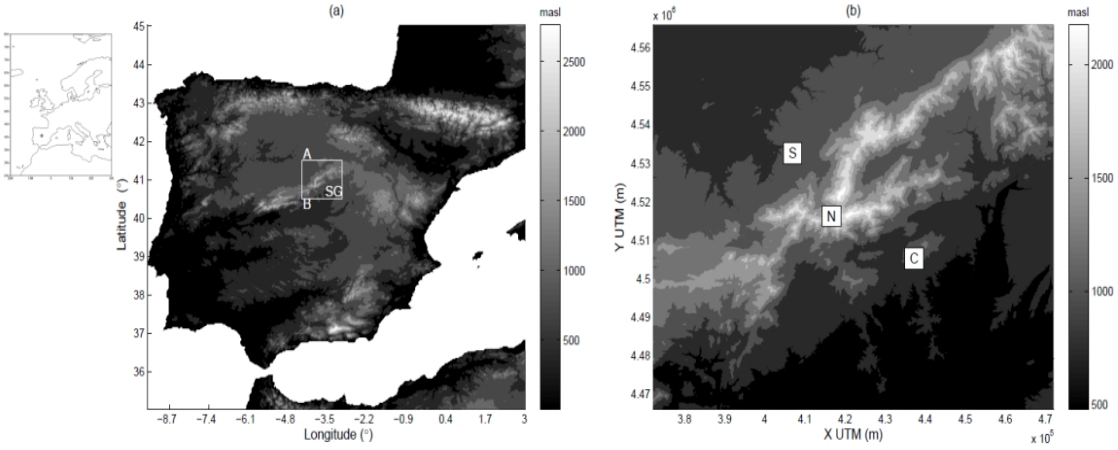

Figure 3.5. (a) Elevations of IP showing location of Guadarrama and points A and B used in this work. (b) Elevations of Guadarrama with locations of rain observatories used in this study: Segovia (S) located in the northern side of the range, Navacerrada (N) located on the top of range and Colmenar Viejo (C) located in the southern side of the range.

Figure 3.6.a represents the accumulated annual precipitation at the observatory at top of the range, *N*, for the period 1990-2013 and for hydrological years, defined as the period going from September to August. Also accumulation for years with maximum and minimum accumulated precipitation is highlighted. It can be seen how average precipitation at *N* site is around 1240 mm. Lowest accumulation at this observatory was 750 mm, reached during the hydrological year 1994/1995. Highest record is 1788 mm, reached the next year, in 1995/1996. This year was characterized by strong precipitation all over the IP (Losada et al., 2007). This Figure also shows the high inter-annual variability of precipitation at this area. For the IP, most of the anomalous precipitation in winter has been related to a small number of large-scale atmospheric modes (Rodríguez-Puebla et al., 1998). Some authors have stressed the

importance of the North Atlantic oscillation (NAO) (Hurrell et al., 2003) on winter precipitation at IP (Rodríguez-Puebla et al., 1998; Rodríguez-Fonseca and Serrano, 2002; Trigo et al., 2004). Recent results by Sanchez López et al. (2015) using a conceptual lake model and limnological variables (ice phenology records) found how anomalous precipitation related with NAO is strongly influencing the ice cover of Laguna de Peñalara, a small lake located at the highest lands of Guadarrama. It is well known how alpine lakes are excellent indicators of these kinds of teleconnections (Rodó et al., 1997)

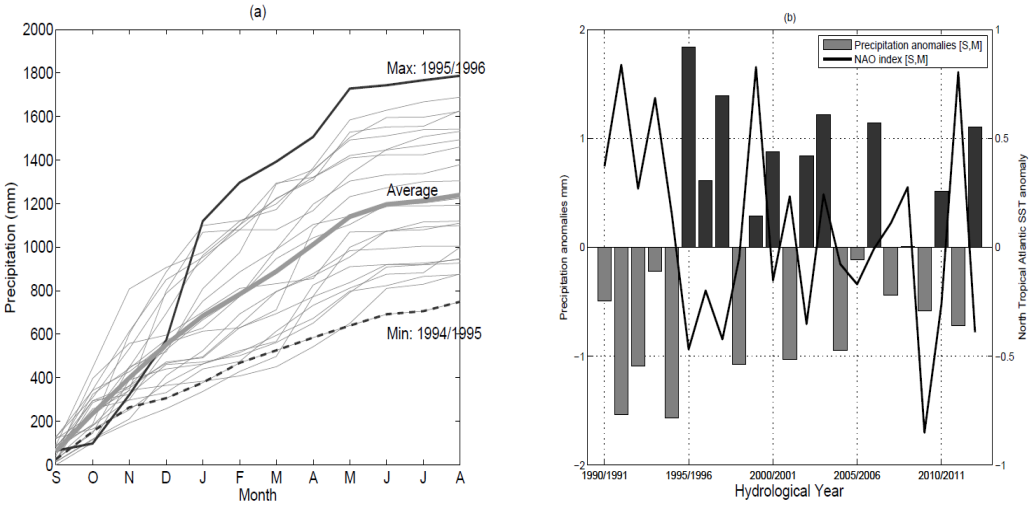

Figure 3.6. Accumulated annual precipitation at the top of mountain observatory (N) for the period 1990-2013 and for hydrological years going from September to October. Upper solid line represents accumulated precipitation for the year that reached the maximum precipitation. Solid gray line represents the average accumulation. Lower black dashed line represents the accumulated precipitation for the year with lowest precipitation. (b) Standarized anomalies of precipitation at N for the period 1990-2013 for hydrological years. Black bars represent years with a total precipitation higher than average. The scale shows how many times the anomaly is compared to the standard deviation of the time series. Gray bars represent years drier than average. Solid line represents the average North Atlantic Oscillation Index for the period 1990-2013 averaged for the same hydrological years.

Figure 3.6.b shows the standarized anomalies of precipitation at *N* for the period 1990-2013 also for hydrological years but only for the wet months (from September to May).

It shows the high inter-annual variability of this region (see Durán et al., 2013 for more details). The period analyzed here starts with a persistent drought that lasted until 1994/1995. Some authors (Rodríguez-Fonseca and Castro, 2002; Rodríguez-Fonseca et al.,

2006; Losada et al., 2007) have documented how 1995 and 1996 were characterized by an anomalous warming of the Subtropical North Atlantic sea surface temperatures due to a transition of the Atlantic Multidecadal Oscillation (Knight et al., 2006) from its negative to its positive phase. This drought finished next year, 1995/1996, with the highest precipitation reached for the period of study. Regarding the drought of 2004/2005, García-Herrera et al. (2007) concluded that it might be attributable to three main factors that occurred successively: a NAO positive pattern from November to January, a positive East Atlantic pattern in February, and a record-breaking blocking episode, which extended from mid-February to mid-March.

Figure 3.7.a shows again the marked summer drought and the strong variability observed during winter months. Figure 3.7.b shows how most of the precipitation at this location falls as snow from November to April. If we assume hail precipitation as a good indicator of heavy convective storms, this figure would shows how these events are mainly concentrated between April to September with a moderate contribution to total precipitation (see Durán et al. (2013) for a detailed discussion).

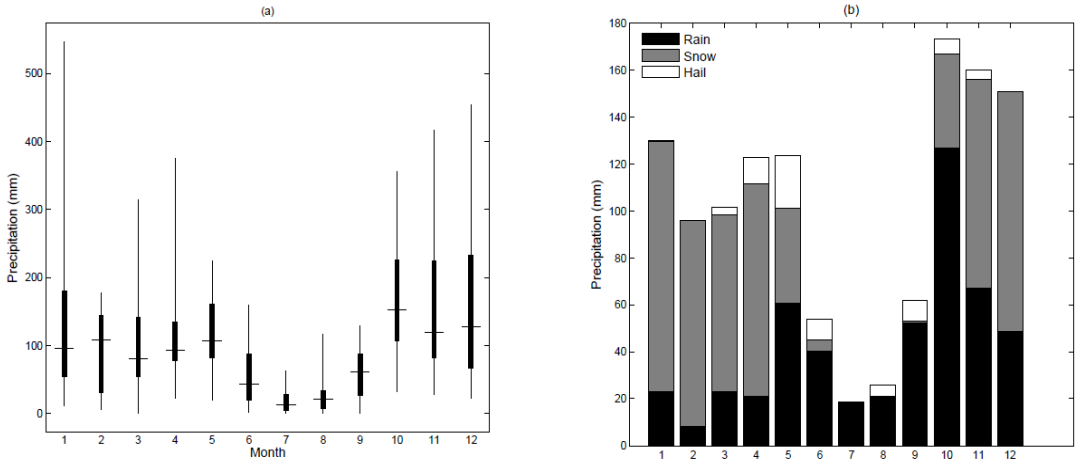

Figure 3.7. (a) Box plots for monthly precipitation at N for the period 1990-2013. (b) Monthly precipitation at N for the period 1990-2013 differentiating between types of precipitation: rain, snow or hail.

3.4.2. Data

One of the strengths of LMOP is its low requirements in terms of input data. The following data sets have been used in this work:

- ECMWF ERA-Interim data for determining the meteorological initial conditions of the air masses reaching Guadarrama.

- IGN-MDT200 (National Geographic Institute, Spain) digital elevation terrain model for detailed orography description.

- AEMET precipitation data from three observatories for model tuning and evaluation of results.

i. ECMWF ERA-Interim

The ERA-Interim dataset is a product from European Centre for Medium-Range Weather Forecast (ECMWF) describing the large scale atmospheric state from the period 1979 to present. The horizontal grid is approximately of 70 km.

LOPM is driven by the input data taken from this dataset. Vertical profiles were extracted from two points: A (41.75º N, 4.22º W) and B (40.35º N, 4.22º W) referred to as the northern and southern input points respectively (see Fig. 3.5.a). The data is taken from the original vertical levels and positions are located at the original ERA-Interim (not interpolated) grid. The terrain heights in ERA-Interim at these points are 903.6 m for A (northern) and 817.7 m for B (southern).

ii. AEMET Data

The three precipitation observatories from used in previous sections are used: N, C and S. Figure 3.3.b shows the location of these observatories along with the domain of this study.

Observations coming from these observatories have very good quality and have 100% data completeness for the period 1990-2013 (see Durán et al., 2013, for a detailed discussion on this). It can be seen how these three observatories are strategically located since there is always one on the leeward side and the other on the windward, representing an excellent workbench for testing the performance of LMOP.

But precipitation observations using rain gauges are not perfect and should be always be taken with a certain degree of uncertainty. Representativeness of these measurements depend on many factors and measurements often need extra corrections (Goodison et al., 1989; Groisman and Legates, 1994; Sevruk, 1996; Adam and Lettenmaier, 2003; Cheval et al., 2011; Isotta et al., 2015). For example, only the influence of wind at the upper part of a rain gauge can be responsible of more than 15% losses in the case of rain and of 30% for snow. It is generally accepted that rain gauges tend to underestimate real precipitation. (Chvíla et al., 2005; Paulat et al., 2008; Nitu et al., 2012).

The observing method used at the three observatories (*S*, *N* and *C*) is a Hellman rain gauge (Sevruk and Klemm, 1989) without wind shield. Every six hours precipitation is collected and measured manually by professional observers. In case of snow or hail, precipitation is melted and measured as the equivalent in water. Data used in this study do not suffer from data gaps and and homogeneity has been checked (see Durán et al., 2013 for more details).

iii- IGN-MDT200

IGN-MDT200 (from the National Geographic Institute, Spain) digital elevation model has been used as input of LOPM. The digital elevation model has a grid resolution of 200 m. With this high resolution, this terrain model is expected to reflect accurately enough the main terrain features of Guadarrama. Highest peak of this Sierra, *Pico de Peñalara*, with a real altitude of 2428 masl has an altitude of 2418 masl on IGN-MDT200.

A squared modeling domain has been defined going from 39º52'38''N to 5º4'45''W. This domain includes the whole Iberian Central System and part of northern and southern plateau and is shown in Figure 3.5.a. The area where results of LMOP are expected to be valid and the validation will be performed is a centered sub-domain of 500 x 500 grids that covers Guadarrama (Figure 3.5.b).

3.4.2 Linear Model of Orographic Precipitation

LMOP is based on the Smith and Barstad (2004) proposal for a linear steady-state theory of orographic precipitation. This theory includes airflow dynamics, cloud physics, condensed water advection, and downslope evaporation (a full description of the method can be found at Smith et al. (2005) and Smith (2006) and to Barstad and Smith (2005) for its evaluation). LMOP, has been tested and applied to different areas evolving from its initial conception but keeping its simplicity and conceptuality (Barstad et al., 2007; Smith and Evans, 2007; Crochet et al., 2007; Schuler et al., 2008).

LMOP finds a simple solution for airflow dynamics, using the 3D airflow pattern over complex terrain solved using linear mountain wave theory; and cloud physics, using a linear cloud physics representation including cloud time scales for the formation and fallout of hydrometeors.

i. The Solution of the Advection Equations

Linear Orographic Precipitation Model proposes a simple way of considering part of the physical processes that occur when a humid air mass reaches an orographic obstacle and is forced to progress upslope. This theory starts with the formulation of two steady-state advection equations describing the vertically integrated cloud water density $q_c(x, y)$ and hydrometeor density $q_s(x, y)$.

$$\frac{D q_c}{Dt} = S(x, y) - \frac{q_c}{\tau_c} \qquad (3.6)$$

$$\frac{D q_s}{Dt} = \frac{q_c}{\tau_c} - \frac{q_s}{\tau_f} \qquad (3.7)$$

Linear equations (3.6) and (3.7) are used to describe the vertically integrated cloud water density $q_c(x,y)$ and hydrometeor density $q_s(x,y)$ where τ_c is the time constant for conversion from cloud water to rain or snow and τ_f is the time constant for hydrometeor fallout. In Eq.(3.6), $S(x,y)$ is the rate of cloud water generation by moist adiabatic uplift (Blader and Roach, 1977).

Note that last term in Eq.(3.7) represents precipitation at the ground: $P(x, y) = \frac{q_s}{\tau_f}$

Assuming steady state, the only variation of q_c and q_s are due to advection, so the material derivatives in Eqs.(3.6) and (3.7) can become: $\frac{D(\,)}{Dt} = \vec{U} \nabla(\,)$, where $\vec{U}$ is the horizontal wind vector

with components U and V. Thus Eqs. (3.6) and (3.7) can be rewritten as:

$$\frac{D q_c}{Dt} \approx \vec{U} \nabla q_c = S(x, y) - \frac{q_c}{\tau_c} \tag{3.8}$$

$$\frac{D q_s}{Dt} \approx U \nabla q_s = \frac{q_c}{\tau_c} - \frac{q_s}{\tau_f} \tag{3.9}$$

Thus, Eqs. (3.6) and (3.7) can be rewritten as

$$u \frac{\partial q_c}{\partial x} + v \frac{\partial q_c}{\partial y} = S(x, y) - \frac{q_c}{\tau_c} \tag{3.10}$$

$$u \frac{\partial q_s}{\partial x} + v \frac{\partial q_s}{\partial y} = \frac{q_c}{\tau_c} - \frac{q_s}{\tau_f} \tag{3.11}$$

A way of solving this set of equations linked by a common term in a simple way is to solve then on the Fourier space. It is known that spatial derivatives are very simplified in this space: $\frac{\partial}{\partial x} \to ik$, $\frac{\partial}{\partial y} \to il$. The intrinsic frequency of the resultant wave is then $\sigma = uk + vl$, and k and l are the components of the horizontal wave number vector. Eqs. (3.10) and (3.11) can now be transformed into Fourier space like:

$$uik \hat{q}_c + v il \hat{q}_c = \hat{S}(k, l) - \frac{\hat{q}_c}{\tau_c} \tag{3.12}$$

$$uik\,\hat{q}_s + v\,il\,\hat{q}_s = \frac{\hat{q}_c}{\tau_c} - \frac{\hat{q}_s}{\tau_f} \qquad (3.13)$$

From Eq. (3.12) $\hat{q}_c = \frac{\hat{S}(k,l)}{i\sigma + \frac{1}{\tau_c}}$. Now, introducing this term in Eq. (3.13), it can be rewritten as: $\hat{q}_s\, i\sigma = \frac{\hat{S}(k,l)}{\tau_c\left(i\sigma + \frac{1}{\tau_c}\right)} - \frac{\hat{q}_s}{\tau_f}$, leading to $\hat{q}_s\left(i\sigma + \frac{1}{\tau_c}\right) = \frac{\hat{S}(k,l)}{\tau_c\left(i\sigma + \frac{1}{\tau_c}\right)}$, multiplying both sides by τ_f and with some algebra, this equation leads finally to the following simple expression for precipitation in the Fourier space as a function of a source function $\hat{S}(k,l)$ and two dumping parameters: τ_c and τ_f

$$\hat{P}(k,l) = \frac{\hat{S}(k,l)}{\left(i\sigma\tau_f + 1\right)\left(i\sigma\tau_c + 1\right)} \qquad (3.14)$$

Eq. (3.14) can be brought back to real space to obtain precipitation distribution in real space:

$$P(x,y) = \int\int \hat{P}(k,l)\, e^{i(kx+ly)}\, dkdl \qquad (3.15)$$

It is not only the simplicity of the physics of this model that contributes to LMOP being so computationally cheap, it is also the simplicity of the solution of the governing equations in the Fourier space that makes this possible. Calculation of direct and inverse

Fourier transforms can be achieved nowadays really quickly using Fast Fourier Transform algorithm on regular computers.

The use of Fourier space is really useful in 3D mountain wave theory (Sawyer, 1962; Smith, 1979) giving a wavy behavior to the air movement that would be very cost effective to achieve real space models.

ii. The Source Function

The term $S(x, y)$ in Eq.(3.8) is the vertically integrated condensation rate arising by moist adiabatic uplift:

$$S(x, y) = \frac{C_w}{H_w} \int_0^\infty w(s, y, z) e^{-z/H_w} dz \qquad (3.16)$$

In Eq. (3.16), the air is assumed to be near saturation and C_w is an uplift sensitivity factor depending on surface humidity and lapse rate, H_w is the thickness of the ambient moist layer, and $w(x, y, z)$ is the terrain-forced vertical air velocity.

$$C_w = \rho_{wv} \frac{\Gamma}{\gamma} \qquad (3.17)$$

$$H_w = \frac{-R_v T^2}{L\gamma} \qquad (3.18)$$

Where ρ_{wv} is the surface water vapor density, γ is the environmental lapse rate, and Γ is the average moist adiabatic

lapse rate, T is the surface temperature, L is the latent heat of vaporization, and R_v is the gas constant for vapor.

The terrain-forced vertical velocity at ground level is determined from the horizontal wind and the terrain gradient following Smith (1979):

$$w(x, y, 0) = \vec{U} \nabla h(x, y) \qquad (3.19)$$

As pointed out by Crochet et al. (2007) this calculations of the vertical velocity with altitude using linear mountain-wave theory allows to capture important features of the airflow such as decay of vertical velocity with altitude leading to a reduction in the amount of condensation, lateral airflow around topographic features leading to reduced uplift, and the formation of gravity waves. The effect of vertical stability of the air column is incorporated in the source term. In neutral conditions, vertical velocities at the lower boundary will propagate through the entire moist layer, while in stable conditions, they tend to reduce aloft. In the latter case, the source field is smoothed and reduced.

To describe the dynamics of forced ascent, we use well known results from linear Boussinesq mountain wave theory (e.g., Queney, 1947; Sawyer, 1962; Smith, 1979, 2002; Wurtele et al., 1996). For each Fourier component *(k, l)*, the vertical velocity takes a complex exponential form:

$$\hat{w}(k, l, z) = \hat{w}(k, l, 0) e^{imz} \qquad (3.20)$$

Where the vertical wave number is given by:

$$m(k, l) = \left[\frac{N_m^2 - \sigma^2}{\sigma^2}(k^2 + l^2)\right]^{1/2} \qquad (3.21)$$

Substituting Eq. (3.20) into the Fourier transform of Eq. (3.16), after some algebra :

$$\hat{S}(k,l)=\hat{w}_0(k,l)\left(\frac{C_w}{H_w}\right)\int_0^{\infty} e^{-z/H_w}e^{imz}dz \qquad (3.22)$$

Thus,

$$\hat{S}(k,l)=\frac{C_w\hat{w}_0(k,l)}{(1-imH_w)} \qquad (3.23)$$

Using $\hat{w}_0(k,l)=\hat{w}(k,l,0)=i\sigma\hat{h}(k,l)$ from mountain wave theory, Eq.(3.23) yields to a transfer function relating the transform of the terrain and the condensed water source function:

$$\hat{S}(k,l)=\frac{C_w i\sigma\hat{h}(k,l)}{(1-imH_w)} \qquad (3.24)$$

As pointed out by Smith and Barstad (2004), the denominator of Eq. (3.24) contains the effect of vertical velocity variations up through the moist layer. If $N_m^2-\sigma^2$, m is positive imaginary and the forced ascent decays with height. Then, the denominator of Eq. (20) is real, positive, and greater than unity, reducing the amount of condensation. If the static stability (N_m) is large or the intrinsic frequency s is small, m will be real. In this case, the vertical structure oscillates with height and partial cancellation occurs. The denominator of Eq. (3.24) is complex with a magnitude exceeding unity. Again, the total condensation is reduced.

In both these cases, the depth of the moist layer (H_w) plays a key role in the penetration of the vertical motion through the moist layer. Also the effect of static stability enters several ways in Eq.

(3.24) increases the available water vapor (C_w and H_w), but decreases the depth of the lifting (see Smith and Barstad (2004) for a complete discussion on these aspects)

Combining Eq. (3.14) and (3.24) gives a single equation that represent LMOP model:

$$\hat{P}(k,l)=\frac{C_w i\sigma \hat{h}(k,l)}{(1-imH)_w(i\sigma\tau_f+1)(i\sigma\tau_c+1)} \qquad (3.25)$$

Eq. (3.25) shows at a glance all the input parameters necessary to run LMOP:

- Terrain: *h(x,y)*.
- Surface temperature, entering in H_w trough Eq.(11).
- Average wind entering through σ.
- surface water vapor density entering trough C_w
- Stability: N_m
- Moist layer thickness: H_w
- Cloud delay times: τ_c and τ_f

For a clarifying and interesting discussion about the implications of the terms in the denominator of Eq. (3.25) the reader can refer to Crochet et al. (2007).

Eq. (3.25) can be brought back to real space by an inverse fast Fourier transform to compute the precipitation field:

$$P(x,y)=max\left[\iint P(k,l)e^{i(kx+ly)}dkdl+P_{\infty},0\right] \quad (3.26)$$

3.4.3 Enhancements from Original Formulation

LMOP has been given good results even with its original formulation (Smith and Barstad, 2004). Nevertheless there has been some improvements that keeping the same philosophy has shown to improve, to a certain extent, the performance of the model. Next sections show of the enhancements that were susceptible to improve the results for this application.

i. Drying Ratio

Original formulation of LOPM considered precipitation to be proportional to the upstream advection of water vapor flux. This simple assumption might work fine for isolated and round mountains or mountain ridges with general flow going perpendicular of the axis of the ridge. Very often, water vapor flux at Guadarrama reach the sierra almost along its axis (see Durán et al., 2013; Durán et al., 2014). For this reason, this original simplification was considered that might induce significant errors.

A simple way of dealing with this was already proposed in Smith and Evans (2007). They proposed to correct the precipitation with the local fraction of water vapor remaining after upwind precipitation. This was estimated to be:

$$P_{reduced}(x,y)=P(x,y)\Theta(x,y) \quad (3.27)$$

where $P(x,y)$ is computed with Eq. (3.26) and $\Theta(x,y)$ is the fraction of vapor remaining defined as:

$$\Theta(x,y)=1-\int_{-\infty}^{x,y} P_{reduced}(x',y')ds/F_0 \qquad (3.28)$$

Where $F_0=\rho q_w U H_w$ is the incoming upstream horizontal water vapor flux and $ds=(U_x dx'+U_y dy')/|\vec{U}|$. Eq. (3.28) can be expressed as:

$$\Theta(x,y)=e^{-D R_{ref}(x,y)} \qquad (3.29)$$

where

$$D R_{ref}(x,y)=\int_{-\infty}^{x,y} P(x',y')ds/F_0 \qquad (3.30)$$

ii. Sub-saturated Upstream Conditions

In addition to Smith and Evans (2007) correction which adjusts for the drying of the water flux across mountain ridges, we will introduce a new correction which to some degree takes into account sub-saturated upstream conditions. We start with considering the background wind vector $\vec{U}=U\vec{i}+V\vec{j}$ where U and V are wind components, and defining the vertically-integrated water vapor flux as:

$$\vec{F}_{ref}=\rho_{wv}\vec{U}H_w \qquad (3.31)$$

Further discussions on the flux may be found in, e.g. Barstad et al. (2007). Moreover, we assume there is a sub-saturated water vapor flux expressed as:

$$\vec{F} = \theta \vec{F}_{ref} \tag{3.32}$$

where the $\vec{F}_{ref}$ is the saturated flux. Now, using Eq. (3.31 and 3.32) and assuming homogeneous reduction throughout the air column, H_w is unaffected and only the humidity ρ_{wv} is influenced, thus we have:

$$\frac{\rho_{wvs} - \rho_{wv}}{\rho_{wvs}} = (1 - \theta) \tag{3.33}$$

Using definition of relative humidity, $Rh = 100\,\rho_{wv} / \rho_{wvs}$, and

$$\theta = Rh / 100 \tag{3.34}$$

The condensation source term in Eq. (3.24) can be also expressed as:

$$\hat{S}(k,l) = \frac{i\,\rho_{wv}\,\gamma / \Gamma\,\sigma\,\hat{h}}{1 - imH_w} \tag{3.35}$$

Since the intrinsic frequency can be written as $\sigma = \vec{U} \cdot \vec{K}$ where $\vec{K} = k\vec{i} + l\vec{j}$, we have:

$$\hat{S}(k,l) = \frac{i\,\rho_{wv}\,\gamma / \Gamma\,\hat{h}\,\vec{F} \cdot \vec{K}}{H_w(1 - imH_w)} \tag{3.36}$$

or with the relative humidity adjusted flux, $\vec{F}$, from (3.32),

$$\hat{S}(k,l) = \frac{i\theta\,\gamma / \Gamma\,\hat{h}\,\vec{F} \cdot \vec{K}}{H_w(1 - imH_w)} \tag{3.37}$$

Where now (3.37) has some adjustments taking into account a reduced flux due to sub-saturated conditions. This assumption violates to some extent the original idea behind the linear model as it was intentionally designed as a perturbation model, assuming saturation in the base state. However, it will to some extent reduce the condensation relative to the relative humidity level of the incoming air.

iii. Topographic Flow Blocking

It has been widely analyzed how a mountain barrier interact with an atmospheric flow (e.g. Smith, 1979; Medina et al., 2005; Armi and Mayr, 2015). Several factors like height of the obstacle, wind velocity and stratification play a role whether or not the flow is able to get over, split or even being blocked. It seems clear that not taking into account this fact can lead LOPM to overpredict precipitation. Blocking cases are expected to happen with a strong stratification and weak winds Under these conditions, the dynamical height of the mountain is high. A simple way to deal with this effect is using the concept of Nondimensional Mountain Height, *M*. This can be defined as:

$$M = \frac{N \cdot h}{|\vec{U}|} \qquad (3.38)$$

Which is the inverse of the Froude number $Fr = \frac{1}{M}$ where $\vec{U}$ is the wind velocity, N is the Brunt-Väisälä frequency and h is the mean height of the mountain range.

This parameter has been widely used for describing nonlinear features of fluxes over mountains and it has been shown how it describes in a simple way accelerations at the lee and windward slopes (Smith and Grønas, 1993).

There are some variations on literature about the values of M (Bousquet and Smull, 2006; Hughes et al., 2009). As a rule of thumb it is accepted that values of M=1 guarantee free upslope humid flow and values higher than 2 will block the flow.

For this work, a 6 hours characterization of topographic blocking flow due Guadarrama massif has been done. For $M<1$ result in air flowing over the obstacle, while a $M>2$ indicate blocking. These cases have not being simulated. A mean orographic altitude of the massif has been set to h=1600 m, which is the maximum height of a well connected orographic barrier. Values of M between these thresholds have been linearly interpolated and converted to a blocking factor, b_f. This factor is zero for $M=2$ and is 1 for $M=1$. Then it has been used to diminish partially the value of the source function S in the following way:

$$S''(k,l)=b_f S \qquad (3.39)$$

3.4.4 Model Set-up

Terrain preprocessing is crucial in upslope models like LMOP. Dynamical uplifting due to wind and orographic obstacles is the dominating factor for producing condensation and, subsequently, precipitation. Since LOPM assumes a steady and unperturbed flow on its boundaries, it is necessary to preprocess the orography in such a way that air reaches the model domain relatively

undisturbed by mountains. Also, since the equations are solved in the Fourier space, it is necessary to leave a considerable distance from the area of interest to the lateral boundaries of the model in order to avoid aliasing or spurious wave behavior. For these reasons, orography in band of 250 grid points (50 km) at all sides has been smoothed out.

In previous applications of this model at coastal areas sea level has been chosen as the reference level. Nevertheless for this continental application, choosing a right reference level has required more attention. Even though Guadarrama is surrounded by two relatively flat and extensive plateaus that facilitate the mentioned unperturbed flow prerequisite, they have different mean heights. Northern plateau is about 200 m higher that southern plateau (see Figure 3.3.a). These differences can be even higher depending on wind direction. This makes questionable to choose a single reference level for all the simulations and for all wind directions. In order to tackle this problem in a simple way, a case dependent orography was used. This means that reference level will depend on every case wind direction. For sake of simplicity, only six different sectors have been considered. LMOP is an upslope model, so artificial precipitation from incorrect elevations on the downwind areas will not enter the results.

The vertical profiles extracted from ERA-Interim at points *A* and *B* (Figure 3.3.a) were used for initializing LMOP with a 6 hours step. ERA-Interim surface temperature in the reanalysis has been adjusted to compensate for the deviation from the reference level taken of terrain height. For this adjustment an environmental lapse rate of Γ=0.06 K km^{-1} has been used. In addition to surface temperature, the linear model also needs winds and stability at some height. For wind of the air mass the 870 m above reference level was chosen. For temperature near surface, temperature at 10

m was chosen. For upper temperature for snow precipitation characterization, temperature at 1100 m was chosen since this is a reasonable height for cloud base height. For relative humidity of the air mass, the average relative humidity between levels at 525 to 3300 m above surface was calculated. This an approximate thickness of the moist layer ignoring levels too influenced by soil.

In order to separate precipitating events from non-precipitating events, a threshold on the average relative humidity was calculated using observed precipitation at *N*. This threshold is supposed to represent a threshold for near saturating conditions. A classification of every case into wet (*W* hereafter) and dry (*D* hereafter) has been performed. A day is considered wet if total precipitation for those 6 hours case is equal or higher than 1 mm. Precipitation at *N* has been chosen for such classification for two reasons. First, this observatory is located at top of the range so it is representing the higher lands, where more reliability of results is wanted. Also, as pointed out by Duran et al. (2013), the probability of having precipitation at *S* or/and *C* and not at *N* is very low. Except in summer (JJA), when the frequency of wet days with only precipitation at *S* is 15% of the summer wet days.

The 1 mm threshold for considering a wet day is selected so 25^{th} percentile of wet population has maximum distance from 75% percentile of dry population.

The near saturation threshold has been taken as the 25^{th} percentile of the wet population for each season.

Two parameters of the model needed to be also determined. These are τ_c and τ_f. The falling time was considered fixed and equal to an average terminal velocity, V_t, of 6 m s^{-1} for rain and 1 m s^{-1} for snow. Then $\tau_f = H_w/V_t$. In order to determine the kind of

precipitation a snow temperature threshold need to be defined. For this purpose the ERA-Interim profile temperature from 10 to 3000 m above surface has been used. For each level two populations out of the temperature values were made: one for snow (*S1*) and the other for rain (*R1*) depending on kind of precipitation recorded at *N*. The level that gives the maximum distance between 25th percentile of rain and 75th percentile of snow for all seasons, except summer, is taken as snow reference level. The threshold used is the 75th percentile of the snow population for each season.

For τ_c a value of 1000 s was taken from bibliography. As has been stated, τ_f depends on the type of precipitation. In order to determine the temperature threshold that better could differentiate populations of snow and rain, the temperature at different level of observatory *N* were compared. The optimum separation between populations was temperature at a height of 1100 m above reference level.

With this set-up LMOP simulations were conducted for simulating from 1st of January of 1990 to 31st of December of 2013 with a 6 hours time step with a 200 m. For every case, mean wind direction was calculated. Depending on the sector, terrain model was selected and initial meteorological conditions upwind used. The results obtained are shown in section 4.4.

Supercooled water in fog formed ice needles near Dos Hermanas betraying wind direction

Chapter 4. Results

4.1 Results From the Peñalara Meteorological Network

4.1.1 Description of the Network

At the present time RMPNP consists of five automatic meteorological stations that cover the area of Massif of Peñalara and the lower lands of Valle del Lozoya. Also a manual observatory of temperature and precipitation has been established

at one of the automatic sites for calibration purposes and research. Figure 3.1.b shows the location of the sites.

Table 4.1 shows the code, name, coordinates, starting year, variables codification, magnitudes measured and sensor used at the present time.

Even though location of sites are tried to be as much representative as possible of the general environmental conditions of a broad area, this is sometimes difficult, specially for some variables. Table 4.2 includes some general comments about the representativeness of the sites that any future user of the data should take into account (Woodruff et al., 1998). This brief information, should not substitute an in-situ visit of the site, something that is always recommended before using the data.

Since first stations (Zabala and Cabeza Mediana) were installed in 1999 at a height of 2079 and 1691 masl the network has suffered a set of changes as a result of technological evolution and acquisition of knowhow (Durán, 2003). Regarding changes in sensor and data logging system technology, the evolution has been less marked than in telecommunications and quality assurance. Data logging was made first using a NRG9000 data logger (renewablenrgsystems.com). With the irruption of the Global System for Mobile (GSM hereafter) communications, loggers were progressively substituted with Gantner IDL101 loggers (gantner-instruments.com) and Wavecom (sierrawireless.com) modem was used for data transfer.

Table 4.1.Description of the location and characteristics of the observing sites of Peñalara Meteorological Network. Instrumentation has changed since first installation but last one is included in this table.

Code	Name	Coordinates (City, Province)	UTM (m) Altitude (masl)	Starting year	Variable code	Magnitude (Units)	Sensor (in 2014)
001	Ontalva	40º52'20''N 3º53'1'' O (Rascafría, Madrid)	X: 424736 Y: 4524980 Z: 1196	2008	TA01	Air temperature at 2m (ºC)	Vaisala HMP45
				2008	HR01	Relative humidity at 2 m (%)	Vaisala HMP45
				2008	LL01	Liquid precipitation at 3 m (mm)	NovaLynx 260-2500
				2008	VV01	Wind velocity at 6 m (m s-1)	NRG #40
				2008	DV01	Wind direction at 6 m (º)	NRG
002	Cabeza Mediana	40º50'13''N 3º54'15''O (Rascafría, Madrid)	X: 423450 Y: 4521790 Z: 1691	1999	TA01	Air temperature at 2m (ºC)	Vaisala HMP45
				1999	HR01	Relative humidity at 2 m (%)	Vaisala HMP45
				1999	LL01	Liquid precipitation at 3 m (mm)	NovaLynx 260-2500
				1999	VV01	Wind velocity at 6 m (m s-1)	Young Wind monitor
				1999	DV01	Wind direction at 6 m (º)	Young Wind monitor
				2008	PA01	Atmospheric pressure 1.75m (hPa)	NovaLynx
003	Refugio Zabala	40º50'20''N 3º57'1'' O (Rascafría, Madrid)	X: 419300 Y: 4521330 Z: 2079	1999	TA01	Air temperature at 6m (ºC)	Vaisala HMP45
				1999	HR01	Relative humidity of air at 6 m (%)	Vaisala HMP45
				1999	LL01	Liquid precipitationat 4m (mm)	Young Wind monitor
				2008	LL02	Liquid precipitation at 4m (mm)	Lambrecht
				1999	VV01	Wind velocicity at 10m (m s-1)	Young Wind monitor
				1999	DV01	Wind direction at 10m (º)	Young Wind monitor
				2008	PA01	Atmospheric pressure 2m (hPa)	NovaLynx
004	Cotos	40º49'31''N 3º40'''O (Rascafría, Madrid)	X: 418955 Y: 4519800 Z: 1857	2008	TA02	Air temperatute at 2m (ºC)	E+E Elektronic
				2005	TA01	Air temperature at 10 m (ºC)	E+E Elektronic
				2008	HR02	Relative humidity of air at 2m (%)	E+E Elektronic
				2005	LL01	Liquid precipitation at 1.5 m (mm)	Nova Lynx
				2005	VV01	Wind velocity at 10 m (m s-1)	NRG #40
				2005	DV01	Wind Direction at 10m (º)	NRG
				2008	HN01	Snow heigth (m)	Judd Comunicatio
005	Alameda	40º54'53''N 3º50'39'' O (Alameda, Madrid)	X: 428934 Y: 4529640 Z: 1104	2009	TA01	Air temperature at 4m	E+E Elektronic
				2009	HR01	Relative humidity of air at 4m	E+E Elektronic
				2009	LL01	Liquid precipitation at 4 m	Nova Lynx

Table 4.2.Representativity of sites.

Code	Name	Metadata and representativity of sites
001	Ontalva	This station is located in the lower land of the valley. Land use is natural grass immersed into a pine forest in a sheltered clear. Wind observation is not very representative of the boundary layer wind due to obstacles, much higher than tower. The not heated rain gauge might under sample in winter due to snow blocking. Minimum temperatures might be lower than expected for this altitude since this location is immersed in Valle de la Umbría, a north oriented valley within Lozoya Valley with possible air drainage from higher elevations.
002	Cabeza Mediana	Mountain site. Land use is natural pasture with some small trees. Excellent location in top of a flat and round ended hill in the middle of Valle del Lozoya. Very good representativity of wind measurements. Not heated rain gauge is surely under sampling real precipitation in winter.
003	Refugio Zabala	Very High mountain environmental conditions. Land use is mainly bare rock with snow cover during many months. Sensors are located in the top of small construction for security and impact reasons, so some impact is expected in wind an precipitation measurements. Good representativity of temperature at 4 meters but rime might be influencing temperature measurements in winter. Not heated rain gauge, so precipitation measurements are surely under sampled in winter.
004	Cotos	High mountain site. Land use is natural pasture with tall pine trees at 100 meters. Good representativity but the site is located not in a very flat area. Local effects of catabatic cold air drainage from higher terrain is expected due to the slope. Not heated rain gauge, so precipitation measurements are surely under sampled.
005	Alameda	Good representativity of all measurements. Land use is natural grass. Even though rain gauge is not heated, under sampling might be less important due to less snow precipitation at this altitude, but needs to be taken into account in winter.

4.1.2 Data Completeness

Table 4.3 shows the annual average data completeness of the stations based on the availability of air temperature data. This table shows the performance of the network in relation to problems related with power failures, general malfunction due to a general breakage of the stations and also human errors. This table shows also the increment of data volume through the years and also the technology change that the network has suffer from first years to present, specially in relation to telecommunications and data storage systems.

Before 2005 data collection was made locally accessing to the sites walking and downloading data directly from the logger to a computer (Local hereafter). This method was proven to be very robust since power requirements were minimum and loggers could be operated by small power panels and batteries. Nevertheless this was unsustainable with more sites needed to be visited. GSM communications opened a new horizon, since stations could be accessed remotely for data downloading and configuration. But poor quality of the signal at these mountains and problems due to a still incipient technology with not many automatization software possibilities, made this technology not very reliable. GPRS (General packet radio service) and evolution of GSM oriented to data transfer through the cellular network was the ultimate solution that gave the needed reliability to the communications at RMPNP. Telecommunications not only gave the possibility to have data at the desktop, saving man power, but also made possible to have an almost online diagnostic of the station status. It really made a difference on data completeness no matter the increment in the number of sites.

Table 4.3. Annual average of data completeness of the stations based on availability of air temperature observations (Blue for completeness>=75%, orange for completeness <75%, and white for not fully operative). Collection method are Local that stands for in-situ downloading of data, GSM for analog GSM data collection using modem and GPRS for GPRS TCP/IP protocol using dynamic IPs. Regarding Storage, ASCII stands for individual raw files from datalogger, S. Sheet stands for spread sheets for every variable organized in years with individual validation code and SQL stands for PosgreSQL database storage.

Year	Collection method	Volume of data	Storage	Station				
				Ontalva	C.Mediana	Zabala	Cotos	Alameda
1999	Local	202039	ASCII		34	42		
2000	Local	722874	ASCII		98	100		
2001	Local	1015623	ASCII		96	94		
2002	Local	1698549	ASCII		83	73		
2003	Local	2198111	ASCII		63	61		
2004	Local	2850198	ASCII		84	89		
2005	Local	3613656	S. Sheet		91	85	96	
2006	GSM	4219771	S. Sheet		55	58	51	
2007	GSM	5375096	S. Sheet		66	80	56	
2008	GPRS	7510050	SQL	84	92	90	96	
2009	GPRS	9911400	SQL	88	87	88	98	21
2010	GPRS	12634429	SQL	81	100	75	95	99
2011	GPRS	15261155	SQL	95	80	83	98	88
2012	GPRS	18022734	SQL	97	93	84	99	100
2013	GPRS	20629862	SQL	100	80	79	100	82
2014	GPRS	21966337	SQL	99	77	75	99	55
Average				92	80	79	89	75

Another important technological evolution was the way data is stored. With a few stations and during the first years, individual ASCII (American Standard Code for Information Interchange) was feasible. Nevertheless, soon it was necessary to tag data as valid ('V'), null ('D'), corrected ('C') or temporal ('T') as a result of the QA/QC process. This was first solved using spreadsheets, that also offered an easy solution for calculation of some statistics and daily and monthly time series but turn not to be very practical with the fast growing of data stored. The solution was found using PosgreSQL that brought new possibilities like programing of Python algorithms for data validation, automatization of report

generation and exchange of information with third parties. Also, gave reliability to the system thanks to the powerful capabilities of this environment.

4.1.3 Representativity of the Measurements and Statistics

The measurement of temperature using automatic techniques has shown to be robust at RMPNP. Data gaps at temperature time series is mainly due to general failure problems of the station, like power failures (Figure 4.1). Drift of sensors has shown to be under factory specifications and regular replacement of sensor filters showed to be less necessary than in other more contaminated atmospheres.

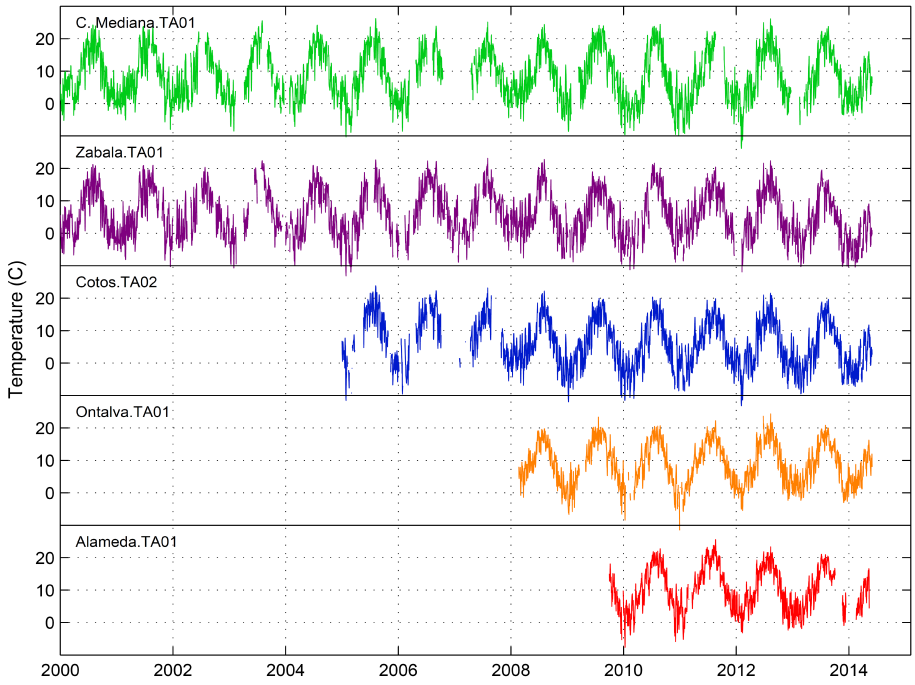

Figure 4.1. Time series of air temperature at the sites from 2000 to present in ºC.

The measurement of temperature using automatic techniques has shown to be robust at RMPNP. Data gaps at temperature time series is mainly due to general failure problems of the station, like power failures. Drift of sensors has shown to be under factory specifications and regular replacement of sensor filters showed to be less necessary than in other more contaminated atmospheres. The progressive substitution with new sensors have not affected its homogeneity.

In order to check the homogeneity of the temperature data sets, an Alexandersson test (Alexandersson, 1986) has been performed with Zabala and C.Mediana temperature data sets for the period 2000-2014. As reference station a less than 10 km distant temperature observatory belonging to the Spanish Meteorological Agency has been used. Puerto de Navacerrada (1893 masl) observatory uses professional staff and follows standardized observation methods. Since this observatory is operated by independent staff from RMPNP and uses a completely different method of measurement, a homogeneous behavior with this observatory should be robust enough. Figure 4.2 shows the results obtained. As can be seen the T value of this test on the annual mean temperature is below the critical value (6 for 13 points) and can be concluded that the time series at these two sites are homogeneous.

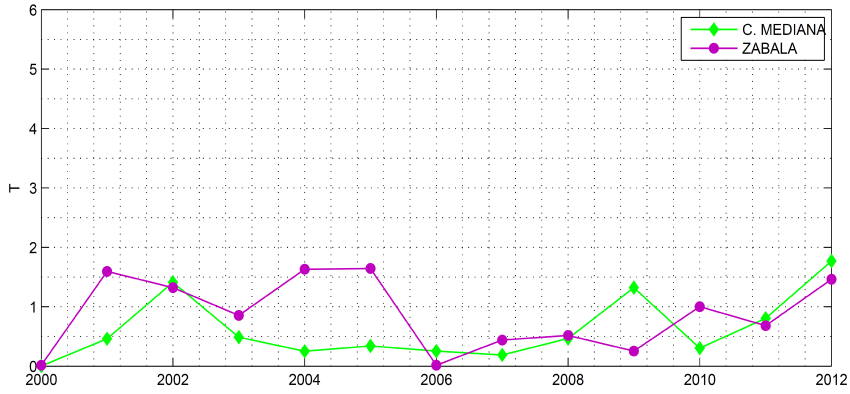

Figure 4.2 Values of T of an Alexandersson test for annual mean temperature observed at Cabeza Mediana and Zabala using Puerto de Navacerrada AEMET observatory as a reference station. The critical T value for 5% confidence level and 14 samples is 6.

Temperature time series recorded at RMPNP seem to be a good estimate of the real temperatures expected during all these years at this area of Sierra de Guadarrama. Nevertheless, there are some factors that could be influencing the representativeness of these estimations and would deserve a deeper analysis in the future. These are:

i) effect of rime freezing on the naturally aspirated radiation shield. Under this situation, a decoupling of the sensor from the measurand is expected (Leroy et al., 2002; Appenzeller et al., 2008);

ii) effect of down-up short wave radiation reflected from ground due to snow cover. Radiation shields are designed for an up-down direction;

iii) effect of ground level to rise due to snow height in winter;

iv) effect of evaporation of water drops condensed over temperature sensor;

One aspect that has shown to be useful for data validation is the relationships between values observed simultaneously by different sites (spatial coherency checks). Figure 4.3 shows the mean hourly temperature for every site and season. The difference between maximum and minimum temperature is a good estimator of the mean daily temperature amplitude. This figure shows how this relationships have an altitude forcing that needs to be taken into account. Higher altitude sites show a much lower temperature amplitude than valley bottom sites.

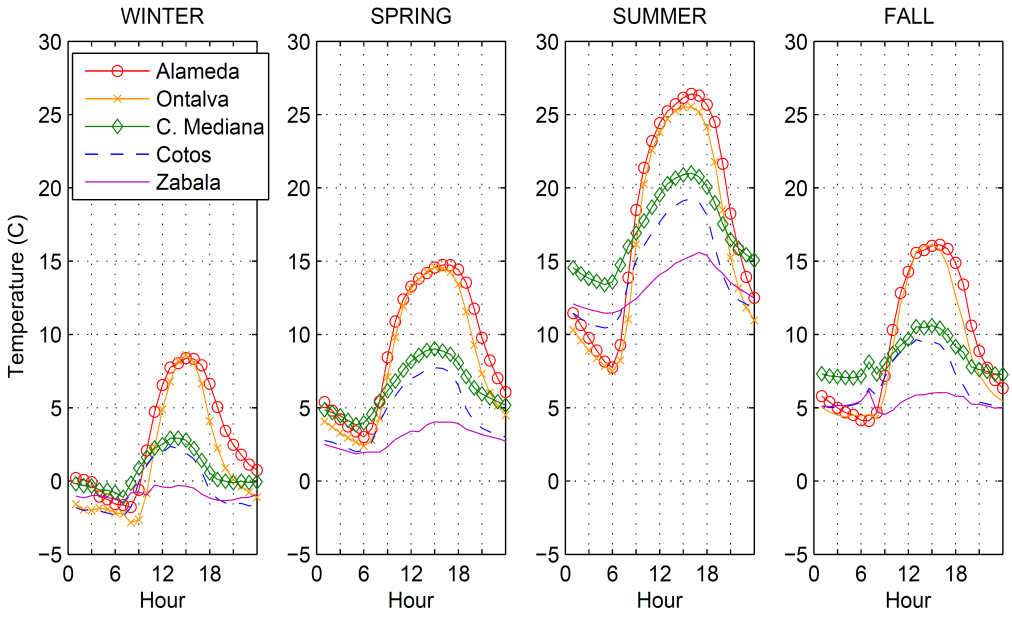

Figure 4.3: Mean hourly temperature for every hour, site and season. Difference between maximum and minimum can be taken as the mean temperature amplitude.

Figure 4.4 shows the correlation between the hourly air temperatures for all the sites and for their common period. As expected the correlation is high since the sites are relatively close. Higher correlations are found among the higher altitude sites (Zabala, Cotos and C.Mediana) and the valley bottom sites (Ontalva and Alameda).

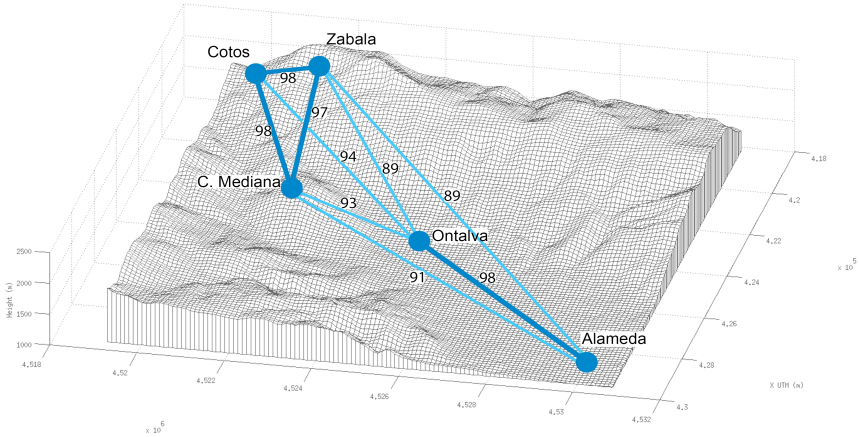

Figure 4.4 Correlation coefficients of air temperature 10 minutes time series between all the sites of the network. Width of the lines is proportional to the Pearson correlation factor value.

One advantage of having such high density of stations highly correlated is that it might be feasible to complete the data gaps of one site out of the observations from the others. Figure shows an example of such simple data completion procedure calculating a temperature lapse rate between Zabala and C.Mediana. This lapse rate is then used to calculate air maximum, minimum and average temperature at Cotos. Figure 4.5.a shows the scatter plots of calculated versus observed temperature using this simple lapse rate method. Figure 4.5.b shows the root mean square error (RMSE) between these two data series. It is shown how this method gives higher RMSE for summer and lower values for the rest of the year inviting for a more sophisticated method. Whether or not these errors are acceptable for future users of this data base depends on the application since there are other more sophisticated methods to do this (Henn et al., 2013).

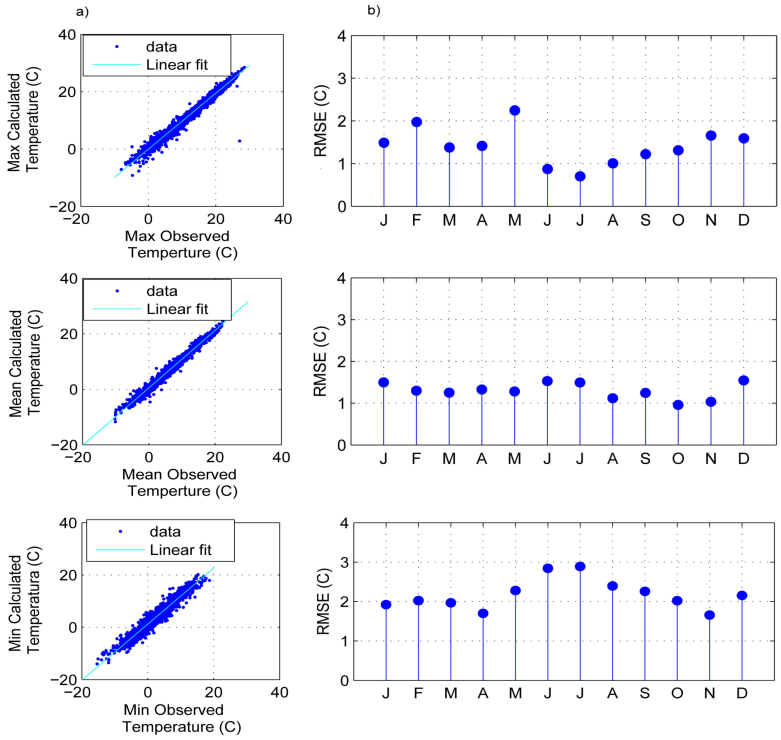

Figure 4.5 (a) Scatter plot of observed and calculated t*ime series of daily* maximum (up), average (center) and minimum (bottom) *temperatures* at Cotos site (b) Monthly RMSE of the calculated maximum (up), average (center) and minimum (bottom) *temperatures.*

A similar discussion could be followed by relative humidity measurements, since both variables are close related and measured by very close sensors.

Regarding total radiation, this variable shows relatively small interferences if micro-sitting of the sensor is properly done avoiding shades. The situation changes dramatically in winter when snow or

rime deposits over non-heated pyrometers. Under this situation, measured radiation will be much less than real, and it will be difficult to detect during the QA/AC process.

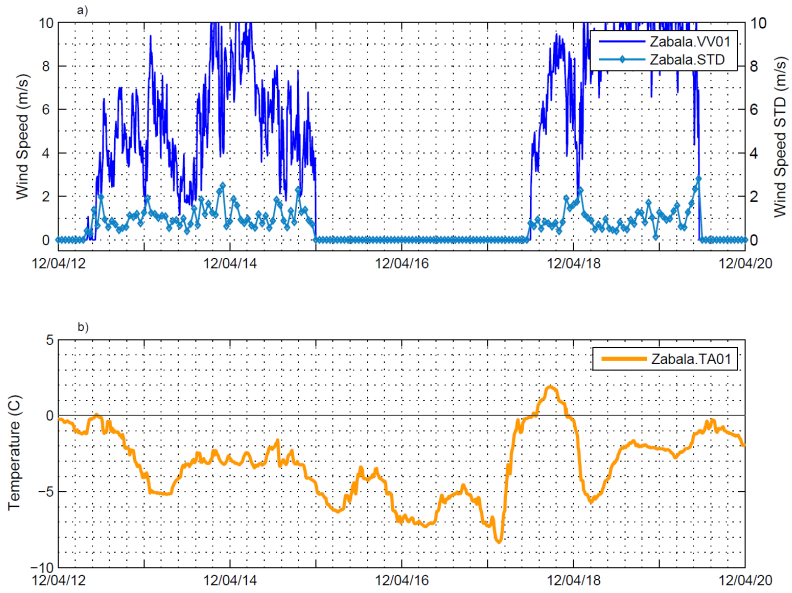

Figure 4.6.(a) Wind speed (Zabala.VV01) and standard deviation of wind speed (Zabala.STD) at Zabala site during a period affected by freezing rime. (b) Air temperature (Zabala.TA01) at Zabala during the same period.

For wind speed and wind direction, mechanically driven sensors have been chosen. In the last years cup anemometers and wind vanes have been substituted by four blade helicoid propeller wind and direction sensors which has shown to be more reliable and robust. Both kind of sensors are susceptible of being blocked and broken frequently by rime acting together with high winds (Makkonen et al., 2001; Fortin et al., 2005). Figure 4.6.a shows the wind speed measured at Zabala during some days in winter as long with the standard deviation in the same period. This is just an example of the effect of rime on anemometers. Supercooled water

freezes immediately when touching the anemometer that finally looses its mobility after a certain time. This process occurs under freezing conditions and can last for some days, Figure 4.6.b. When temperature rises, ice melts and very often the anemometer recovers functionality. Often, an asymmetrical melting process on the rotor of the anemometer can cause it to break and loose functionality. Since this is a winter phenomena, substitution of sensor delays in time waiting for safe conditions for the maintenance crew, increasing the data gaps considerably.

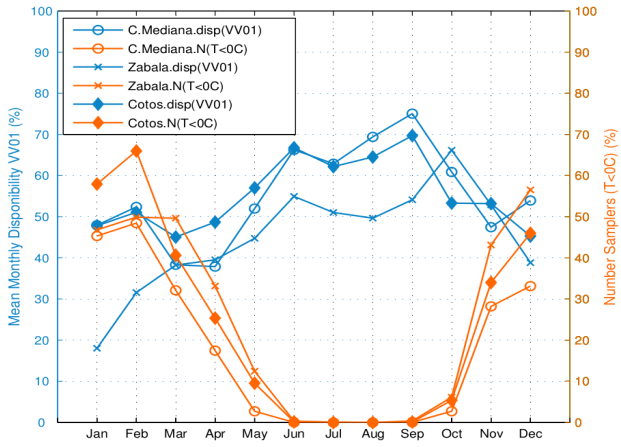

Figure 4.7.Data completeness (blue) for three stations of RMPNP and relation of samples taken under freezing conditions (orange)

Figure 4.7 shows completeness of wind data for some sites at different height and for all seasons. Also number of wind measurements taken under freezing conditions is shown. This graph shows the strong relationships between both variables and how higher elevation sites are more susceptible to this kind of phenomena. Figure 4.8 reinforces this showing the percentage of valid data and gaps produced either by a general failure of the

powering system, effect of rime and sensor breakage. It seems clear how it is still difficult to have good data coverage in winter and at high elevation sites without heated sensors.

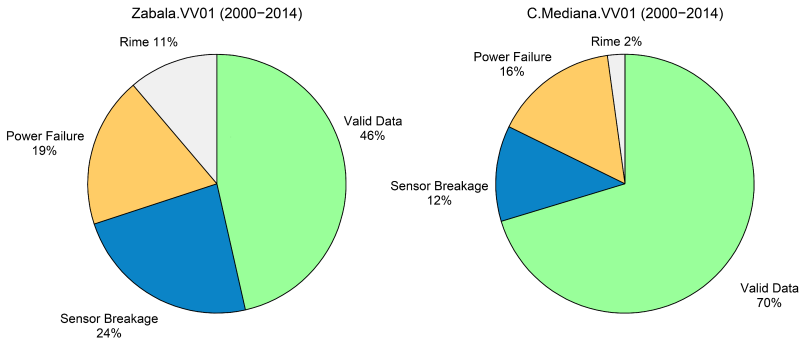

Figure 4.8 Percentage of factors that lead to wind speed data loss (rime, power failure and sensor breakage) and total valid data at Zabala and Cabeza Mediana sites.

Besides the complexity of measuring wind under these conditions, and taking into account that the loss of data is causing a bias that would need further evaluation, a first assessment of wind at this area of Guadarrama can be obtained using C.Mediana site which showed 70% of completeness for more than a decade. For illustrating purposes the seasonal wind distribution has been calculated (Figure 4.9.a) and the wind roses for this excellent wind monitoring site (Figure 4.9.b).

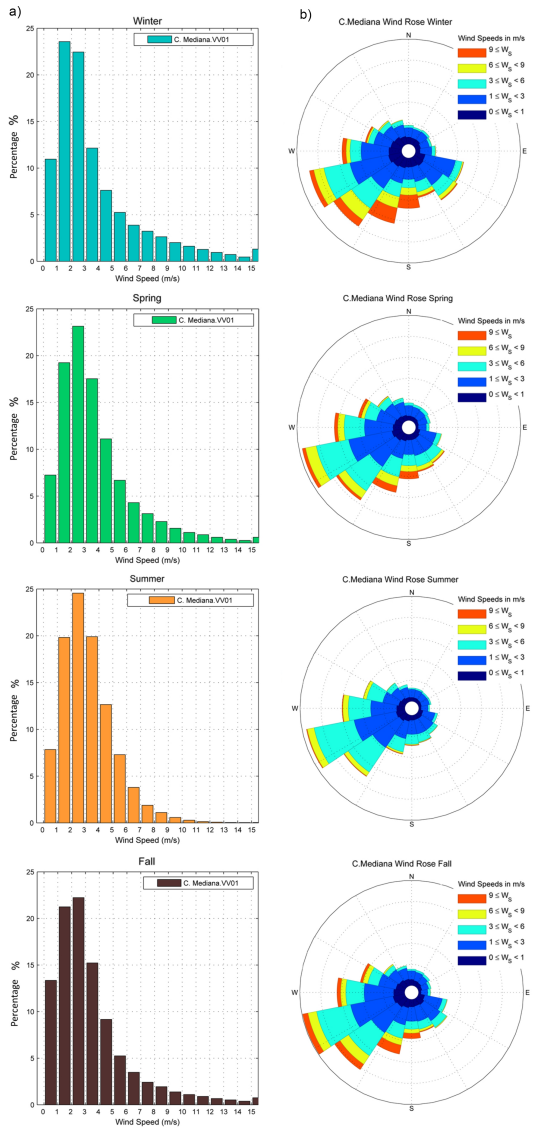

Figure 4.9.(a) Seasonal wind velocity distribution at Cabeza Mediana for the period 1999-2014. (b) Seasonal wind rose at Cabeza Mediana for the same period.

Regarding precipitation, this magnitude has shown to be extremely difficult to measure at these mountains. Under the absence of wind, rain gauges perform fairly well since precipitation falls down vertically and is collected by the effective area of the collector. But in real field conditions the catching process is less efficient and depends on other factors, mainly on wind speed and precipitation rate. Even neglecting other sources of errors, only the influence of wind at the upper part of the rain gauge can be responsible of more than 15% losses in the case of rain and of 30% for snow, depending on wind speed and precipitation rate (Goodison et al., 1989; Groisman and Legates, 1994; Sevruk, 1996; Sieck et al., 2007; Paulat et al., 2008; Cheval et al., 2011). Thus, it is generally accepted that rain gauges tend to underestimate no matter the measuring principle.

Besides the loss of precipitation due to the aerodynamic effect of wind, the non-heated rain-gauge used at RMPNP have been blocked with snow during many winter, fall and spring precipitation events. When temperatures rise, the blocking snow at the funnel melts and spurious precipitation is recorded at the tipping-bucket under clear sky. This double effect of erroneous precipitation measurement is shown in Figure 4.10.a where manual observations made at Cotos using a Hellman manual rain gauge combined with the automatic measurements made possible to make an deep analysis of this effect. During the 27th and 28th of October snow precipitation is collected manually. During these days nothing is detected by the tipping bucket rain gauge, which is collapsed with the snow. The 2nd of March, the sky is clear as shown by the radiation sensor, and temperature rises above zero degrees (Figure 4.10.b). Snow starts to melt during the central hours of the day giving precipitation at a very constant and artificial rate (Figure 4.10.b). This process is confirmed by the snow depth sensor

installed at the same site (Figure 12.a). Normally the total amount of this spurious rain is very similar for other episodes and it stops at night, when temperatures go again below zero. This pattern is repeated with every snow storm, so proper validation algorithms can be programmed to filter them out.

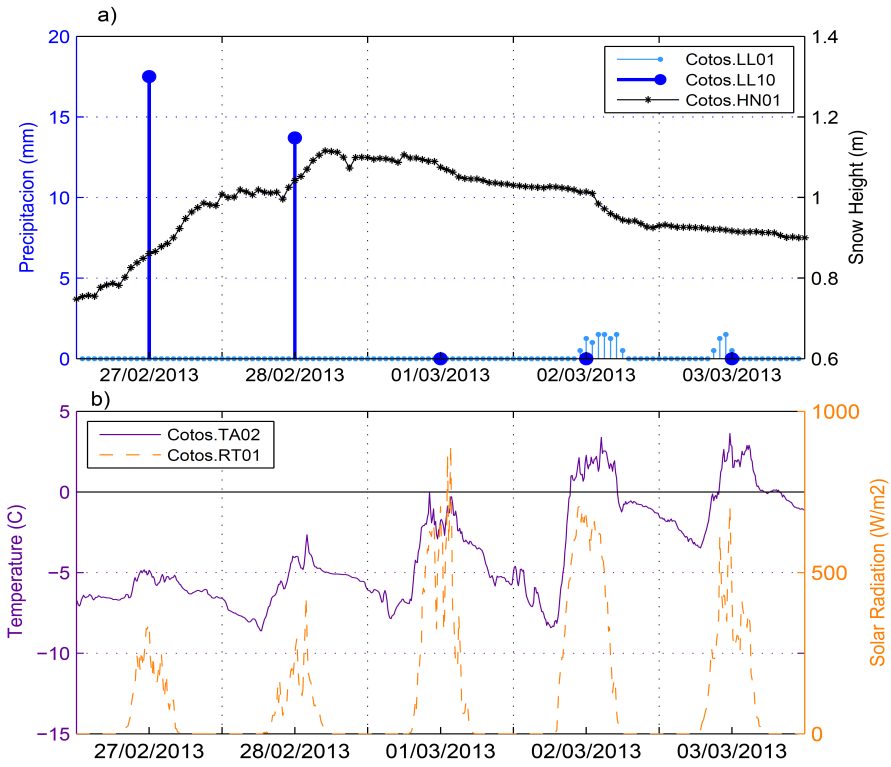

Figure 4.10.(a) Precipitation observed using both a manual (Cotos.LL10) and a non-heated tipping bucket (Cotos.LL01) rain gauge, and the snow height (HN01) in Cotos site for the same period. (b) Air temperature (Cotos.TA02) and solar radiation (Cotos.RT01) observed at Cotos site.

At Guadarrama, most of the precipitation that falls along the year except for summer and some months in spring and fall is snow (Durán et al., 2013). Figure 4.11.b shows a scatter plot of days with precipitation below 1 mm (orange) and days with snow (light blue) and rain (dark blue) precipitation over 1 mm and mean daily relative humidity and mean air temperature observed at Cotos using a manual rain-gauge and an automatic station. First it can be seen how precipitation occurs normally with mean daily relative humidity values higher than 80% (Figure 4.11.c). This result can be used with higher refinements to build a precipitation algorithm for precipitation validation. The refinement could be done discriminating between seasons and hour, since relative humidity follows a clear daily cycle. Precipitation events with low mean relative humidity correspond to days with convective storm activity with a sudden and isolated increase of relative humidity for some hours. This opens again many possibilities for using relative humidity of an excellent variable for precipitation data validation. This graphs also shows how snow, as expected, occurs mainly under freezing conditions, but again some exceptions are found and probably attributable to a cooling process due to evaporation of the snow flakes on their falling down (Figure 4.11.a).

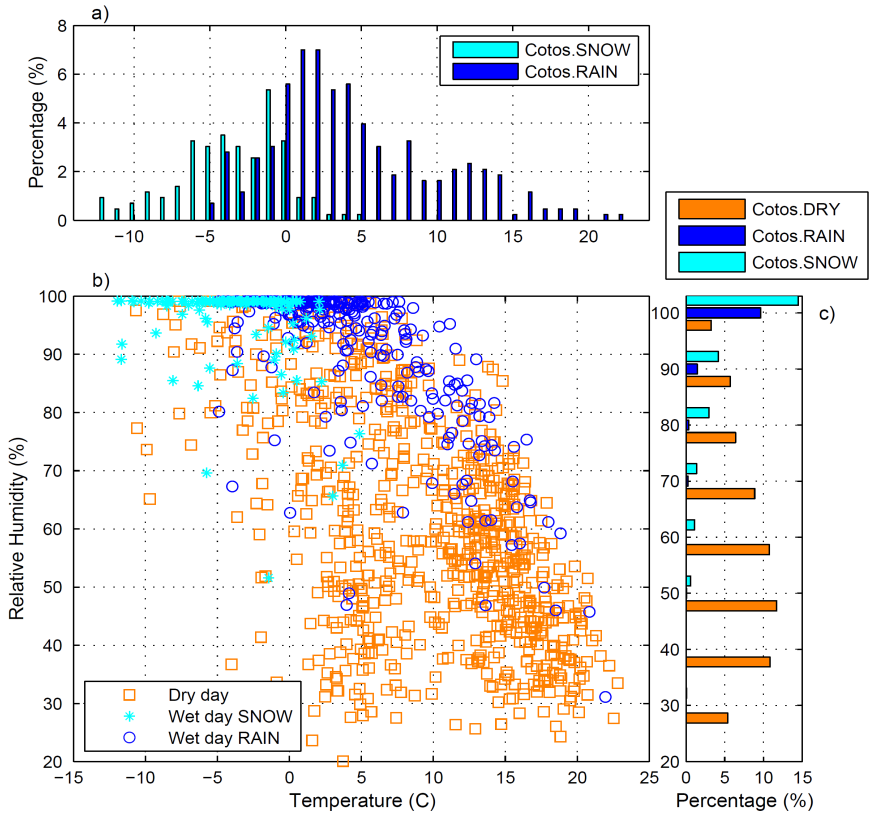

Figure 4.11.((a) Bar plot of rain (Cotos.RAIN) and snow (Cotos.SNOW) observed using a manual rain gauge at Cotos for different values of daily mean air temperature. (b) Scatter plot of daily relative humidity against daily temperature for days with precipitation under 1 mm (squares), days with snow precipitation above than 1 mm (asterisks) and days with rain precipitation above 1 mm (circles) at Cotos. (c) Bar plot of percentage of days with precipitation under 1mm (Cotos.DRY), days with snow precipitation (Cotos.SNOW) and days with rain precipitation (Cotos.RAIN) above 1 mm and mean daily relative humidity.

In an attempt to evaluate the impact of using non-heated tipping-bucket rain gauges for measuring precipitation at Guadarrama a comparison between manual and automatic methods used at Cotos has been performed. Figure 4.12 shows the relationship found

between the monthly differences between the two methods and the number of hours per month with saturating conditions (relative humidity over 80%), and near freezing temperatures (air temperature under 5ºC), as an estimator of potential snowy hours. A significant linear relationship between the automatic sensor underestimation and number of hours potentially having snow precipitation have been found. This relationship could be used to estimate the amount of underestimated precipitation at other close locations that use the same rain-gauge or for QA/QC.

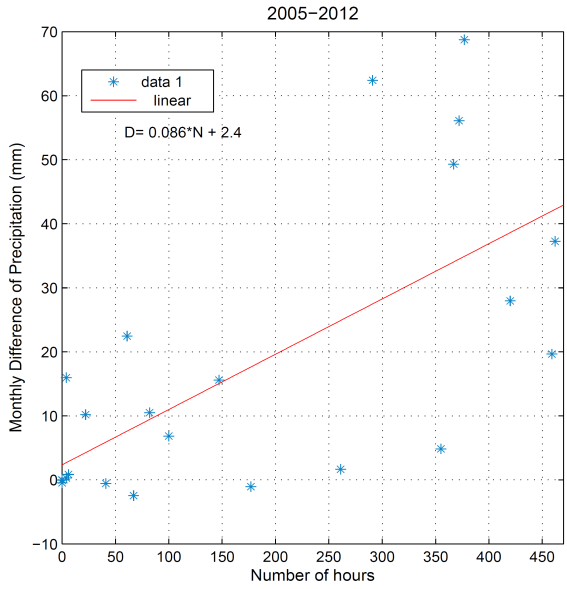

Figure 4.12. Relationship found between the monthly precipitation differences between a manual and a non-heated tipping bucket rain gauge and the number of hours per month with relative humidity over 80% and air temperature below 5ºC (snow precipitation conditions).

Figure 4.13 shows the mean zero isotherm calculated from the common period of sites. It shows how during many of the winter and some fall and spring months most of the sites, except Ontalva and Alameda, have average freezing temperatures. This concludes that this underestimation is potentially occurring at most of the observatories and that observations should be used with precaution.

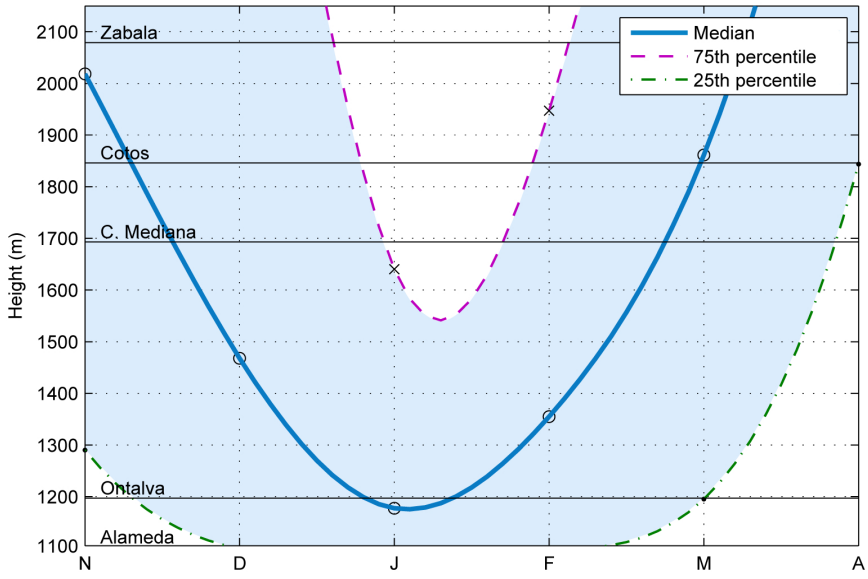

Figure 4.13. Median, 75th percentile and 25th percentile of elevations of the zero isotherm for winter months calculated out of the temperatures observed at all sites.

Figure 4.14 shows an estimation of the climograms at every site and for the available period. Due to the limitations on observing precipitation at this area, monthly totals at these sites using a high resolution precipitation model (Sec. 4.4) are shown here.

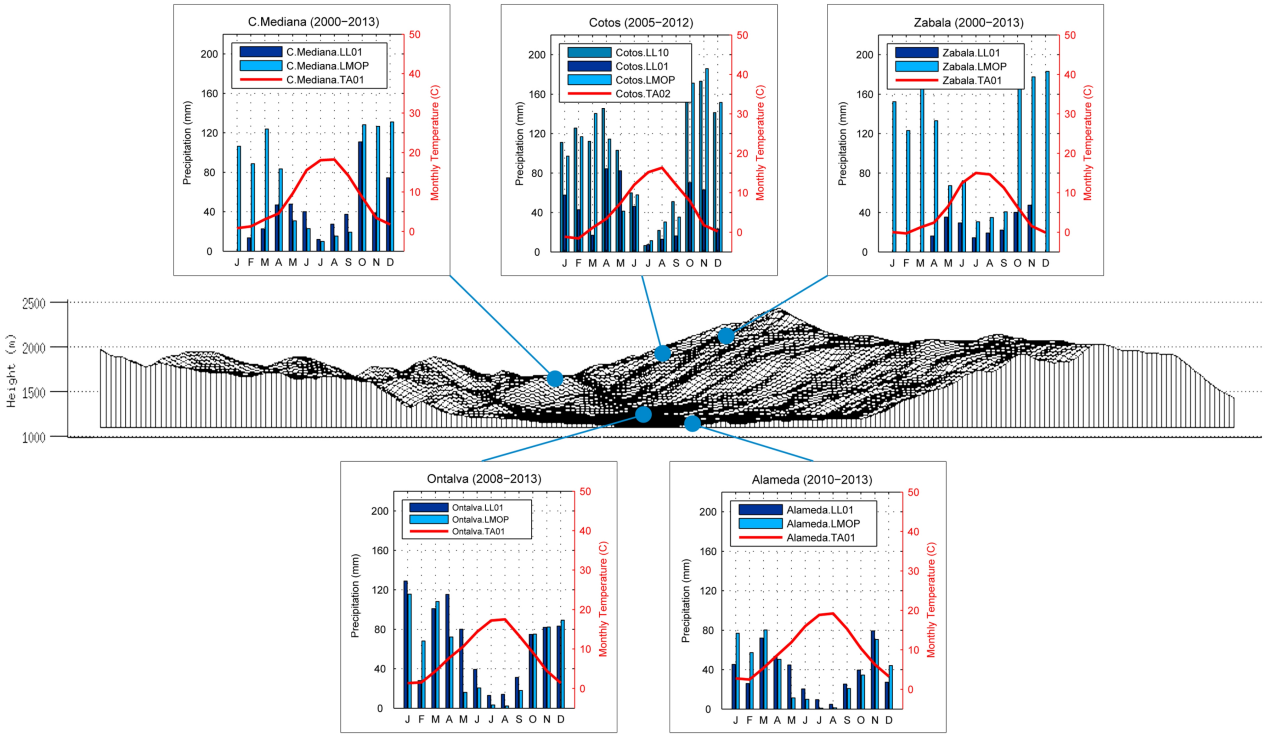

Figure 4.14. Mean monthly temperature (TA01, TA02) and precipitation observed (LL01, LL10) and modeled (LMOP) at all sites.

Snow fall over Valle de la Umbría as seen from Las Suertes, Rascafría.

4.2 Climatology of Precipitation at Guadarrama[4]

4.2.1. Main Climatic Characteristics of Precipitation at Guadarrama

An Alexandersson homogeneity test (Alexandersson, 1986) has been performed using Madrid (Retiro) observatory as the reference station, since this observatory has been shown to be homogeneous (Gonzalez-Rouco et al., 2001). Figure 4.15 shows the T value of the

[4] *This chapter follows closely the publication: Durán L., E. Sánchez and C. Yagüe (2013). "Climatology of precipitation over the Iberian Central System mountain range". Int. J. Climatol., 33, 2260–2273. DOI: 10.1002/joc.3602 © 2012 Royal Meteorological Society*

t-test obtained for the rest of the observatories. As the critical value for rejecting the null hypothesis that the series are homogeneous at a 5% confidence level for 22 samples is 7, then it can be concluded that the series are homogeneous.

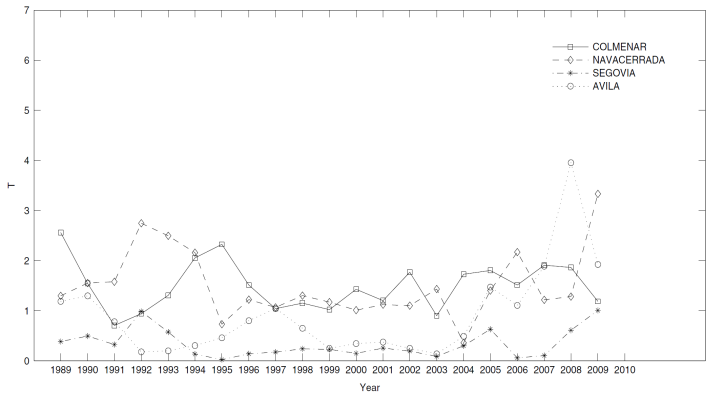

Figure 4.15. Values of T of an Alexandersson test for Colmenar Viejo (C), Navacerrada (N), Segovia (S) and Avila (A) using Madrid (M) as reference station. The critical Tvalue for 5% confidence level and 22 samples is 7.

In Table 4.4, the main statistics for the whole period (1989-2010) are shown. As expected, the mean precipitation is much higher over the mountainous station (*N*), with 1229 mm yr^{-1}, meanwhile, both sides show values smaller than 600 mm yr^{-1}. Mountainous station also exhibits larger spread from year to year (300 mm yr^{-1}), in comparison with the plateau ones (less than 150 mm yr^{-1}).

Table 4.4.Basic annual statistics per observatory.

	Madrid	*Colmenar*	*Navacerrada*	*Segovia*	*Avila*
Mean (mm)	*427*	*567*	*1229*	*479*	*418*
Median (mm)	*435*	*535*	*1160*	*451*	*401*
Standard deviation (mm)	*96*	*158*	*301*	*102*	*108*
Maximum (mm)	*573*	*859*	*2011*	*812*	*679*
Minimum (mm)	*252*	*354*	*806*	*352*	*243*

Table 4.5 also shows the percentage for each of the seasons, with around a 30% for spring, winter and autumn, meanwhile summer only gives around 10% of the total annual amount. It is remarkable how Avila and Segovia show higher summer values than the rest.

Table 4.5. Percentage of total precipitation per season and for Segovia (S), Navacerrada (N) and Colmenar Viejo (C) for the whole period.

	S	*N*	*C*
WINTER (DJF)	*24 %*	*31 %*	*30 %*
SPRING (MAM)	*29 %*	*27 %*	*26 %*
SUMMER (JJA)	*17 %*	*9 %*	*9 %*
FALL (SON)	*30 %*	*33 %*	*34 %*

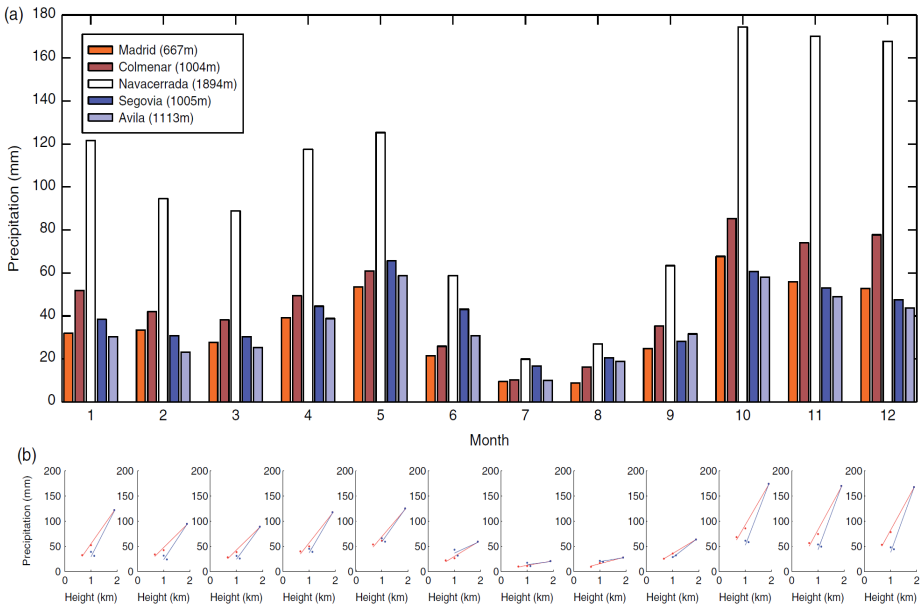

Figure 4.16. (a) Mean monthly precipitation at the observatories for period 1989–2010. (b) Mean monthly precipitation altitude gradients for south side of range (red) and north side of range (blue). Navacerrada observatory is shared for both sides calculation.

Figure 4.16 shows the climatic annual cycle of precipitation at the five observatories. Precipitation at site *N* is always considerable higher than the other stations, as expected due to elevation, with an important percentage of solid precipitation (Figure 4.17). It is important to mention how precipitation shows a very marked decrease from June to September for all observatories. This behavior is characteristic of the Mediterranean climates that dominate most of the IP. Here it is shown how Guadarrama alpine climate seems also to be influenced by such annual precipitation cycle, resulting in a larger decrease of precipitation during summer than other Alpine-like regions (Frei and Schär, 1998). This marked difference between summer and the rest of the year might be

caused by the decrease of the advection of humidity from the ocean due to synoptic disturbances. Along with this, convective systems might be less frequent compared with other mountain ranges, probably due to the lack of local sources of humidity at the northern and southern plateau. It is also remarkable how this summer minimum starts later in the northern side observatories A and *S*, which show higher precipitation in June.

Maximum precipitation is found in spring in northern side and in fall in southern side. It is also shown how precipitation during summer months is closer at all sites, which might indicate a possible decrease in the role of orography in the production or enhancement of precipitation during this season, probably due to the convective origin of precipitation during these months. Regarding *N* site, precipitation is always considerably higher than others, with a shorter summer drought which extends only from July to August. Precipitation at *N* seems to be the result of the phenomena that affects both sides of the range along with its own orographic processes.

Figure 4.16(b) shows the vertical linear precipitation gradient calculated for every month and for southern and northern side of the range (*N* observatory is shared for both sides calculation). These gradients would be useful for calculating a simple monthly precipitation atlas of the region using a digital elevation model (Daly et al., 1994). Here it is calculated just to show differences between southern and northern side, and the special behavior of June.

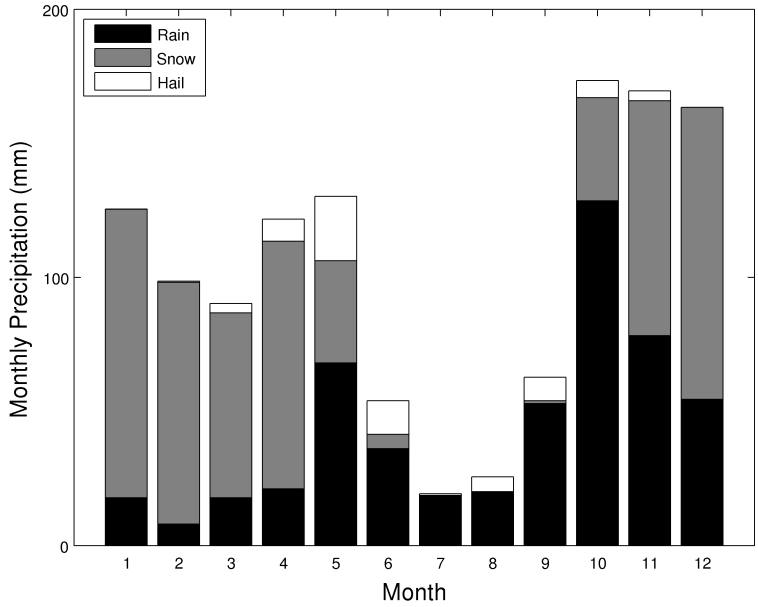

Figure 4.17. Monthly mean precipitation at Navacerrada (N) for the period 1989-2010. Rain, snow and hail precipitation is also shown.

Figure 4.18 shows the time series anomalies, related to the annual climatology, at each of the five observatories, calculated as the annual mean precipitation minus the whole period mean divided by the standard deviation for the whole period. It is shown how precipitation in Gudarrama shows the well-known 1990s persistent dry anomaly and the shift in 1996 that affected the whole Peninsula. This feature has been documented in previous works in relation with changes in the tropical North Atlantic Sea Surface Temperature (Rodríguez-Fonseca and Castro, 2002; Rodríguez-Fonseca et al., 2006; Losada et al., 2007). It is important to mention that larger anomalies at each observatory are reached at different years, indicating again how large-scale phenomena have different impact on precipitation at each side and top of mountain.

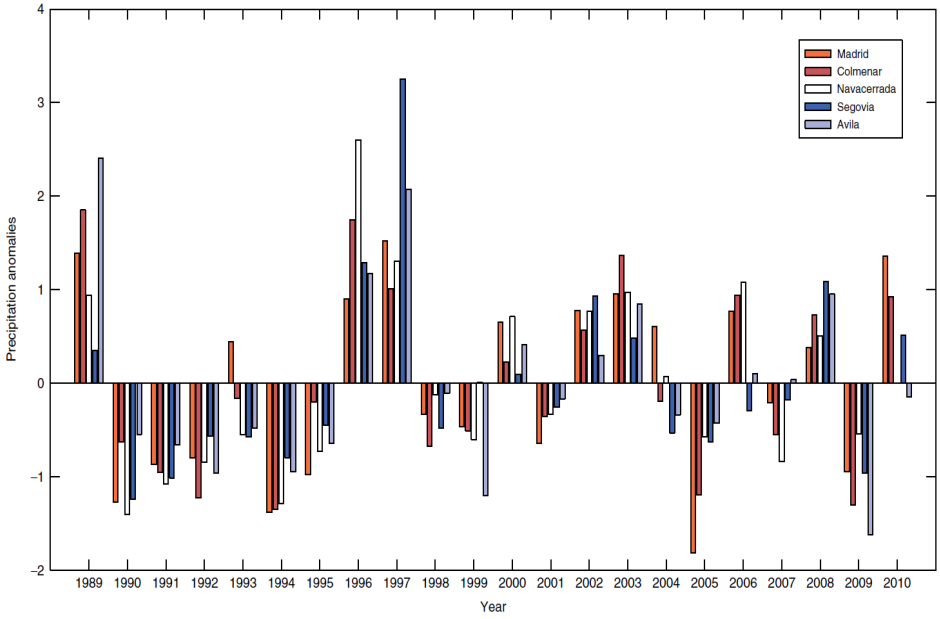

Figure 4.18. Annual standardized precipitation anomalies for the observatories. Anomalies are calculated by subtracting the annual mean to every year total precipitation and then divided by standard deviation for the period 1989–2010.

Table 4.6 shows the results of a t-test on the monthly averages of all possible combinations of pairs of observatories. If marked, the sample means belong to different populations with a 5% significance level. It is shown how during most of the year, mean precipitation at N is significantly different compared to any of the other stations. However, all non-mountainous observatories show equal means except for some months: June, August and February. Important to mention is how Madrid and Colmenar show significant equal means for all year round. The same happens between Avila and Segovia. This fact is used to simplify the analysis to observatories S, N and C. S would be representative of

the northern side of Guadarrama, N representative of the mountain range and C representative of the southern side.

Table 4.6. Results of a t-test on the monthly averages. If marked, it means that the two mean values come from distributions of different means at the 5% significance level.

Sites/Month	*1*	*2*	*3*	*4*	*5*	*6*	*7*	*8*	*9*	*10*	*11*	*12*
S-N	*X*	*X*	*X*	*X*	*X*				*X*	*X*	*X*	*X*
C-N	*X*	*X*	*X*	*X*	*X*	*X*	*X*		*X*	*X*	*X*	*X*
S-C						*X*						

In such complex orography, density of stations would not be enough to perform a spatial interpolation as done by other authors (Daly et al., 1994; Frei and Schär, 1998; Kyriakidis et al., 2001; Marquínez et al., 2003; Guan et al., 2005). Nevertheless, in order to have an idea of the spatial extent of the rain episodes, eight different spatial precipitation sizes are defined using precipitation from S, N and C; considering all the possible combinations of wet and dry days at each observatory (wet day is defined as a day with a precipitation higher than 0.1 mm d^{-1}). Classes are shown in Table 4.7. Each of these classes represent the minimum known size of the rain event. For example, a day classified as '*SNC*' would mean that rain was observed that day at the three observatories: S, N and C. Not much is known about the exact precipitation field, but at least it is sure that daily rain field has a minimum size equal to the distance from S to C.

Table 4.7. Definition of spatial precipitation patterns according to the observatories that record simultaneously daily precipitation

Pattern	*Rain at S*	*Rain at N*	*Rain at C*
SNC	*YES*	*YES*	*YES*
SNo	*YES*	*YES*	*NO*
oNC	*NO*	*YES*	*YES*
oNo	*NO*	*YES*	*NO*
Soo	*YES*	*NO*	*NO*
ooC	*NO*	*NO*	*YES*
SoC	*YES*	*NO*	*YES*
ooo	*NO*	*NO*	*NO*

Results using this classification are shown in Figure 4.19 for each season. Around half of the days during winter, spring and fall are wet days (rain at least at one of the three sites: all patterns but '*ooo*') in Guadarrama. Of these wet days, only half of them, rain falls simultaneously at the three sites (*SNC*). The rest of wet days, rain falls at only two sites or one site. When rain falls at only two sites, these sites are adjacent. Except in summer, with just 37% of occurrence, broad rain pattern (*SNC*) becomes the most frequent pattern being around 50% of all the wet days. The second most frequent pattern, except in summer, is rain only at the top of the mountain and at northern side of the range ('*SNo*'), followed very closely in frequency by rain only on the top of the mountain ('*oNo*'), with an almost constant frequency all the year round. North side and top pattern ('*SNo*') is more frequent than South side and top pattern ('*oNC*'). Considering that monthly rain means (Figure 4.18) are higher during winter, half spring and fall in the southern side, rain episodes are less frequent in the South side but with higher amounts. Rain at only one side of the range ('*Soo*' or

'*ooC*') is very infrequent, except in summer. These wet days, without rain on the top of the mountain, might be associated to local convective storms, that can be related to temperature changes associated to mountain conditions. Frequency of rain at both sides of the mountain but with no rain on the top ('*SoC*'), is almost negligible, confirming the consistency of this simple classification. This pattern classification is also dependent on the direction of the fronts that arrive to Guadarrama, as it will be shown on the next section.

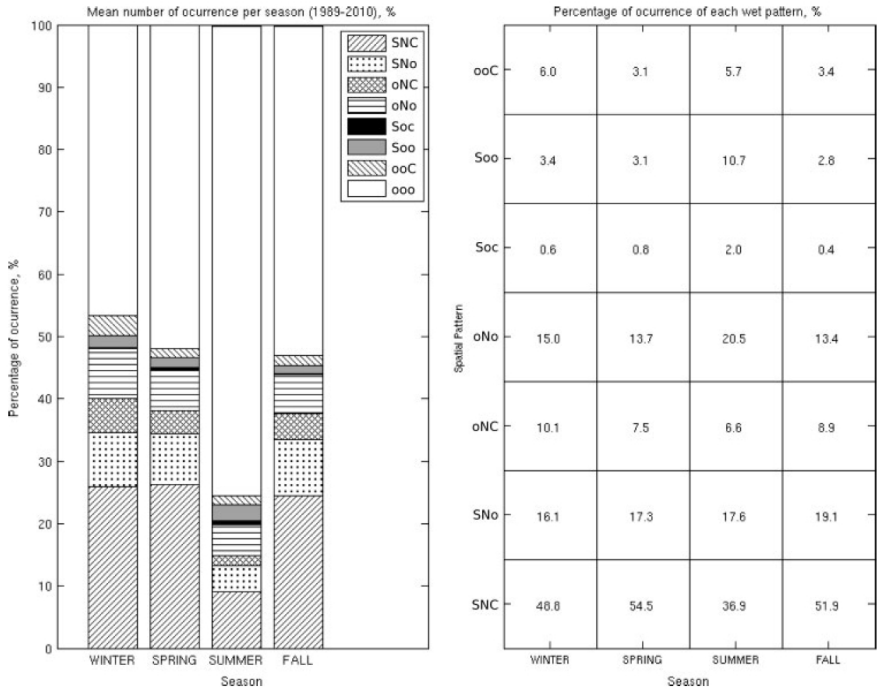

Figure 4.19. Spatial precipitation patterns frequencies (left) and spatial precipitation patterns frequencies for wet days (right).

4.2.2 Relationship Between Precipitation and Humid air Masses Reaching Guadarrama.

Precipitation is the result of a set of conditions in the atmosphere that lead the water vapor to condense and form droplets (clouds) that eventually reach the ground. Sometimes these conditions are reached in a very short time and space, like thermally induced storms, but others, these conditions depend in the state of a very large portion of the atmosphere with an origin of hundreds of kilometers away from where precipitation takes place.

Advection of humid air masses over continents is an essential source of precipitation at extratropical latitudes. One way to analyze advection of humid air masses consists is to study the flux of water vapor in the atmosphere (Rasmuson, 1968). Specific humidity and wind velocity integrated from surface to 200 hPa levels have been used to calculate horizontal total column water vapor flux (TCWVF) using Eq. (3.1), Eq. (3.2) and Eq. (3.3).

Figure 4.20 shows the Pearson linear correlation coefficients between the monthly precipitation anomalies at the three observatories and monthly TCWVF anomalies for each grid point in order to analyze the relationships between moisture advection and precipitation at Guadarrama. Not significant correlations are neglected after applying a t-test with 95% confidence level and monthly anomalies of TCWVF at every grid point and precipitation anomalies at the observatories have been calculated. Anomalies are computed subtracting to the monthly value at each particular year, the climatological monthly mean, dividing the result by the climatological standard deviation (These are known as standardized anomalies). It is noticeable the great correlation found between TCWVF and precipitation anomalies at the three

observatories for all year around except summer. Correlation maps for *N* show positive values during most of the year, indicating that an anomalous higher flux of water vapor into IP is connected to a anomalous increase of precipitation. Maxima is located in the sourthern part of IP, this only indicates that the anomalies of TCWVF at that grid point are highly correlated with precipitation anomalies. This means that it would be a good predictor, but does not give any physical cause-effect connection. These anomalies might be associated with the main teleconnection pattern affecting IP, like NAO and others (Rodriguez-Puebla et al., 1998; Serrano et al., 1999; Goodess and Jones, 2002; Rodriguez-Fonseca and Serrano, 2002; Muñoz-Díaz and Rodrigo, 2004; Trigo et al., 2004; Gallego et al., 2005). Southern observatory behaves slightly different. Here, correlation maps are shifted to the south and a dipole pattern shows for in Febreuary, July and October. These dipole patterns are formed when a band shape flux is shifted to the south parallel to its initial trajectory, leaving northern part with a deficit in relation with climatology and an increase in the the southern part. Mountain observatory, *N*, shares behavior with *C* at the beginning of summer of winter but does it with *S* for the end of summer. All these results confirm the important Atlantic forcing affecting precipitation at Guadarrama. TCWVF seem to be reaching the IP with a great variety of shapes leading to a complex flow as a result of the synoptic configuration.

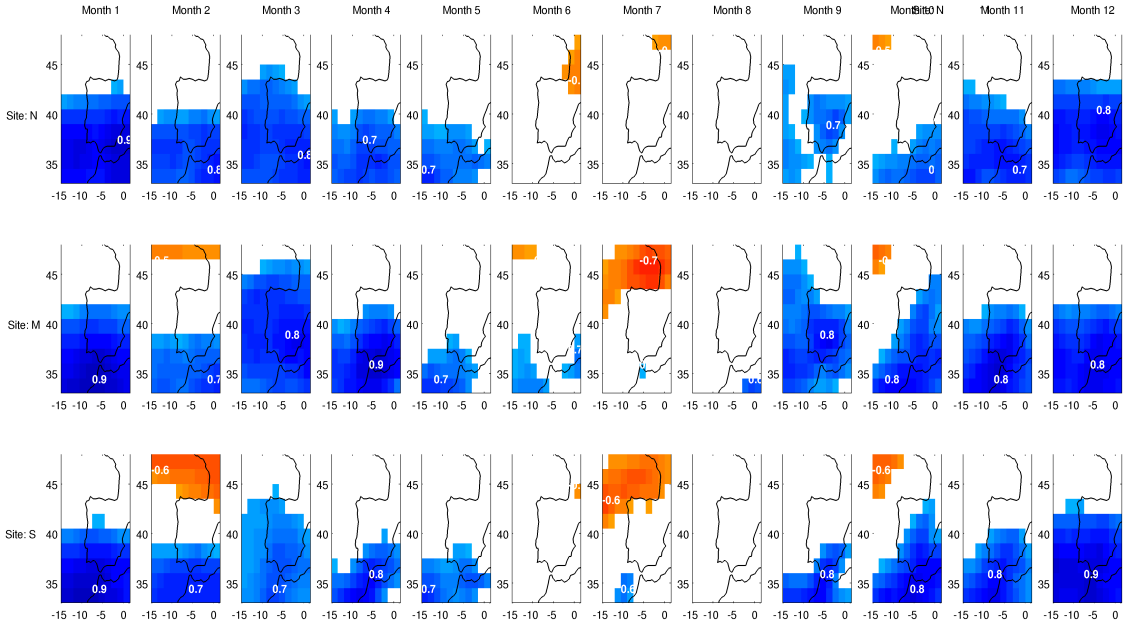

Figure 4.20. Pearson correlation coefficient maps between monthly TCWVF anomalies at each grid point and monthly precipitation anomalies at northern side obseratory (a), mountain top (b) and southern side observatory (S). Only significant correlations are shown.

4.2.3 Average Atmospheric Conditions of the Air Masses that Lead to Precipitation at Guadarrama

An added value of having the reanalysis data is that it is possible to analyze the mean conditions of the advected air masses before they reach the mountain range and before orographic precipitation processes occur. In order to understand the conditions of these masses the following variables are analyzed upwind the mountain range: TCWVF, surface temperature, relative humidity at 950 hPa

and wind speed and direction sector. The level of 950 hPa has been chosen since it is the average pressure level of the plateau.

Figure 4.21 shows box plot diagrams for relative humidity at 950 hPa (the rest of plot diagrams are not shown). Left box corresponds to wet days and right box to dry days. From this figure seems easy to infer that the two populations (wet and dry events) are significantly different, since the notches do not overlap. Similar results are obtained for the rest of variables such relative humidity at low levels, surface temperature and wind (not shown).

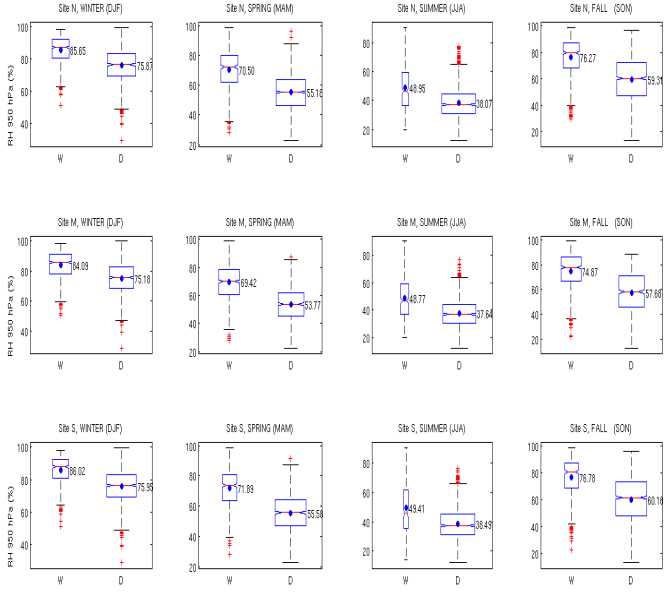

Figure 4.21. Box plot of relative humidity at 950 hPa and precipitation for all sites and seasons.

Table 4.8 summarizes the results obtained for every site and season. This table summarizes the mean conditions of the main variables found in the air masses that reach Guadarrama and lead to precipitation (for wet days). As expected, precipitation seems to be very related with advection of air masses transporting moisture from the Atlantic as seen in the significant different values of TCWVF for wet and dry days. This points out orographic precipitation as the main phenomena in Guadarrama precipitation. This is confirmed by the differences found in the relative humidity of air advecting at 950 hPa for wet and dry days, specially during fall. Relative humidity is a very sensitive variable for orographic precipitation models, specially for low TCWVF (Barstad et al., 2007). Relating wind direction, it is remarkable how the main sector for wet days at site S is always west except in summer. On the other hand, main wind sector for wet days at C is always southwest. The simplicity of this classification scheme makes robust the idea of precipitation at Guadarrama being highly dependent on wind direction at medium levels of the troposphere.

Table 4.8. Significant medians of ERA-Interim variables closely related to orographic precipitation for wet (W) and dry (D) days at the three observatories.

Season	Site	Kind	Upwind TCWVF ($kg\ m^{-1}\ s^{-1}$)	Upwind Surface Temperature (^oC)	Upwind Relative Humidity at 950hPa (%)	Wind Sector and speed at 850 hPa ($m\ s^{-1}$)
WINTER	S	W	165	6	86	W (6.16)
		D	69	5	76	N (1.1)
	N	W	152	6	84	W (4.9)
		D	60	5	75	N (1.26)
	C	W	165	6	86	SW (6.0)
		D	71	5	76	W(1.6)
SPRING	S	W	141	11	71	W (4.15)
		D	78	12	55	SW (0.7)
	N	W	135	11	69	W (3.74)
		D	73	13	54	N (0.8)
	C	W	144	11	72	SW (4.14)
		D	80	13	56	NW (1.1)
SUMMER	S	W	143	21	49	SW (2.5)
		D	100	24	38	W (1.1)
	N	W	139	21	49	SW(2.3)
		D	100	24	38	W(1.2)
	C	W	142	21	49	SW(2.2)
		D	102	24	38	W(1.3)
FALL	S	W	199	12	76	W (5.7)
		D	95	15	59	NW (0.6)
	N	W	190	12	75	SW (5.0)
		D	87	15	58	N (0.66)
	C	W	206	13	77	SW (5.9)
		D	99	14	60	NW (1.16)

In order to illustrate this directional dependency, Figure 4.22 shows rain-roses for the four seasons and the three sites. Here, wind direction is divided in eight sectors containing three filled sectors representing accumulated precipitation at each observatory. This graphs are useful since they show the relationship between wind direction and seasonal total precipitation. Most of the precipitation

at the three observatories come from 'southwest sector', nevertheless 'west sector' is relevant for S while 'south sector' is relevant for C. Taking into account the axis of Guadarrama massif, a rain shadow effect might be the cause of differences between different sides of the range. Again, it seems like site N shares behavior of both sides and is less wind direction dependent. The mountain range would be drying the air masses that travel from the Atlantic inland, sometimes these air masses have a more west component giving precipitation at the windward side of the mountain, in this case the northern side, and the top of the range; and sometimes with a more south component giving precipitation at the southern side and top.

These results reinforces the need of a combination of tools, modeling and high density measurements, if a reliable assessment of precipitation is wanted for such complex orography. Specific orographic precipitation models are very convenient in these cases since they allow the use of higher spatial resolutions, consideration of more complex precipitation phenomena and longer time domains with many resolution (Barstad et al., 2008). These models are sensitive to boundary conditions and respond differently to changes in wind speed and direction, relative humidity, surface temperature and other variables related with orographic precipitation.

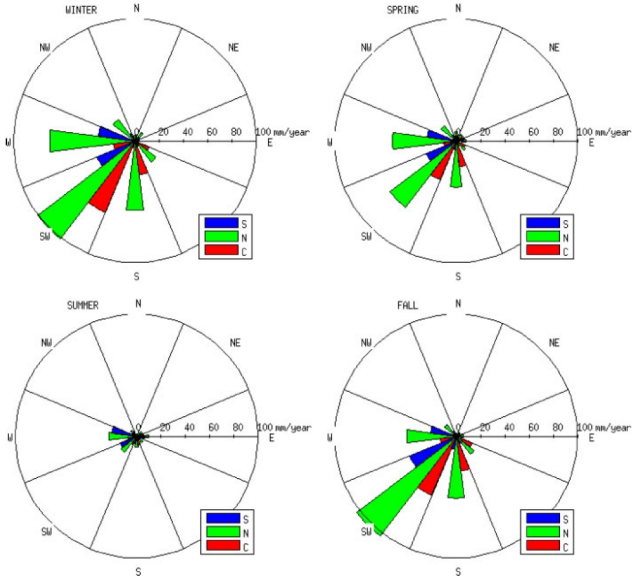

Figure 4.22. Rain-roses for the four seasons. Gray shaded sectors represent seasonally accumulated rain for 850 hPa wind coming from each sector.

Orographic clouds formed along the valley as seen from home.

4.3 Water Vapor Flux Patterns and Precipitation at Guadarrama[5]

Figure 4.23 (bottom panel) shows the climatological fields of the Total Column Water Vapor Flux (TCWVF) for every season and period of study. As expected, a zonal flux from the west is affecting the IP for all seasons and after an EOF analysis of the daily anomalies, three of these EOFs have shown to be accounting for more than 70% of variance and fulfill the North criteria (North et al., 1982) for all seasons. Overall, the flux pattern is significant in

[5] *This section follows the publication: Durán L., Rodríguez-Fonseca, B., Yagüe, C. and Sánchez, E. (2015). "Water vapour flux patterns and precipitation at Sierra de Guadarrama mountain range (Spain)". Int. J. Climatol., 35, 1593-1610. DOI: 10.1002/joc.4079*

all the spatial area, which means that the PCs are significantly correlated with the time series of all points represented.

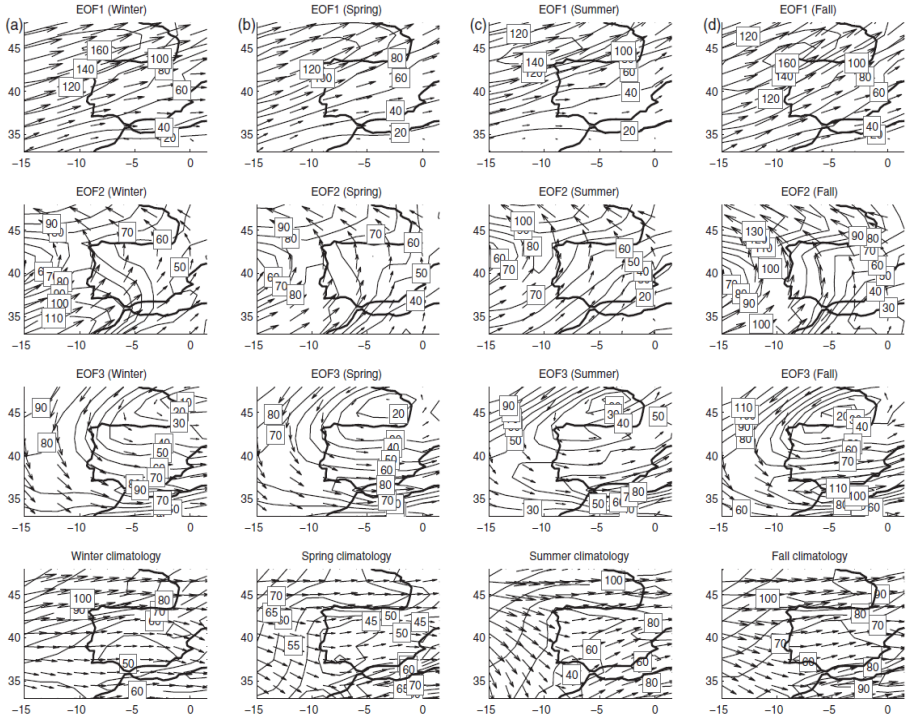

Figure 4.23. First three Empirical Orthogonal Functions of total column water vapor flux (TCWVF) that account for more than 70% of variance during all seasons along with climatology. Arrows represent flux vectors and tags are some values of the magnitude of the vector for a better interpretation. Units: g $cm^{-1}s^{-1}$

The first EOF represents the same flux pattern in the whole region, with a zonal West-East flux of water vapor over the Peninsula. Taking into account that the TCWVF climatology of the Peninsula represents a westerly flow (Figure 4.23, bottom panel), the leading

EOF represents a weakening or an enhancement of the climatology. Regarding EOF2 and EOF3, they represent rotational circulations with centers of actions in the western region (Atlantic) and the northern region. Positive (negative) scores of PC2 will be associated with anomalous cyclonic (anticyclonic) flux of moisture injected from the southwest (northeast). Positive (negative) scores of PC3 will be associated with anomalous anticyclonic (cyclonic) flux of moist injected from the north (Mediterranean).

Then, the PCs daily values have been used to perform a k-means clustering, allowing to establish a single flux pattern for every day. In order to find an equilibrium between not many Water Vapor Flux Patterns (WVFP) and a clear differentiation between wet and dry ones, a number of 7 flux patterns have been chosen according to results obtained applying Eq. 3.5 and analysis of Figure 4.24. Here is evident how significant scores are obtained after 3 clusters, but seven are chosen since the improvement for fall is noticeable.

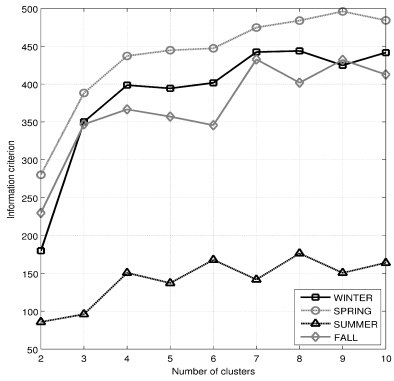

Figure 4.24. Value obtained of the information criterion function used for this study in the determination of optimal number of clusters. Graph shows results for two to ten clusters and for every season.

Figures 4.25 to 4.35 show the seven flux patterns found for all seasons along with an example of a day analysis chart. These figures show the TCWVF vector maps of their corresponding centroids (panel A) along with a shaded map of isolines of the magnitude of the vector with some labels for clearness. Also, composite maps for each flux pattern of MSLP (panel B) and 500hPa geopotential height anomalies (panel *C*) are shown for synoptic interpretation and relation with relevant known teleconnection patterns. The similar structures found for all seasons at surface and at higher levels, in some way, confirm the suitability of keeping the same number of clusters even though some of them will not show the same relevancy among seasons, in terms of contribution to precipitation.

It is remarkable how five of these seven weather types are similar to those found by Santos et al. (2005) for winter, even though the predictant field used here is TCWVF, along with other small

differences in the methodology and the different precipitation data used.

Next sections describe more deeply each WVFP and their relation with observations. Also an analysis chart for some days under wet patterns is also shown.

4.3.1 Cyclonic Flux (CF)

Figure 4.25 shows the spatial structure of the first flux pattern, together with the associated composites of MSLP (panel B) and anomalous 500 hPa geopotential height (panel *C*) for all seasons. The pattern is characterized by westerly fluxes, maximum in the western part of the IP. The associated MSLP pattern presents a minimum of pressure over British Islands and a maximum on northwestern Africa. This MSLP pattern represents, in medium tropospheric levels, an anomalous structure with a minimum north of the IP, indicating a decrease of pressure under this flux. Consequently it has been called Cyclonic Flux (CF) since it seems to be an average of a set of cyclonic systems traveling from the west and passing between the British Isles and the IP. Its structure is very similar to the one obtained for winter by Santos et al. (2005) but with slight differences, like a more southeastern location of the lower MSLP center pressure field (Figure 4.25, panel B) as a consequence of a more eastern location of the observatories and the application of Eq. 3.5. The isolated averaged center of negative anomalies of the geopotential field at 500 hPa (Figure 4.25, panel *C*), reinforces this cyclonic pattern along with a high pressure over Azores as shown in the MSLP composite maps (Figure 4.25, panel B).

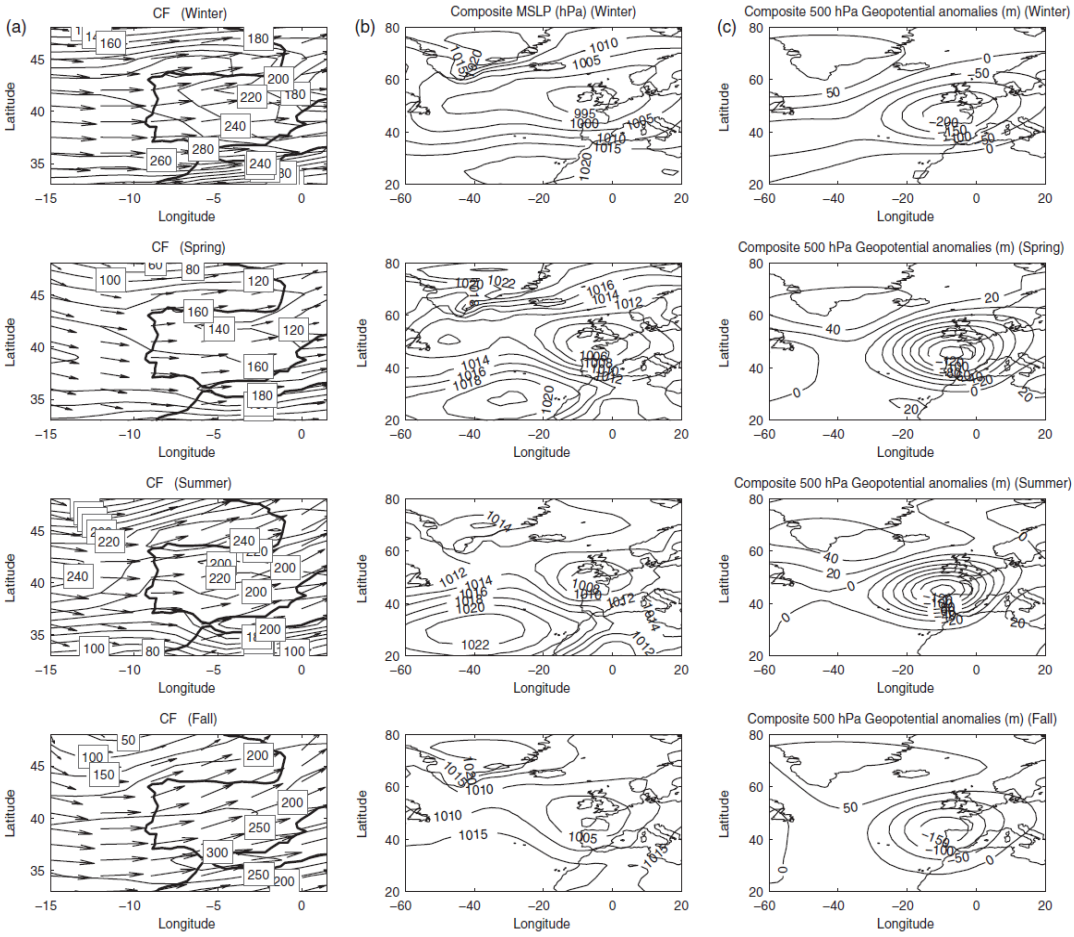

Figure 4.25. Panel A shows mean total column water vapor flux (TCWVF) for days under Cyclonic Flux (CF). Arrows represent the vector flux and the vector magnitude is sometimes shown with tags for better interpretation in g $cm^{-1}s^{-1}$. Panel B shows mean sea level pressure composite maps for those days in hPa.

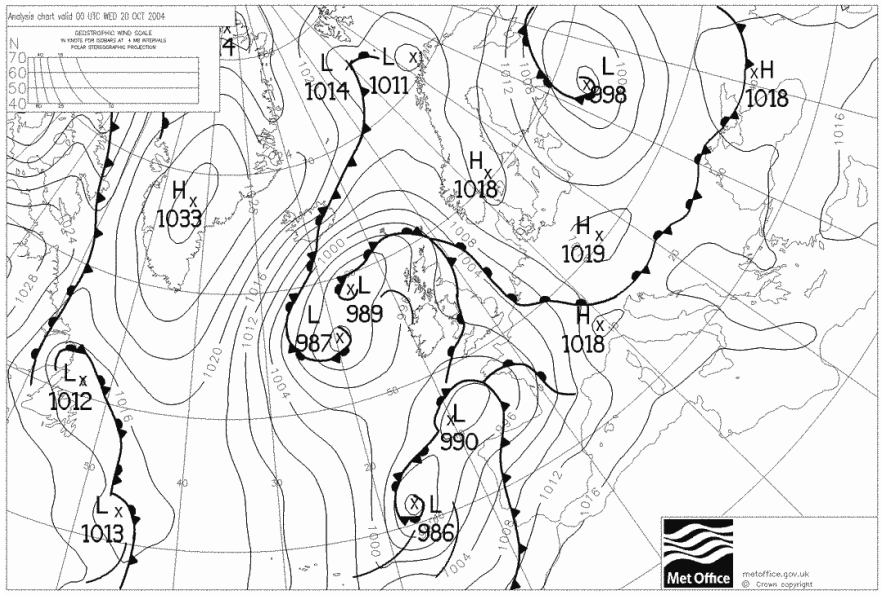

Figure 4.26. Analysis chart for October 20th of 2004 (Courtesy of Met Office, UK). This is a day under CF with a set of cyclones traveling between the British Isles and the Iberian Peninsula and generating on their southern flank cold fronts that swap the Iberian Peninsula.

The strength of the pattern is higher in winter, followed by fall. The location of the maximum fluxes varies from one season to the other, with a maximum in the northern IP in summer and over the south in fall.

As a consequence of the positive cyclonic vorticity, high winds on their southern flank are able to transport cold and dense air from the North Atlantic that can hardly mix with the warmer and humid air masses over Azores. These air masses would be pushed

towards east, forming consecutive cold fronts that are after launched over the IP with almost a west to east direction when reaching Guadarrama. This process is very effective in terms of TCWVF (Figure 4.25, panel A) if compared the average fluxes for this WVFP with the seasonal means (Figure 4.23, panel D), and the frontal structure can explain the marked zonal gradient of TCWVF.

This efficient transport of TCWVF and the frontal development causes a high probability of precipitation, as found for all observatories and seasons (Table 4.9), especially in winter and fall. The contribution of this WVFP to total precipitation is also high for all observatories and seasons, especially in spring and fall. The precipitation processes under this WVFP are mainly related with the thermodynamics of the cold front, and the orography would be enhancing the processes due to an extra adiabatic cooling, as shown by much higher precipitation rates at mountain top (N) than those found at S and C during all seasons except in summer (Table 4.9).

This WVFP is not very frequent, around 10% for all seasons, due to the high traveling velocity of cyclones and its low persistence (Table 4.9), but it is clear that their contribution to total precipitation at Guadarrama is crucial. This WVFP evolves mainly to NAO-F for all seasons and WF except in winter (Table 4.9).

Figure 4.26 shows an analysis chart for October 20th of 2004. This is a day under CF with a set of cyclones traveling between the British Isles and the Iberian Peninsula and generating on their southern flank cold fronts that swap the Iberian Peninsula. This day, precipitation at S was 18.8 mm, at N was 16 mm and at C it was 1mm.

4.3.2 West Flux (WF)

Figure 4.27 displays the second WVFP found, which is also characterized by westerly fluxes. Nevertheless, in this case the fluxes are maximum north of the IP, in association with a maximum MSLP gradient between the IP and British Islands (panel B) corresponding to a dipolar 500 hPa geopotential anomalies pattern (panel *C*) related to a northward displacement of the circulation. It has been called West Flux (WF, Figure 4.27, panel A) and its structure is very similar to the one obtained for winter by Santos et al. (2005).

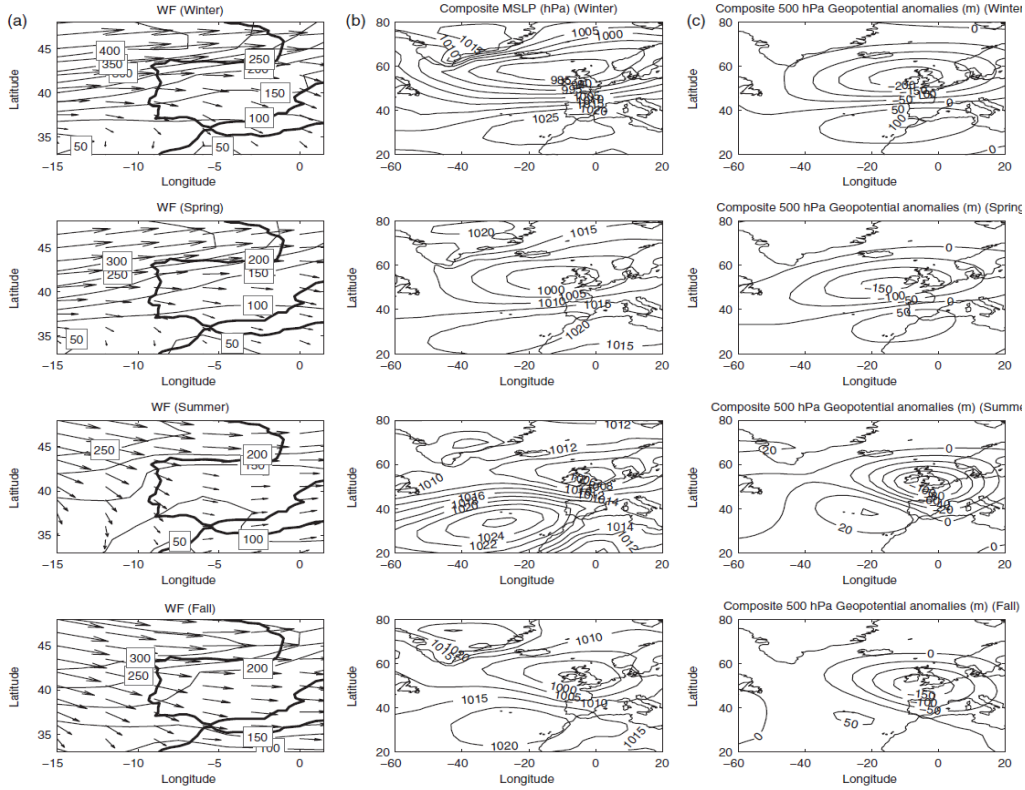

Figure 4.27. As Figure 4.25 but for West Flux (WF)

The configuration of high and low pressures (panel B) translates into an efficient TCWVF, which is considerable higher than climatology (Figure 4.23), but this time, the flux hardly reaches Guadarrama. The high pressure system over Azores presents a different influence depending on the season. In fall the high pressure over Azores is weaker, opening a north west corridor that brings TCWVF to Guadarrama and producing some precipitation at S and N (Figure 4.27, panel A bottom), not much in C, probably enhanced due to orographic forcing. This is the only season and observatories for which this WVFP could be considered as wet since it accounts for a 16% and 14% of fall total precipitation and showing a probability of precipitation of 58% and 72% (Table 4.9). In summer, the probability of precipitation for this WVFP is one of the lowest for all stations (7%, 11% and 4% for S, N and C respectively), (Table 4.9) even though TCWVF over IP is considerable higher than climatology (Figure 4.23). This, along with the fact that the frequency of this WVFP is high in summer (14%), makes this WVFP one of the potential contributors to the summer drought (Figure 4.18).

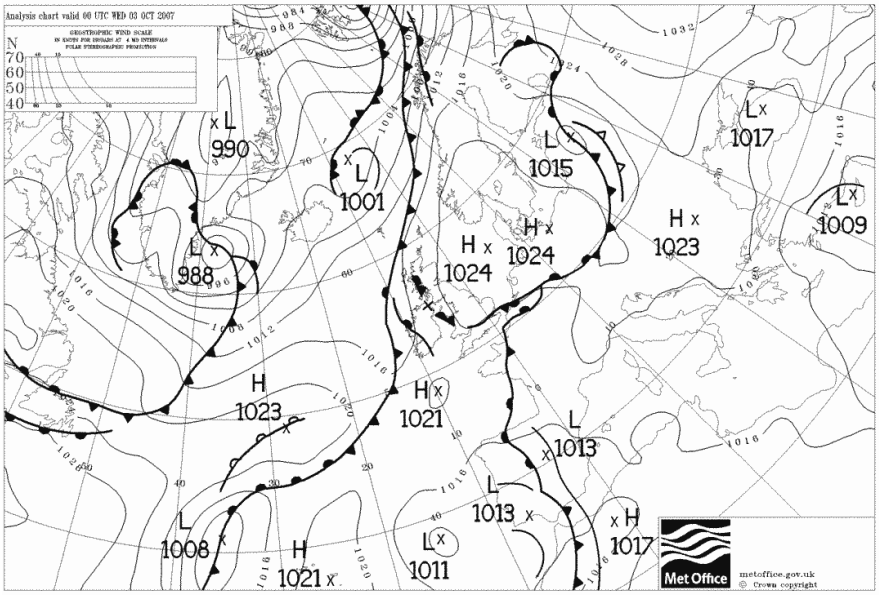

Figure 4.28. Analysis chart for October 3rd of 2007. This was a day with WF (Courtesy of Met Office, UK).

It seems like under this WVFP, and only in fall, the mountain range would be playing a drying role over the air masses that go through Guadarrama, being the southern side of the range in the rain shadow. Obviously this will have to be checked using convenient tools, like modeling. For the rest of the seasons and observatories this WVFP can be considered as moderately dry, even though it shows a considerable probability of precipitation in winter and spring, 57% for winter and 33% for spring at *N*, but its contribution to total seasonal precipitation is quite small, 7% and 3% respectively with low precipitation rates (Table 4.9). Half of the days under this WVFP precipitation is not zero at N, but

contribution to total precipitation is very small with very low precipitation rates. This constant but slight precipitation might be suggesting how this WVFP favors the formation and crossing of not very active warm fronts, but this would need further research.

This WVFP usually evolves to NAO+F and NWF, except in winter that very often evolves to CF (Table Error: No se encuentra la fuente de referencia).

Figure 4.28 shows an analysis chart for October 3rd of 2007. This was a day with WF and precipitation at S was 8.8 mm, at N was 27.4 mm and at C was 6.8 mm. Here a set of cyclones were traveling from west to east with permission from the Azores high that this time let the flux to reach Guadarrama, something that is more frequent in fall.

4.3.3 NAO- Flux (NAO-F)

Figure 4.29 shows what has been called NAO- Flux (NAO-F) since it shows a pattern of a north-south dipole on the 500 hPa geopotential height anomalies (Figure 4.29, panel C) typical of the negative index of the North Atlantic Oscillation (NAO), and very similar to the one obtained in winter by Santos et al. (2005) which was highly correlated with a negative phase of the NAO. The frequency of this WVFP is roughly constant, around 15% (Table 4.9). The negative center over the southern IP (panel C) could be interpreted as an enhancement of the number of cyclones crossing that area, which weaken the climatological behavior of the region. The TCWVF is, thus, maximum over the southern half of the IP, producing 30% of total seasonal precipitation for all observatories and seasons except in fall where precipitation contribution to total

decreases considerably, especially in N and C (Table 4.9). This WVFP brings warmer tropical Atlantic humidity air in spring, summer and fall, but colder north Atlantic air masses in the winter.

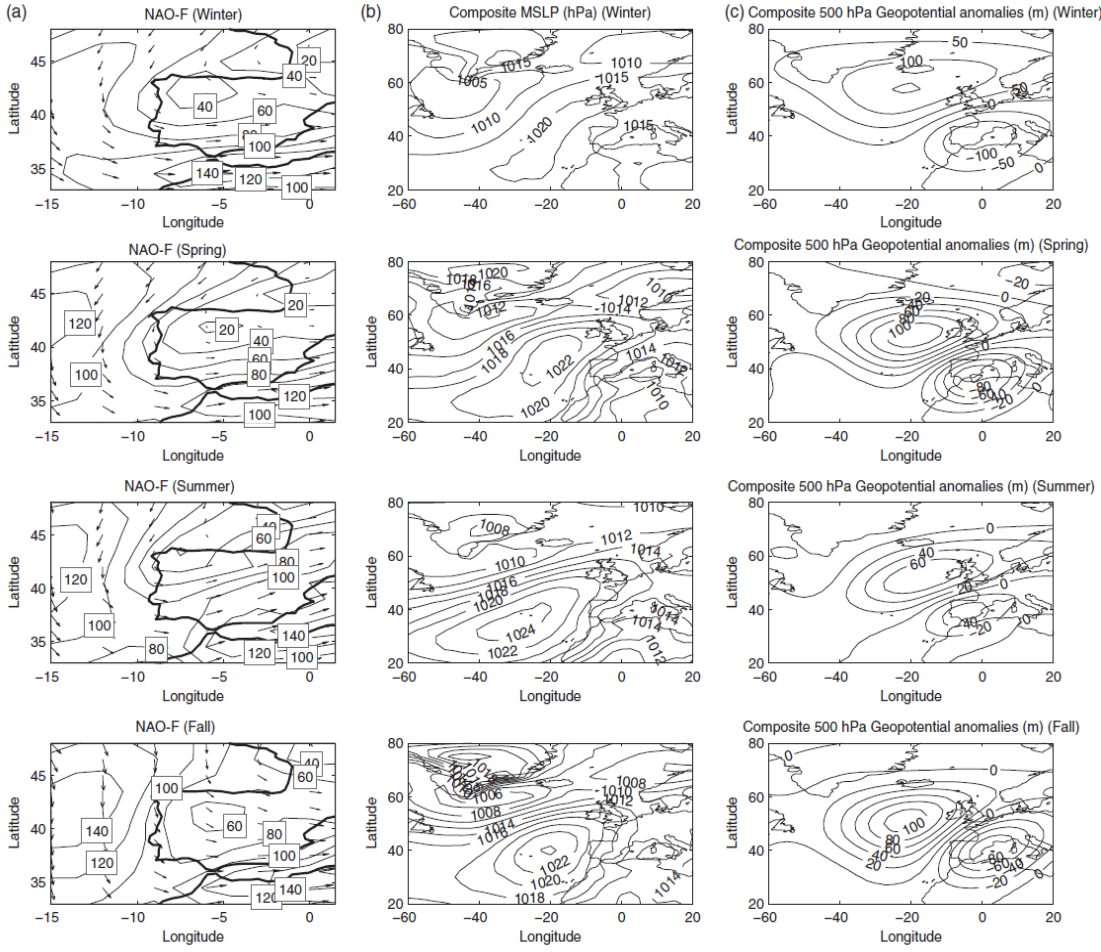

Figure 4.29. As Figure 4.25 but for NAO- Flux (NAO-F)

The MSLP pattern presents a minimum gradient between subpolar and subtropical pressure centers which is more marked in winter, confirming the NAO- identification. It is remarkable how important

is this WVFP for summer precipitation, when it becomes the main contributor to total precipitation showing about 30% for all observatories (Table 4.9). Under this flux TCWVF is slightly higher than climatology (Figure 4.23, bottom) but the combination of this maritime and humid air from northern Atlantic might be favoring the development of convective systems when passing through the heated land of the plateau.

This WVFP evolves mainly to EF (described later) and NWF (described later) for all seasons, as shown in Table Error: No se encuentra la fuente de referencia.

Figure 4.30 shows an analysis chart for the 2nd of December of 2006. a day with NAO-F precipitation at S was 5.9 mm, at N was 15.2 mm and at C was 9.1 mm. It can be seen how a succession of low pressure systems were throwing frontal systems across the IP on their way to the east. Next day, precipitation was 2.4 mm, at N was 15.2 mm and at C was 9.1 mm.

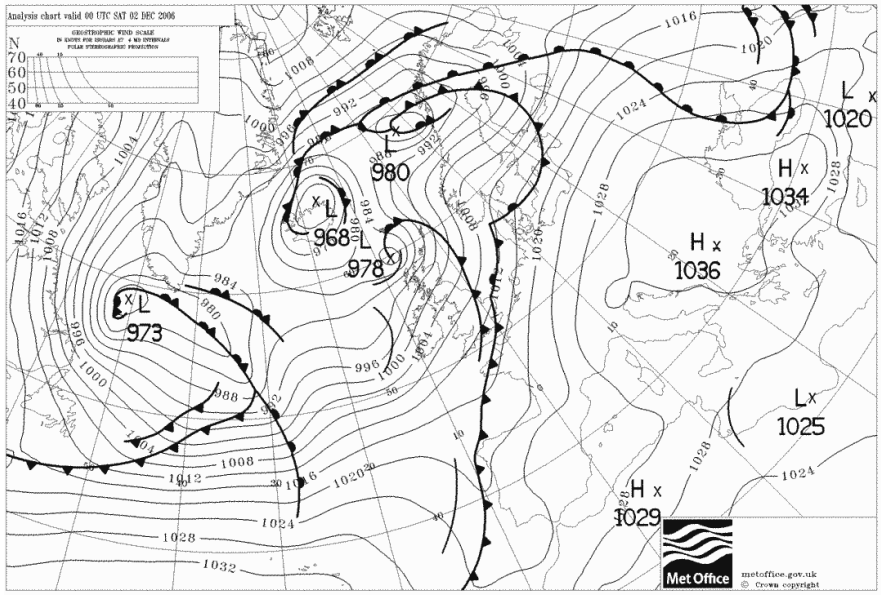

Figure 4.30. Analysis chart for December 2nd of 2006 a day with NAO-F (Courtesy of Met Office, UK).

4.3.4 NAO+ Flux (NAO+F)

Figure 4.31 shows what has been called NAO+ Flux (NAO+F) since the geopotential height shows an anomalous north-south dipole at 500 hPa (Figure 4.31, panel C) typical of the positive phase of the North Atlantic Oscillation (NAO) for all seasons. This pattern is very similar to the one obtained in winter by Santos et al. (2005) which was highly correlated with a positive phase of the NAO.

MSLP maps show an enhancement of the Azores anticyclone together with a weakening of the Icelantic low, producing a strong pressure gradient which is maximum north of the IP. The strong Azores high covers the IP territory blocking the advection of humidity towards the IP. Thus, probability of precipitation under this flux is very low for all observatories and seasons, especially in summer, not even favoring the development of convective storms due to the very little content of humidity of the air and the absence of significant local sources of humidity at the almost arid plateau lands in summer. This is clearly a clear contributor for the summer drought (Figure 4.18) since its contribution of this WVFP to total precipitation is almost negligible, below 6% for all observatories and seasons.

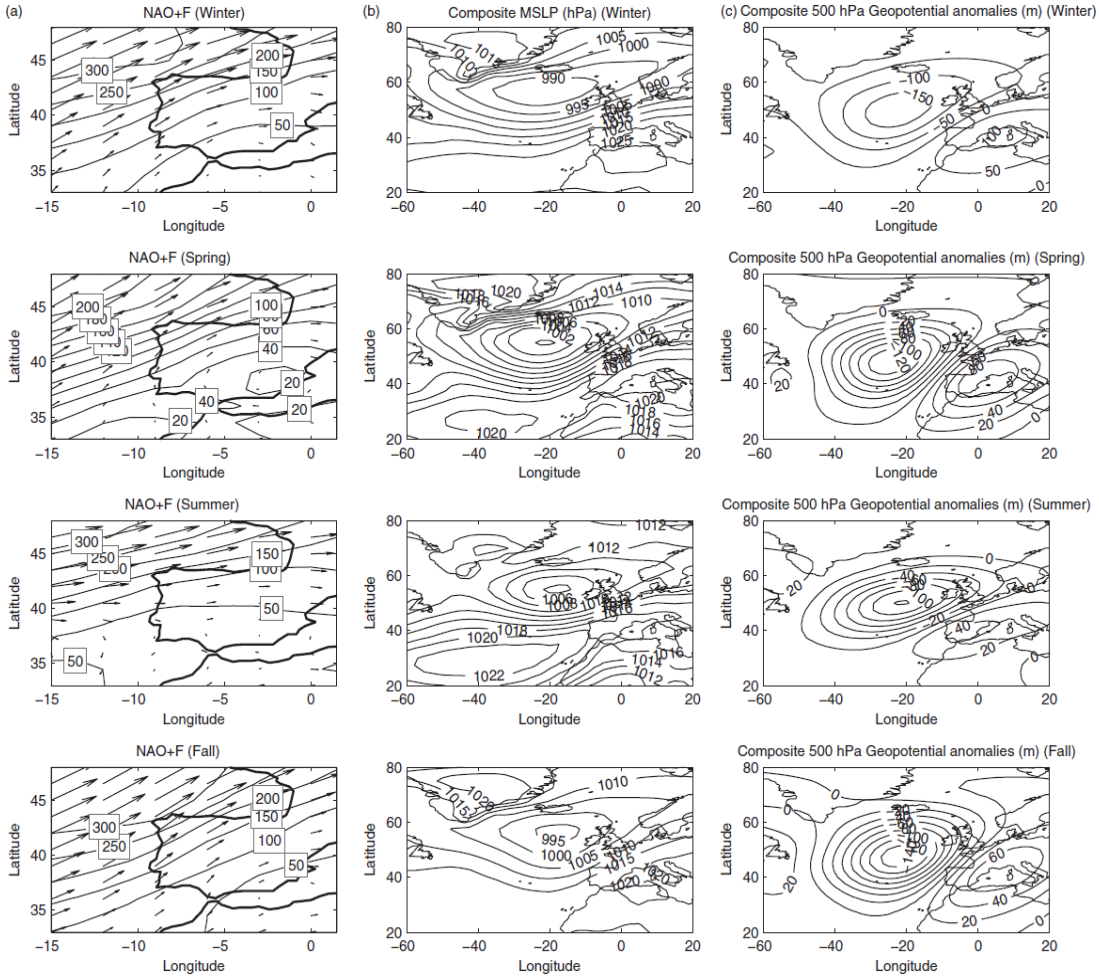

Figure 4.31. As Figure 4.25 but for NAO+ Flux (NAO+F).

This WVFP does not show a marked evolution to other WVFPs (Table Error: No se encuentra la fuente de referencia) except in fall that often evolves to SWF.

4.3.5 East Flux (EF)

Figure 4.32 shows a flux characterized by a maximum TCWVF coming from the east, and, thus, it has been called Eastern Flux (EF). This flux is the most frequent for all seasons, 31% in winter, 22% in spring, 18% summer and 23% in fall. This weak east to west flow when reaching Guadarrama is due to an extended high pressure system on Center Europe that originates, due to the anticyclonic circulation, a flow of cold and dry air of continental origin. These air masses are generally very cold in winter. TCWVF is low and the contribution to total precipitation is one of the lowest for all observatories and seasons except summer (Table 4.9), when the development of a high pressure conditions over north Africa forces a humidity flux from the Mediterranean through the mountain range, favoring the formation of convective storms. The anomalous geopotential height presents one remarkable center over central Europe, with no marked change in the Icelandic low, resembling the Atlantic Ridge pattern in Guemas et al. (2010). Again this pattern is very similar to the one obtained in winter by Santos et al. (2005) for Portugal.

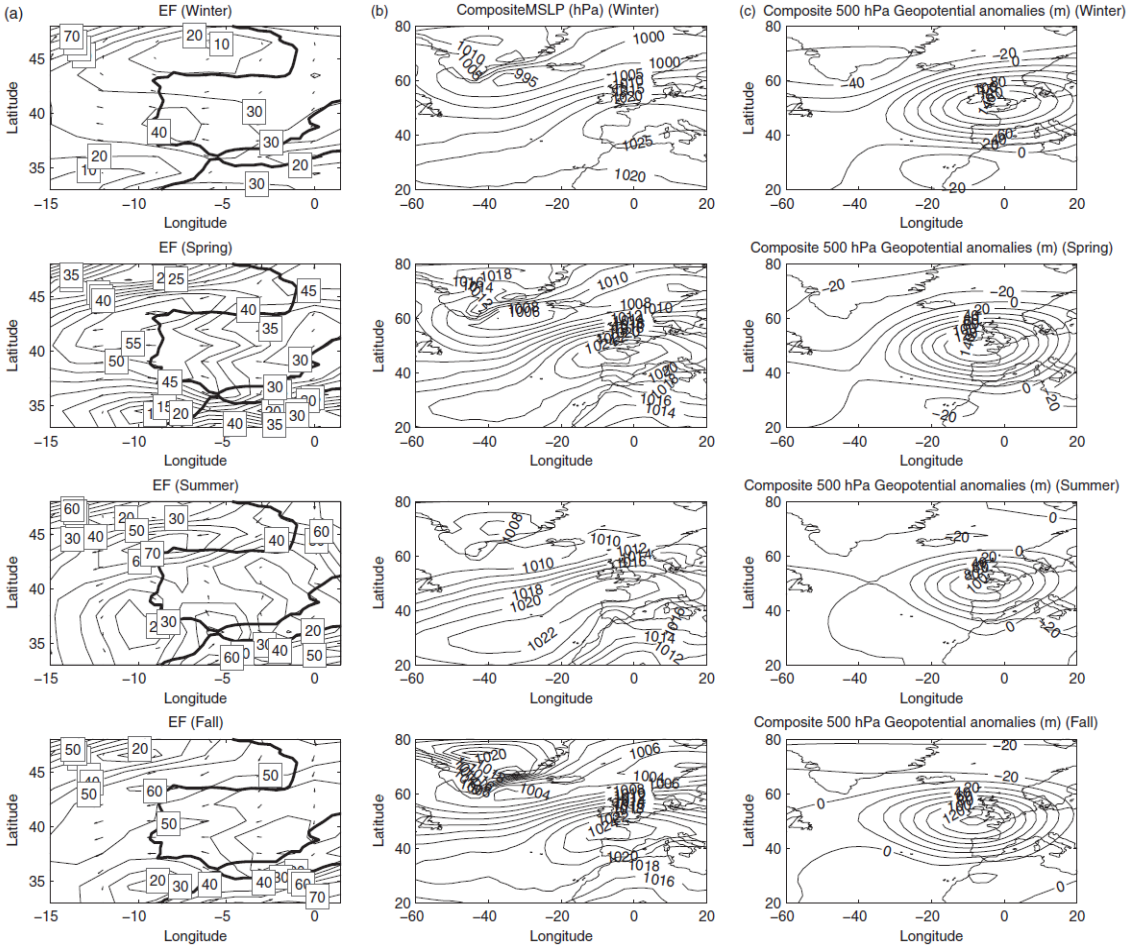

Figure 4.32. As Figure 4.25 but for East Flux (EF).

This WVFP show a variety of preferred transitions depending on the season (Table Error: No se encuentra la fuente de referencia). Transitions to NWF is common in winter, spring and summer, transitions to NAO-F are frequent in spring and summer, while common transitions to SWF are in fall.

4.3.6 South-West Flux (SWF)

Figure 4.33 shows what has been called South West Flux (SWF) This structure is similar to CF, but here the center of action of the cyclone is displaced south west of IP due to development of a high pressure system in Center Europe that is more accused in fall (Figure 4.33, panel B). At 500 hPa, the geopotential anomalies (Figure 4.33, panel A) present negative scores, in accordance with an effective anomalous advection of TCWVF coming from the South West of the IP. These facts have found to be crucial in terms of precipitation, since it forces the advection of warm and humid air masses from the Atlantic to be constrained into a very narrow band. This phenomena is similar to those found by other authors in other parts of the world, like in the American northwestern coast (Neiman et al., 2008; Warner et al., 2012), whith a similar negative anomaly of pressure on high levels, as shown in the Z500 anomalies map, surrounded by a positive anomaly on the west, forming what are usually called atmospheric rivers (Zhang et al., 2008; Rasmussen et al., 2012; Lavers and Villarini, 2013; Durán et al., 2015). This name comes from the fact that a huge amount of precipitable water is contained in a very narrow band. This very localized advection of humidity is transformed into precipitation due to adiabatic cooling when forced orographically to lift. This process starts right after the flux enters the IP and gains altitude when traveling through the South IP plateau producing considerable amounts of precipitation in a short time that sometimes turns into floods in the flat areas.

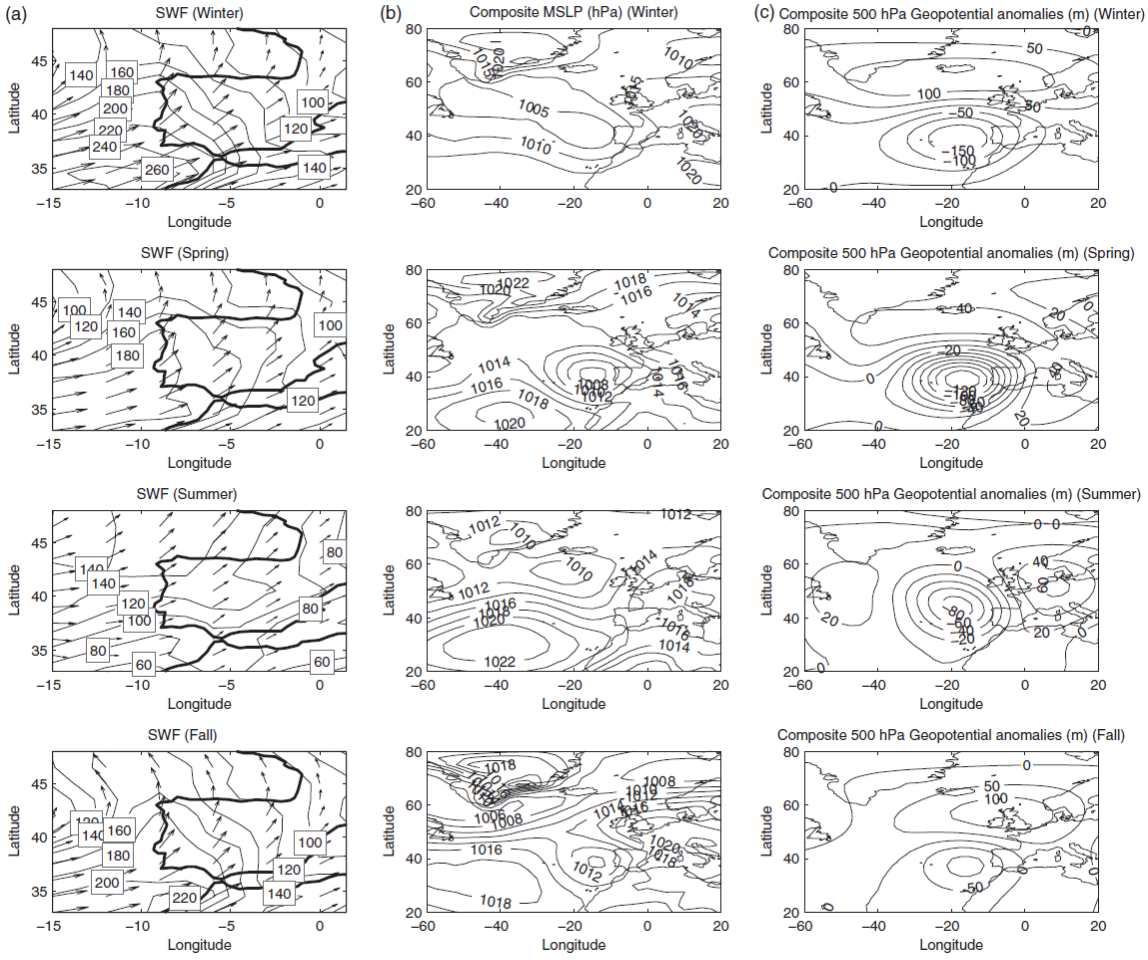

Figure 4.33. As Figure 4.25 but for South West Flux (SWF).

This WVFP is not very frequent, 7% in winter, 10% in spring, 13% in summer and 9% in fall, but it is responsible of a great amount of the total precipitation at N (28% in winter, 24% in spring) and C (38% in winter, 30% in spring). Observatory S show lower

precipitation compared to *N* and *C*, maybe due to fact that this observatory is located downwind of the mountain range. On the other hand, values observed at observatory *C*, on the upwind side of the range, are very high and someway confirm the orographic character of this kind of precipitation that shows also high average precipitation rates, with 20 mm day^{-1} and 14 mm day^{-1} for *N* in winter and fall respectively, and 12 mm day^{-1} and 10 mm day^{-1} for *C* in winter and fall respectively. For *S*, precipitation rates drop to 5 mm day^{-1} (fall) and 4 mm day^{-1} (winter) (Figure 4.9).

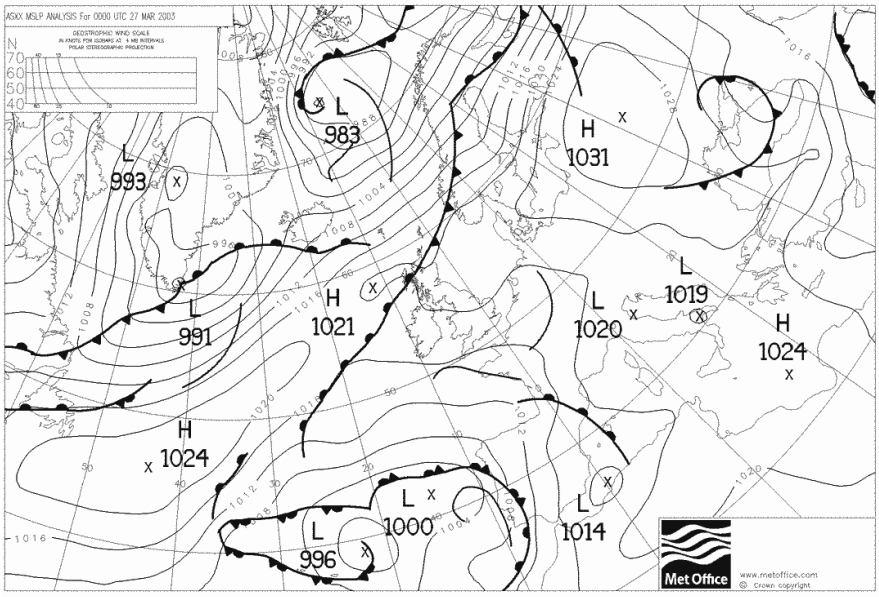

Figure 4.34. Analysis chart for March 27th of 2003, a day with SWF (Courtesy of Met Office, UK).

This WVFP shows clear evolutions to CF and NAO-F for all seasons as shown in Table Error: No se encuentra la fuente de referencia.

An example of a day under this WVFP is presented in Figure 4.34 for March 27th of 2003. Here an analysis chart is shown, where a system of high pressure developed over Central Europe is narrowing the flux of humidity associated to a set of fronts in the southern flank of a couple of low pressure systems with their center of action located in a relatively low latitude. This concentrates the flux of humid and warm air from southern Atlantic to go through IP and leading to important precipitation as this flux travels north through the plateau and then through Guadarrama. Here precipitations are noticeable at the windward observatory, *C*, with 27.7 mm. Precipitation at *N* was 26.4 mm and 6.3 mm at *S*, which is downwind observatory under this flux.

4.3.7 North West Flux (NWF)

Figure 4.35 shows what has been called North West Flux (NWF) due to a TCWVF advecting the IP from the northwest (Figure 4.35, panel C) and shows a frequency from 16% (summer) to 14% (winter and spring) (Table 4.9). This flux is the consequence of an anomalous strengthening of the Azores high in north and western directions, and the existence of a depression in Center Europe (Figure 4.35, panels B and A respectively). In summer, the high pressure system is more spread over the north, producing flows over Guadarrama with a clearer north to south component. As expected, the TCWVF is decreasing along its way along the IP an

drying due to precipitation at the northern mountain ranges of the IP. Thus, this flux seems to be much less efficient in terms of precipitation when reaching Guadarrama, probably due the lack of enough humidity content.

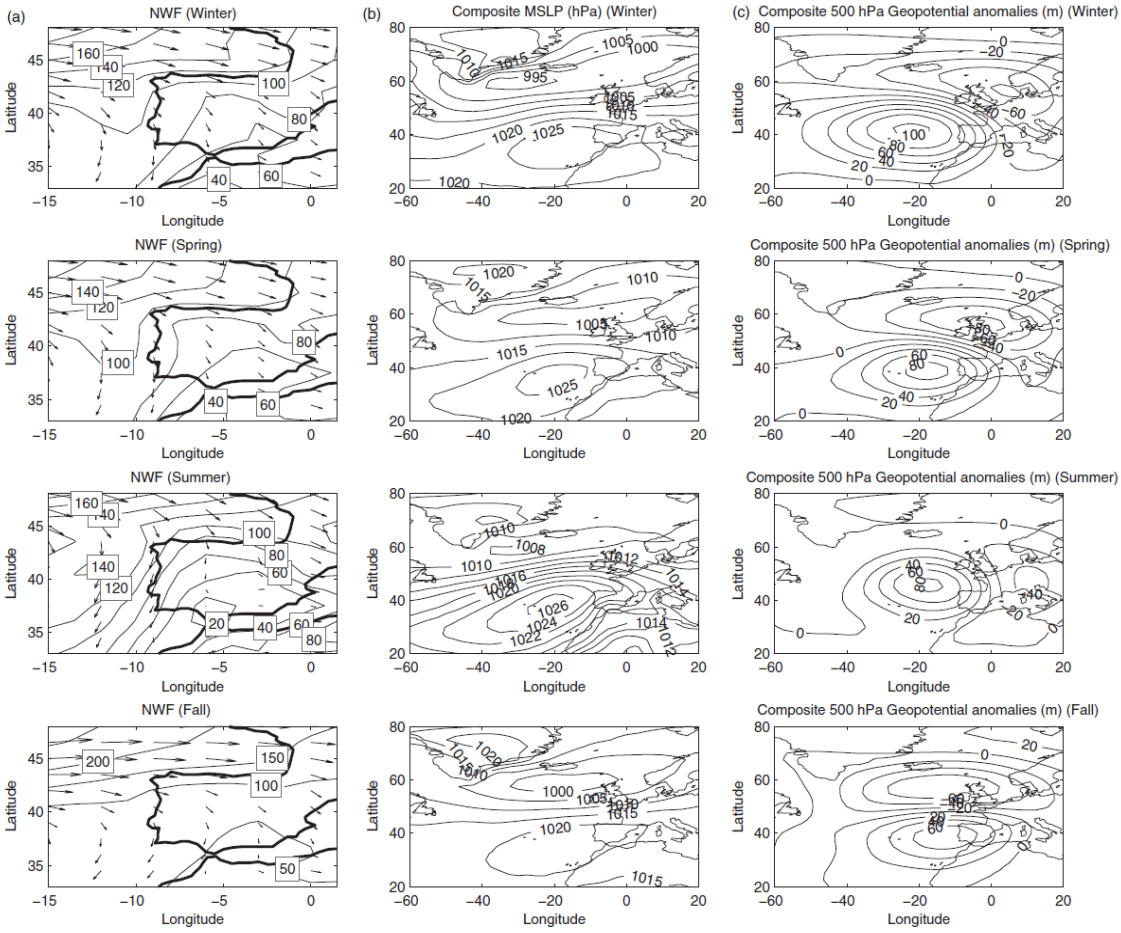

Figure 4.35. As Figure 4.25 but for North West Flux (NWF).

This flux could be considered as a dry one due to the small contribution to total precipitation for almost all seasons and observatories (Table 4.9). Nevertheless there are two noticeable exceptions. The first is the precipitation observed at S in winter, which shows a contribution of 12% (Table 4.9). This is probably due to the fact that this observatory is located upwind from the northwestern flux, and under this situation the mountain range would be acting as a drying factor. A second exception is that precipitation at C in summer under this flux which contributes for almost a 20% of the total, showing also the highest precipitation rates (Table 4.9). It seems like this flux, in summer, favors the convection processes providing enough TCWVF with a northern origin due to the northern displacement of the high pressures. Under this situation, since C is downwind, the mountain range could be acting now as a triggering factor of convective systems forcing the air masses to ascend through it. Obviously this will have to be checked with further research.

This WVFP shows clear transitions to EF for all seasons (Table Error: No se encuentra la fuente de referencia), and to NAO+F, specially in fall.

Table 4.9.Frequency of occurrence of each pattern (bold for values higher or equal than 15%), persistence (bold for values higher than 2 days), probability of precipitation (bold for values higher than 50%), contribution to total seasonal precipitation (bold for values higher or equal than 15%) and precipitation rate (bold for values higher or equal than 10 mm day-1) at every site and for every season.

	Frequency (%)	Persistence (days)	Probability of precipitation (%)			Contribution to total precipitation (%)			Precipitation Rate (mm day^{-1})		
Pattern/ Site			S	N	C	S	N	C	S	N	C
WINTER											
CF	8	1.9	**88**	**98**	**85**	**29**	**22**	**23**	5	**12**	6
WF	8	1.8	45	**57**	37	8	7	3	3	7	2
NAO-F	**15**	**2.3**	**61**	**75**	**54**	**26**	**25**	**24**	4	**10**	6
NAO+F	12	1.9	27	30	28	6	4	5	2	4	3
EF	**31**	**3.6**	10	21	13	5	5	4	2	3	2
SWF	7	2.0	**62**	**79**	**83**	14	**28**	**38**	4	**20**	**12**
NWF	**19**	1.9	33	44	19	12	9	3	2	5	2
SPRING											
CF	13	1.5	**76**	**82**	**63**	**31**	**29**	**24**	5	**10**	5
WF	8	1.9	22	33	14	3	3	1	3	4	2
NAO-F	**16**	2.1	**67**	**77**	**56**	**34**	**28**	**29**	5	8	5
NAO+F	12	2.0	10	14	8	3	2	2	4	4	3
EF	**22**	**2.8**	14	19	15	8	6	11	4	5	5
SWF	10	2.0	**60**	**73**	**67**	**16**	**24**	**30**	4	**12**	7
NWF	**19**	2.0	19	31	12	6	7	3	2	4	2
SUMMER											
CWF	8	1.7	**29**	**35**	**20**	**18**	**20**	13	6	8	4
WF	14	2.0	7	11	4	5	6	3	4	4	2
NAO-F	14	2.1	**34**	**39**	**24**	**31**	**31**	**28**	6	6	4
NAO+F	**16**	2.0	7	7	3	3	3	4	3	3	5
EF	**18**	**2.9**	**21**	**25**	**17**	**23**	**20**	**20**	5	5	4
SWF	13	1.8	17	19	15	**14**	13	13	6	6	4
NWF	**16**	2.0	7	12	8	5	8	**19**	4	5	8
FALL											
CF	10	1.8	**90**	**96**	**88**	**37**	**38**	**40**	7	**19**	**10**
WF	11	1.9	**58**	**72**	39	**16**	14	7	4	8	3
NAO-F	**17**	**2.1**	45	**54**	32	**19**	14	12	4	7	5
NAO+F	12	1.8	23	28	21	5	6	5	3	7	4
EF	**23**	**3.1**	14	21	14	7	8	10	3	7	7
SWF	9	**2.1**	47	**64**	**58**	12	**18**	**24**	5	**14**	**10**
NWF	**18**	2.0	12	19	6	3	2	2	2	2	3

Table 4.10. Transitions in % between weather regimes for all seasons. Transitions are from WVFP on the rows to WVFP on the columns. For clearness transitions equal or higher than an arbitrary limit of 25% are shaded and values are rounded to closest integer.

WINTER

	to:	CF	WF	NAO-F	NAO+F	EF	SWF	NWF
From:	**CF**		22	34	10	2	15	17
	WF	25		12	28	4	1	30
	NAO-F	9	10		7	30	10	35
	NAO+F	19	19	2		24	18	19
	EF	2	4	22	22		22	28
	SWF	47	11	26	2	13		1
	NWF	7	17	21	22	33	1	

SPRING

	to:	CF	WF	NAO-F	NAO+F	EF	SWF	NWF
From:	**CF**		27	27	15	1	12	20
	WF	22		10	25	1	4	37
	NAO-F	8	6		3	34	11	38
	NAO+F	20	23	4		12	19	23
	EF	4	1	26	18		25	26
	SWF	33	7	27	14	14		6
	NWF	5	20	16	23	33	4	

SUMMER

	to:	CF	WF	NAO-F	NAO+F	EF	SWF	NWF
From:	**CF**		26	31	11	1	10	21
	WF	22		11	33	2	3	30
	NAO-F	10	6		3	41	8	32
	NAO+F	22	15	7		15	20	23
	EF	0	3	28	18		21	31
	SWF	39	8	21	13	17		2
	NWF	7	23	14	23	32	1	

FALL

	to:	CF	WF	NAO-F	NAO+F	EF	SWF	NWF
From:	**CF**		26	37	9	2	11	14
	WF	24		13	26	3	2	33
	NAO-F	7	3		4	35	7	44
	NAO+	17	18	1		18	25	20
	EF	3	1	23	20		29	23
	SWF	37	7	25	15	14		3
	NWF	4	18	13	31	33	1	

Hardangerjøkulen glacier in Hordaland, Norway. As an evocation of what the Massif of Peñalara might have looked like in the past.

4.4 Physical Modeling and Assessment of Precipitation at Guadarrama

The objective of this sections is to show the results obtained after doing 6 hour simulations of precipitation from 1990 to 2013 using LMOP with 200 m spatial resolution of Guadarrama. This is a new scenario for LMOP since previous applications of this model were conducted at coastal areas with oceanic climates and Guadarrama is a mountain climate immersed in a typical continental climate.

Results are shown attending to the following different temporal scales:

- *Annual and inter-annual scale*
- *Monthly scale*
- *Daily scale*

4.4.1 Annual and Inter-annual Scale Evaluation

Figure 4.36 shows the scatter plots of observed precipitation versus modeled by LMOP at the three observatories. The correlation is significant for the three observatories

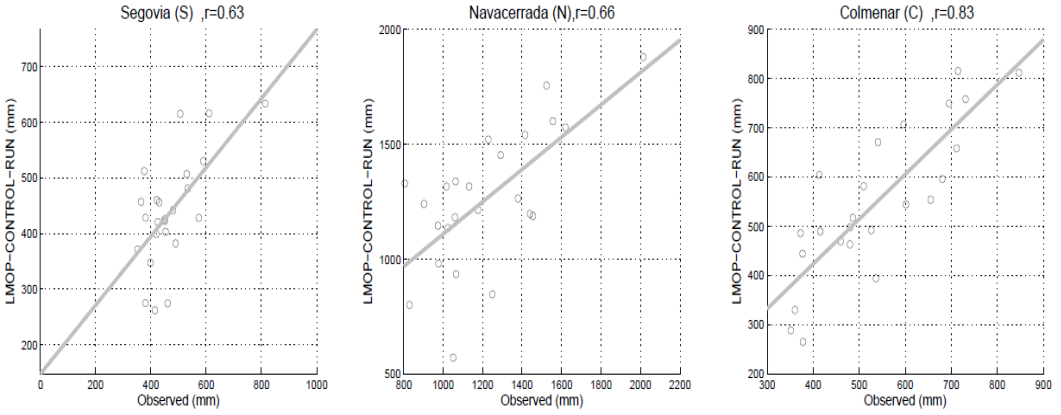

Figure 4.36. Scatter plot of annual measured versus modeled precipitation at the three observatories for the period 1990-2013

Figure 4.37 shows observed (bars) and modeled (lines) total annual precipitation from 1990 to 2013 for the three observatories.

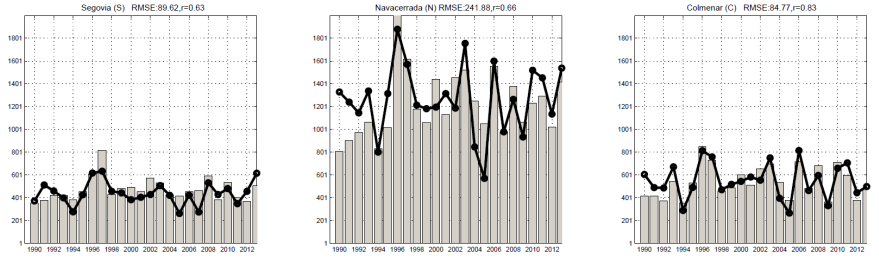

Figure 4.37. Total annual precipitation observed (bars) and modeled (lines) at the three sites for the period 1990-2013

Figure 4.38 shows the anomalies of observed precipitation (bars) versus modeled (lines) for the period 1990-2013 for the three sites.

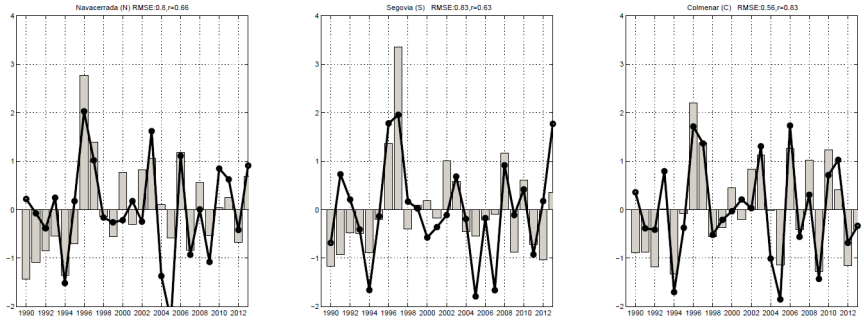

Figure 4.38. Annual precipitation anomalies observed (bars) and modeled (lines) at the three sites for the period 1990-2013

Annual totals simulated by LMOP seem to have a good correlation with observed ones specially for *N* and *S*. For *C*, the correlation is weaker (Figure 4.36). Figure 4.38 shows how LMOP seems to reproduce fairly well the inter-annual variability for the three sites. One exception is the drought before 1995, LMOP is giving higher values than observed specially for *N* observatory. This is not the case for the drought of 2004, that is overestimated. These results are pointing to a different origin of the droughts and deserves further investigation.

In general terms, precipitation anomalies modeled by LMOP are comparable with the observed ones (Figure 4.18), especially for the wet years, not the case for dry years as already pointed out.

4.4.2 Monthly Scale Evaluation

Figure 4.39 shows the monthly total precipitation observed (bars) and modeled (lines) at the three observatories.

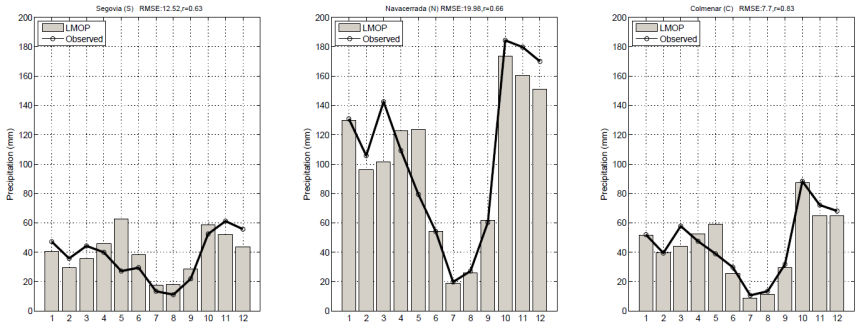

Figure 4.39. Monthly precipitation observed (bars) and modeled (lines) at the three observatories

Figure 4.40 shows the standard deviation of the monthly total precipitation observed (bars) and modeled (lines) for the three observatories. The area between both lines is equal to the root mean squared error (RMSE).

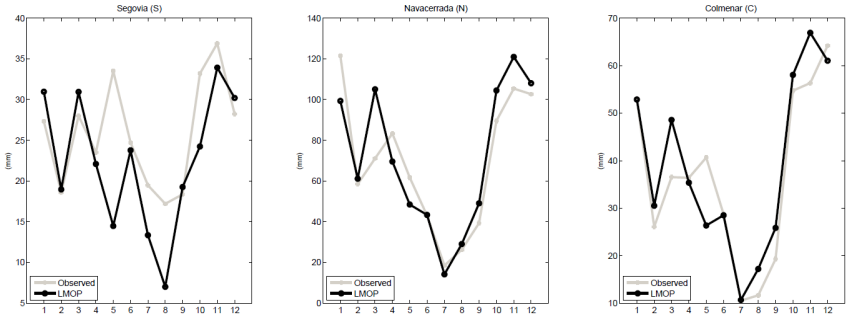

Figure 4.40. Standard deviation of the monthly precipitation observed (black) and modeled (gray) at the three observatories

LMOP formulation does not take into account convective effects. For this reason, the differences found during May and October at *S* might be attributable to this phenomena (Figure 4.39 and 4.40).

Regarding monthly totals, LMOP reproduces very well the observations (Figure 3.6). Average monthly totals seen by LMOP follow the annual cycle very close to observations, accounting for the summer drought at the three observatories. Results are promising for *N*, with highest RMSE values around 20 mm for winter months. LMOP over-estimate precipitation for these months but considering that wind is higher during these months, probably there is an underestimation of the observation.

May is the month that LMOP shows highest difficulties to reproduce observations especially at the plateau observatories (*S* and *C*). Some authors (Iturrioz et al., 2007) have pointed out that from May to October a higher ratio of precipitation events are not stratiform origin but due to thermodynamic instability. Also May is the month with higher ratio of hail precipitation (Figure 4.17.b). If we consider hail as a good tracer of deep convective events, convection is seen as the main factor explaining this difference since LMOP does not consider convection on its formulation.

4.4.3 Daily Scale Evaluation

Regarding daily precipitation, scatter plots (Figure 4.41) show a better correlation for N and C than for S. A finer tunning might be necessary for having better results at S. Considering that monthly averages perform well, maybe a better work should be done on the synchronization of the intial values since their taken away from the mountain range and it takes some hours to reach the massif.

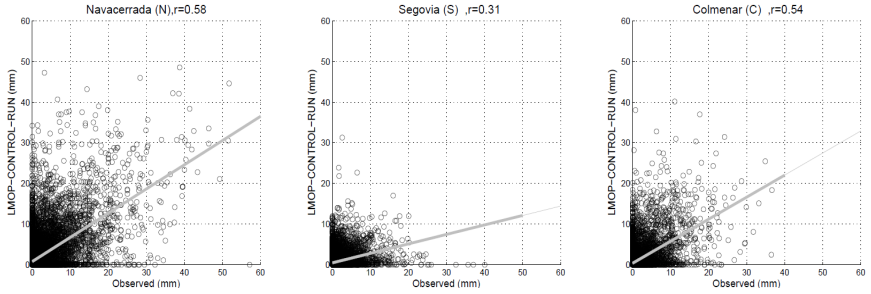

Figure 4.41. Scatter plot of modeled versus observed daily precipitation at the observatories

Figure 4.42 shows daily accumulated modeled precipitation at S, N and C for every hydrological year. Wettest observed year and driest observed year have been marked for comparison (see Figure 3.6). It seems clear how LMOP is able to reproduce fairly well driest and wettest years at N and C observatories. On the other hand, it seems to perform not as good at S.

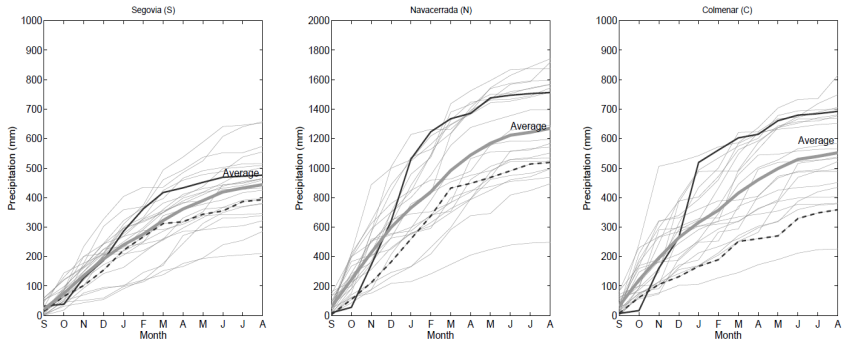

Figure 4.42. Daily modeled accumulated annual precipitation at the top of mountain observatory (*N*) for the period 1990-2013 and for hydrological years going from September to October. As in Figure 3.6 black solid line represents accumulated precipitation for the year that reached the maximum observed precipitation. Solid gray line represents the average modeled accumulation. Black dashed line represents the accumulated modeled precipitation for the year with lowest observed precipitation.

4.4.4 High Resolution Assessment of Precipitation at Guadarrama

In order to evaluate the capability of the high resolution database generated by the LMOP, some results showing different features related to the spatial distribution of precipitation characteristics are presented now. This high resolution gridded data base for Sierra de Guadarrama (SG01 hereafter, Durán and Rodríguez-Muñoz, 2015a) covers the period from 1990 to 2013 with a 200 meters of spatial resolution and a daily time step.

Figure 4.43 compares mean annual precipitation for SG01 and Spain02 gridded database (Herrera et al., 2012) for their common period. This gridded observational database was developed with the highest available density rain-gauge stations over the Iberian Peninsula, generating a 0.2º grid over the whole region. One of

their more clear interests is related to the validation of regional climate model simulations over the Iberian Peninsula (Herrera et al., 2010; Jimenez-Guerrero et al., 2013; Dominguez et al., 2013; Lopez-Franca et al., 2015). Therefore, it can be consider the best gridded database at high resolution for the Iberian Peninsula, compared with other similar databases (Haylock et al., 2008), where just a small amount of the AEMET observational stations were used.

When both data bases are compared, it is clear that Spain 0.2º gridded database can roughly obtain the spatial distribution of precipitation at Guadarrama. As the orography is much more smoothed (slightly higher than 1250 m, compared with the 2400 m of SG01), maximum precipitation obtained there is around 1000 mm yr^{-1}, compared with 1700 mm yr^{-1} shown by SG01 over the highest points of the mountain range (upper figure). This is, nevertheless, an expected result, due to the limitations in the resolution, and therefore, in the real height of the mountains under study.

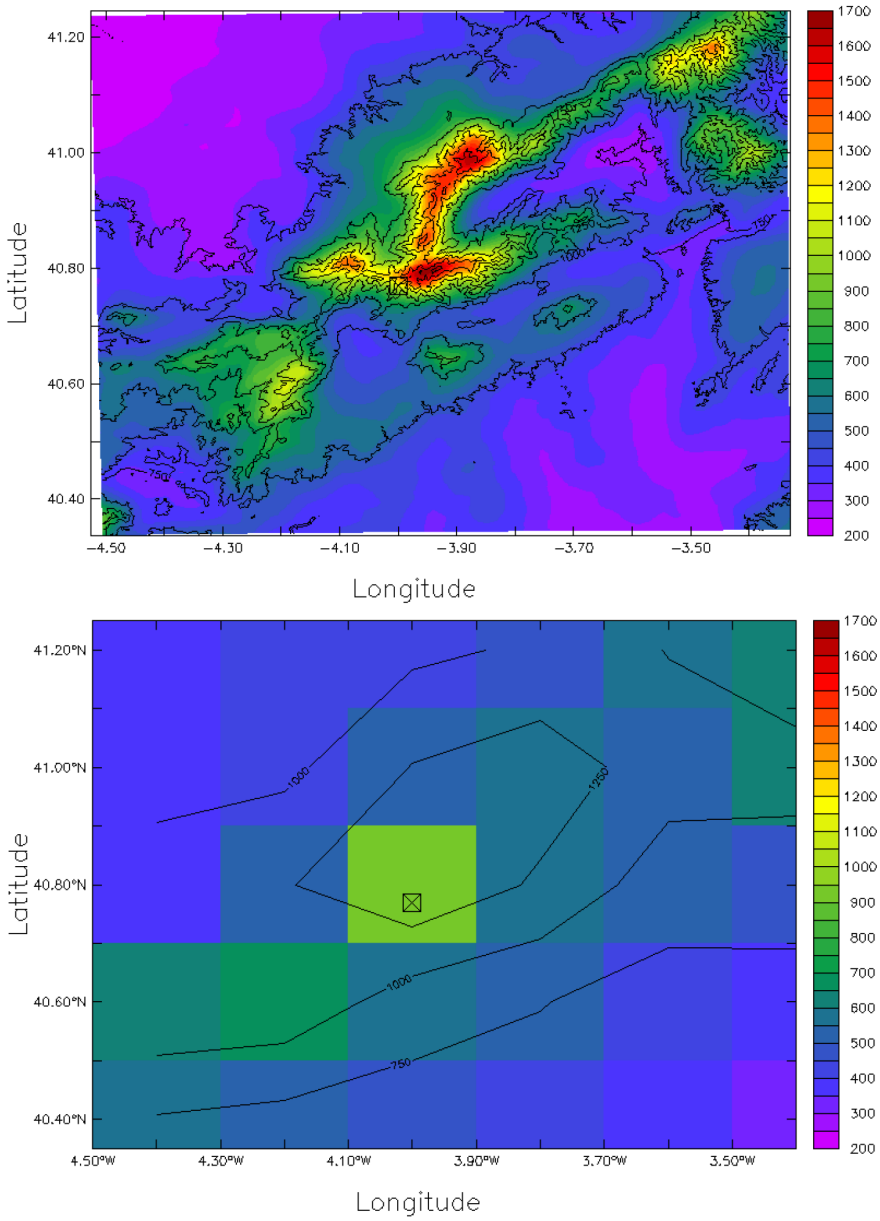

Figure 4.43: Mean annual precipitation in mm year^{-1} for the same domain of SG01 (top panel) and Spain02 (bottom panel) for the common period 1990-2007. Orography for each database is also shown with contour lines. Navacerrada observatory is indicated with a square with a cross in both Figures.

We can then focus on the capabilities of SG01. This first overview of total annual precipitation indicates that usually, the higher the point the larger precipitation is, from a global perspective with a certain shift due to the condensation and precipitation time lags. Valley minimum values can be seen, indicating that large range of precipitation totals from the 1700 mm yr^{-1} on the top levels, values around 500 mm yr^{-1} in the lower lands.

Figure 4.44 shows the interannual variability for the period 1990-2013 calculated out of SG01 data base. As expected, higher variability is found at higher elevations, right where most of the precipitation is snow. This is expected to have a higher impact on the water resources of the region.

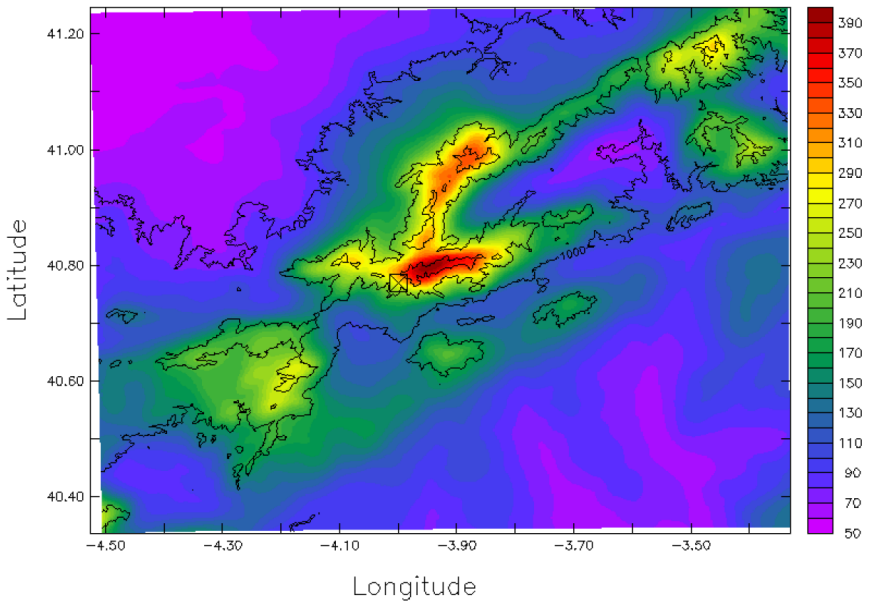

Figure 4.44. Interannual variability in mm $year^{-1}$ defined as the standard deviation of the annual precipitation for the period 1990-2013

Another simple to calculate feature of precipitation is the number of rainy days (precipitation higher than 1 mm day^{-1}) per year. This is shown in figure 4.45 for the whole period. This database allows to see how values range from around 120 days per year over the highest peaks, to values around 55 days on the lower part of the valleys.

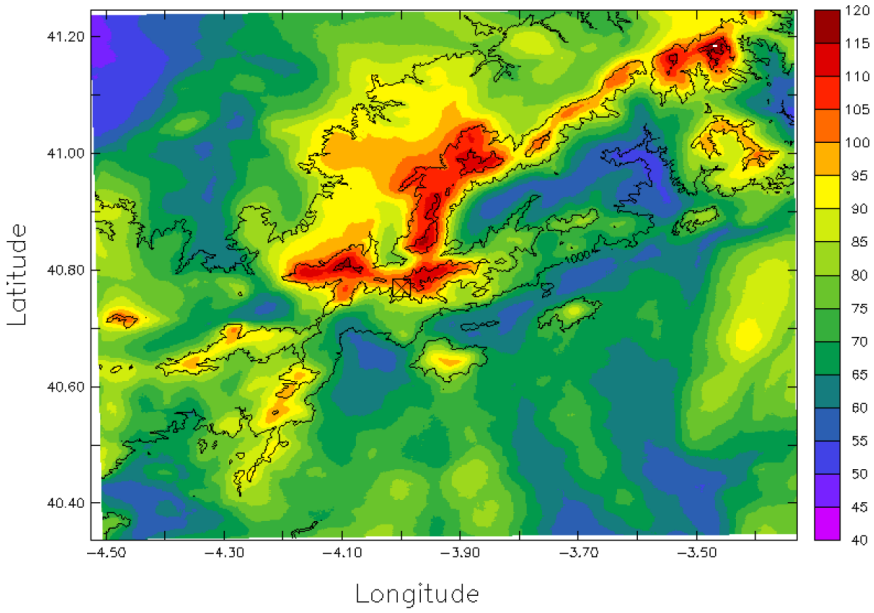

Figure 4.45: Number of precipitation days per year (days with precipitation higher than 1 mm) and for the period 1990-2013

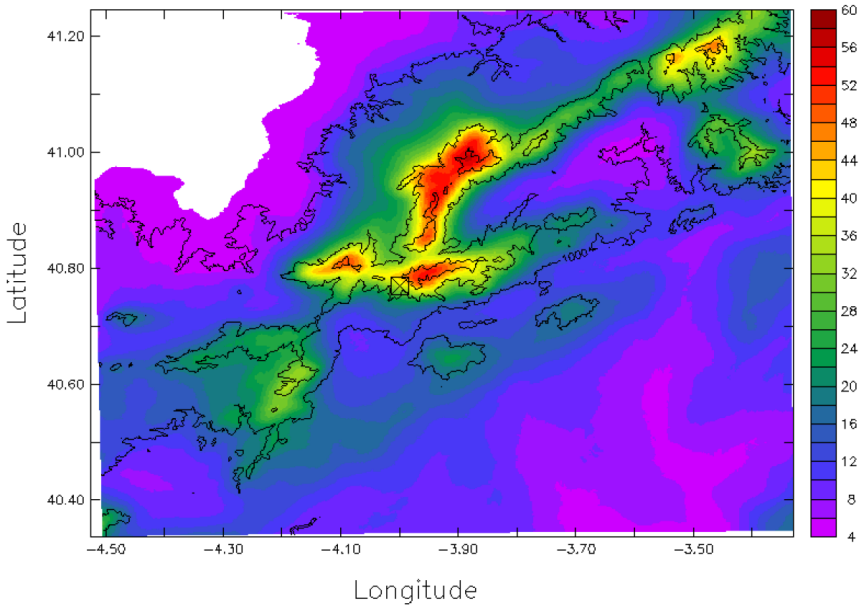

Figure 4.46: SDII (simple daily intensity index) for Guadarrama calculated using SG01. Units are mm day^{-1}

SG01 database allows to calculate many other features.. In particular, index related with extremes can be of high interest. Following Zhang et al. (2011), where a set of index for temperature and precipitation were defined, here some of them have been analyzed. One of the simplest ones is SDII (simple daily intensity index), which is defined just as the ratio between the two previous fields already shown: annual total precipitation over the number of wet days ($>$ 1 mm). Results of this index can be seen on Figure 4.46. As a measure of the intensity of rain when it rains, the results indicate that the areas with higher elevation have more than 15 mm day^{-1} on average, meanwhile, lower points have values around 5-6 mm day^{-1}. It is clear that the shape of the distribution is much smoother than the orography, and not all the peaks lead to the

same amount of precipitation, being the ones around Peñalara massif those with slightly comparative larger values.

Some simple measures of extreme events are those related to days with heavy precipitation: R10 and R20, defined by the annual count of days when precipitation is larger than 10 and 20 mm, respectively. The results are shown in Figure 4.47 and Figure 4.48.

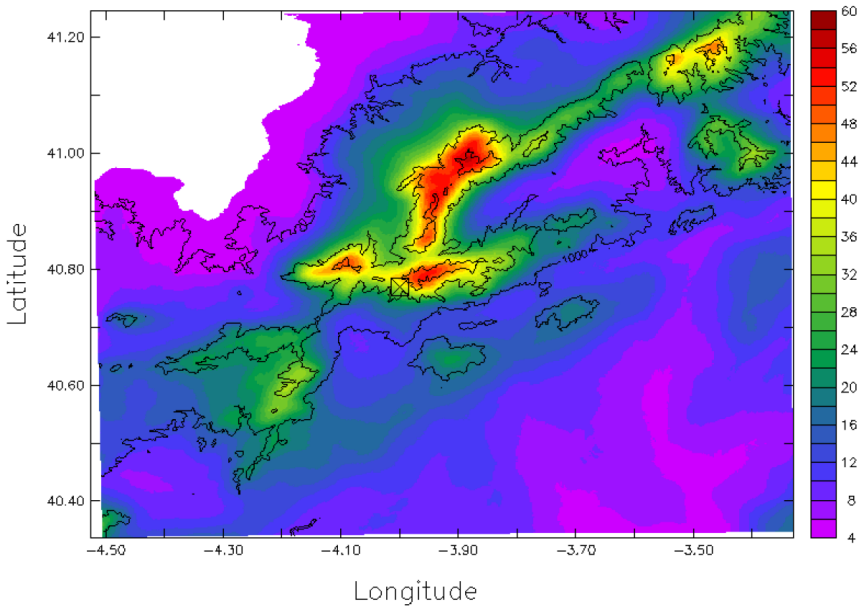

Figure 4.47: R10 defined by the annual count of days when precipitation is larger than 10 mm using SG01

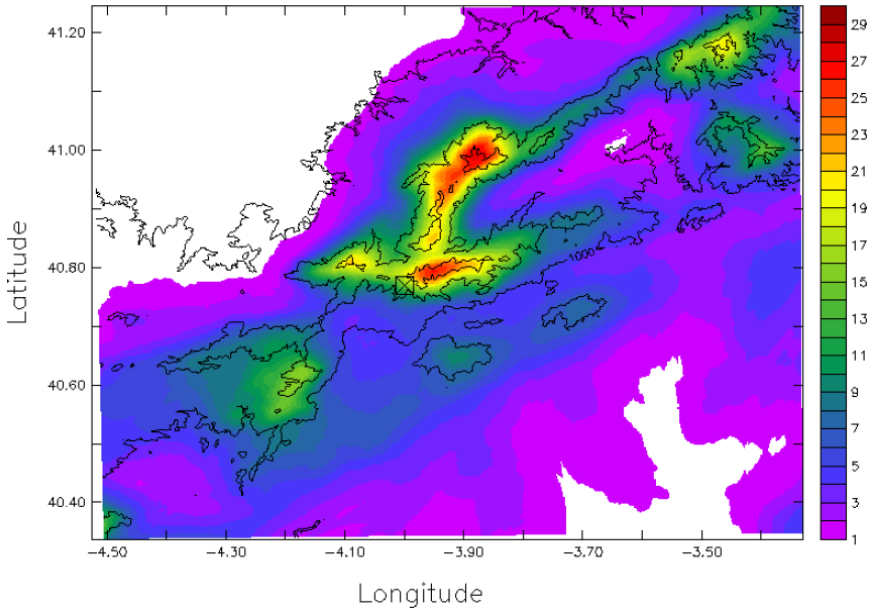

Figure 4.48 R20 defined by the annual count of days when precipitation is larger than 20 mm as estimated using SG01

When looking at days with more than 10 mm, it can be seen once again the orographic pattern, with values up to 60 days (among those 120 obtained as rainy days, that is, around 50% of the total days of precipitation) over the highest peaks, and 10 days or less on the deeper valleys. If 20 mm are considered (Figure 4.48), a similar pattern is obtained, but now highest values are around 30 days, with less than 5 days for the lower elevations.

Dry and wet spells can also be calculated with very high resolution using SG01. Annual maximum length of dry and wet spells, averaged for the 24 years are shown on figures 4.49 and 4.50, respectively. Some relevant features can be seen on these figures.

Dry spells can last for several months on the valleys, as already shown by Sanchez et al. (2011), using regional climate models at 50 and 25 km resolution over the whole Iberian Peninsula. The spatial variability is quite high over this small region, ranging from values around 25 days over the highest peaks, to those 90 around the valleys. Although the altitude seems to be the main aspect to determine the length of the dry spell, also some other interesting results are obtained, probably related to the orientation of some valleys or peaks, as it can be seen with the large differences around Navacerrada, for example. When looking at the largest wet spells (Figure 4.50), a somewhat opposite figure is obtained, being now the peaks the areas where largest values can be seen (around 10 days, on the average over the 24 years), and around 4 days on the valleys.

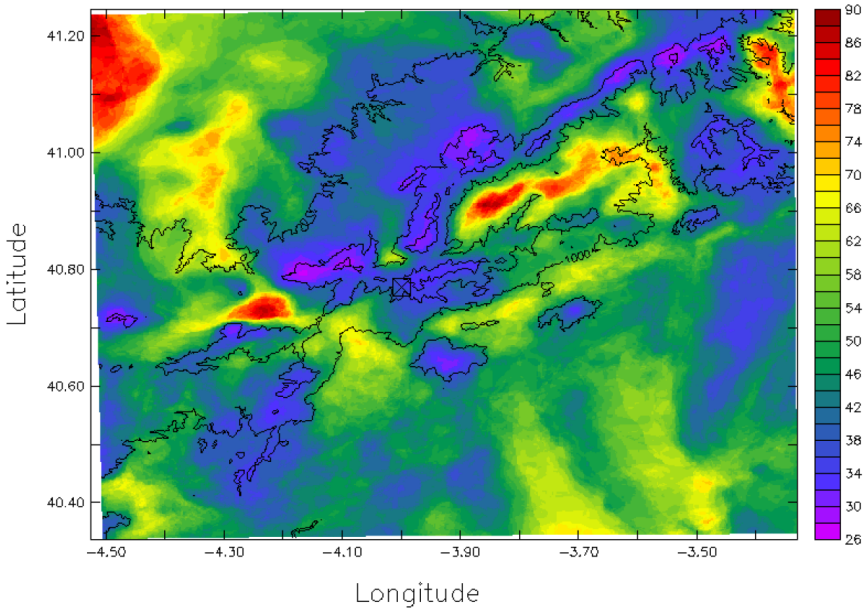

Figure 4.49. Annual value in days, averaged for the 24 years (1990-2013) of the largest dry spell, defined as the greatest number of consecutive days with daily precipitation amount below 1 mm

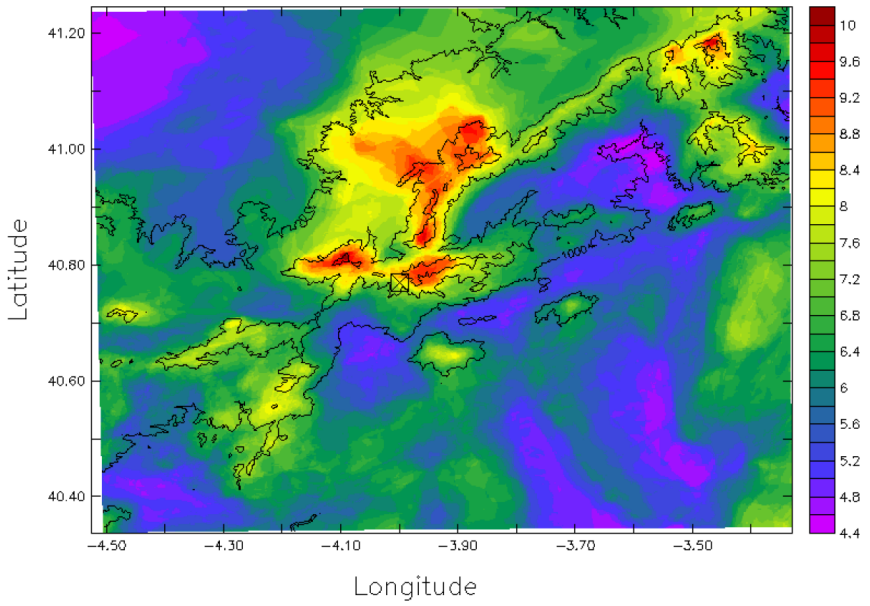

Again, following the indices proposed in Zhang et al. (2011), to measure the intensity, and not only the frequency, of extreme precipitation events, values related to the largest rainfall percetiles have been calculated. Figure 4.51 shows directly the values of the annual 95th precentile, that is, only a 5% of the rainy days give more precipitation amounts than that value. Maximum values around the peaks reach 50 mm day^{-1}, being near to 10 mm day^{-1} around the valleys. The global pattern is as smooth as other magnitudes, such as R10 or R20.

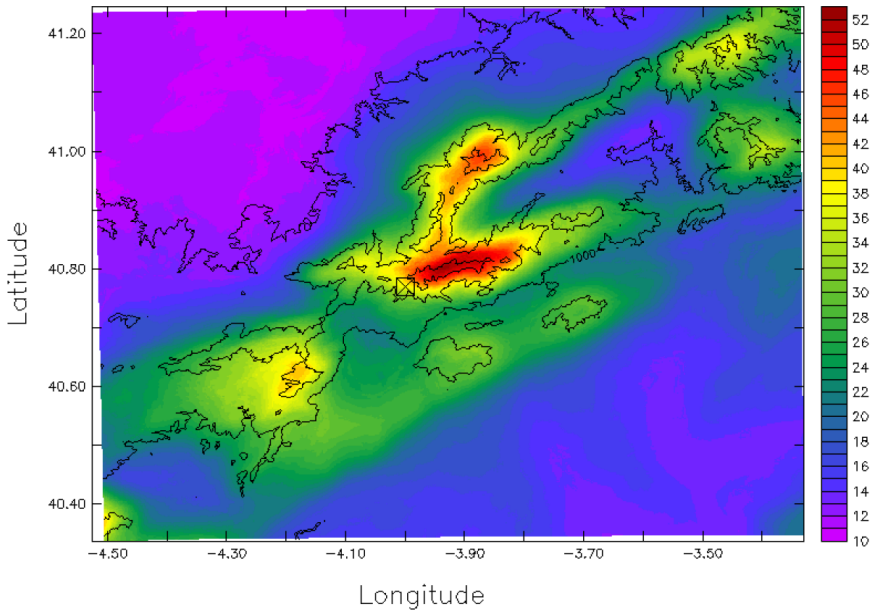

The parameter R95p is proposed as a measure of rain intensity. It is defined as the total annual precipitation from days above that 95th percentile. Figure 4.52 shows the ratio between R95p and the total annual precipitation (Figure 4.43) expressed in %. The Figure shows a clear asymetry between northern and southern side of Guadararma. Southern side shows a higher percentage of precipitation confined in the higher part of the distribution. This means that heavier precipitation concentrates in less days than in northern side. This could connect with the southwest flux pattern described in section 4.3 (Table 4.9). It is remarkable how the orographic pattern seen in other figures is here not shown.

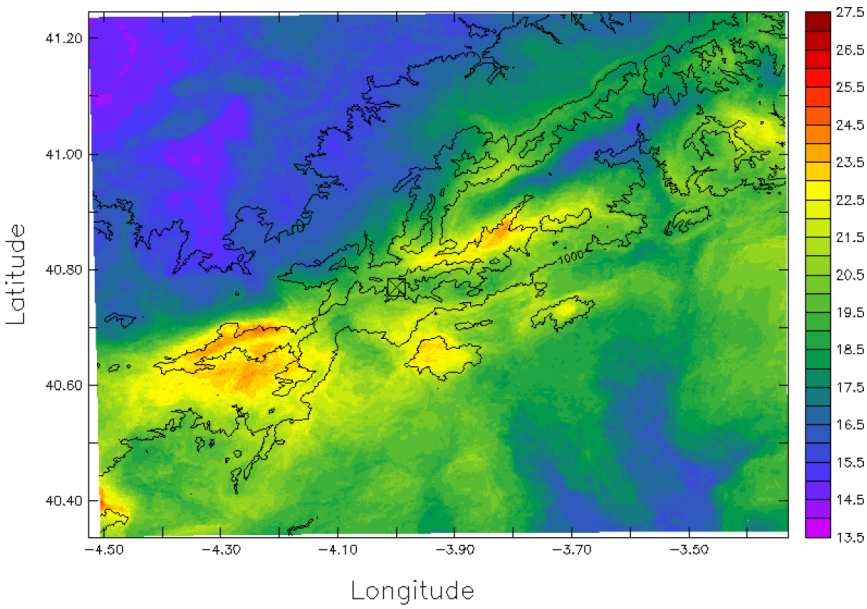
41.20
41.00
40.80
40.60
40.40
Latitude
−4.50
−4.30
−4.10
−3.90
−3.70
−3.50
Longitude
1000
27.5
26.5
25.5
24.5
23.5
22.5
21.5
20.5
19.5
18.5
17.5
16.5
15.5
14.5
13.5

Chapter 5. Conclusions

The main conclusions of this Thesis can be summarized as follows acording to four different aspects:

a) Monitoring Meteorology at Mountains:

- It is possible to use automatic techniques for measuring weather and climate at mountains but there are some factors that affect their representativity, inducing biases, specially in winter.

- Five monitoring sites covering the altitudinal range of Peñalara and area of influence has shown to be enough to find relevant altitudinal differences and to have a first assessment of climatology at this area.

- Regular non-heated tipping bucket rain gauges have shown not to be very appropriate for higher elevations. Other alternative non-heated sensors, like gravimetric or vibrating wire rain-gauges, with wind shields should be considered in the future.

- Significant errors are expected if precipitation at this area is assessed based only on surface measurements. A combination of observations with other techniques, like physical modeling, is seen as the best option.

b) Climatology of Precipitation at Guadarrama:

- Significant differences regarding total precipitation, interannual variability and summer drought have been found between close observatories in Guadarrama.

- Total snow precipitation at higher elevations of Guadarrama is higher than rain precipitation.

- Most of the precipitation events in Guadarrama are related with the advection of humid air masses coming from the Atlantic Ocean.

c) Relationships Between Synoptic Flows and Precipitation:

- Seven total column water vapor flux based regimes are responsible of modulating precipitation at Guadarrama.
- In general terms, three of these flux patterns are responsible of most of the precipitation at Guadarrama (Cyclonic, NAO- and South West), while four can be considered as dry patterns (West, NAO+, East and North West).
- South West pattern gives normally the higher precipitation rates giving a good example of interaction between orography and moisture flux.

d) Multi-Scale Assessment of Precipitation at Guadarrama

- The hypothesis that assumes that total precipitation at Guadarrama is the sum of large scale precipitation, orographic precipitation and a minor contribution of thermally driven convective precipitation has proven to be solid.
- Orographic precipitation phenomena is accounting for the big differences found between precipitation measured at the plateau observatories and top of mountain observatory.
- Linear Model has shown to be a valid tool for assessing precipitation at Guadarrama at different scales. SG01 has shown to be a valid high resolution data base for assessing precipitation at this area and opens new research an water management horizons.

References

Achour, M., Betz, F., Dovgal, A. and Lopes, N. (2006). "PHP manual".

Adam, J. C. and Lettenmaier, D. P. (2003). "Adjustment of global gridded precipitation for systematic bias". J. Geophys. Res.: Atmos., 108, D08112.

AEMET Spanish Meteorological Service (2011). "Iberian climate atlas". http://www.aemet.es/documentos/es/divulgacion/publicaciones/Atlas-climatologico/Atlas.pdf.

Alexandersson H. (1986). "A homogeneity test applied to precipitation data". Int. J. Climatol., 6, 661–675.

Álvarez, R. and Sierra, F. (2011). "Paisajes glaciares del macizo de Peñalara". Biólogos: Revista del Colegio Oficial de Biólogos de la Comunidad de Madrid, 3, 16-19.

Amat, M. E., Vargas, P. and Gómez, J. M. (2013). "Effects of human activity on the distribution and abundance of an endangered Mediterranean high-mountain plant (Erysimum penyalarense)". Journal for Nature Conservation, 21, 262-271.

Andres, M., Tomas, C. and de Pablo, F. (2000). "Spatial patterns of the daily non-convective rainfall in Castilla y Leon (Spain)", Int. J. Climatol., 20, 1207-1224.

Appenzeller, C., Begert, M., Zenklusen, E. and Scherrer, S. C. (2008). "Monitoring climate at Jungfraujoch in the high Swiss Alpine region". Science of the total Environment, 391, 262-268.

Armi, L. and Mayr, G. J. (2015). "Virtual and real topography for flows across mountain ranges". J. Appl. Meteor. Climatol., 54, 723-731.

Arribas. A., Gallardo, C., Gaertner, M.A. and Castro, M. (2003). "Sensitivity of the Iberian Peninsula to a land degradation". Clim. Dyn., 20, 477-489.

Auer, I., Böhm, R., Jurkovic, A., Lipa, W., Orlik, A., Potzmann, R., Schoner, W., Ungersbock, M., Matulla, C., Briffa, K., Jones, P., Efthymiadis, D., Brunetti, M., Nanni, T., Maugeri, M., Mercalli, L., Mestre, O., Moisselin, J.M., Begert, M., Muller-Westermeier, G., Kveton, V., Bochnicek, O., Stastny, P., Lapin, M., Szalai, S., Szentimrey, T., Cegnar, T., Dolinar, M., Gajic-Capka, M., Zaninovic, K., Majstorovic, Z. and Nieplova, E. (2007). "HISTALP – historical instrumental climatological surface time series of the Greater Alpine Region"- Int. J. Climatol., 27, 17–46.

Bader, M.J., and Roach, W.T. 1977. "Orographic rainfall in warm sectors of depressions". Q. J. R. Meteorol. Soc., 103, 269-280.

Baonza, J. and Montouto, O. (2001). "Lycopodiella inundata (Lycopodiaceae) en el Parque Natural de Peñalara (Sierra de Guadarrama, Madrid). Síntesis corológica y conservación". Botanica Complutensis, 25, 299.

Barros, A. P. and Lettenmaier, D. P. (1993). "Dynamical modeling of the spatial distribution of precipitation in remote mountainous areas". Mon. Wea. Rev., 121, 1195–1214.

Barry, R. G. (2013). "Mountain Weather and Climate, Third Edition". Cambridge University Press; 2008; xxiv, 506 pp.; ISBN 978-0-521-86295-0.

Barstad, I., Grabowski, W. W. and Smolarkiewicz, P. K. (2007). "Characteristics of large-scale orographic precipitation: evaluation of linear model in idealized problems". J. Hydrology, 340, 78-90.

Barstad, I. and Smith, R.B. (2005). "Evaluation of an orographic precipitation model". J. Hydrometeorol., 6, 85-99.

Barstad, I., Sorteberg, A., Flatøy, F. and Déqué, M. (2008). "Precipitation, temperature and wind in Norway: dynamical downscaling of ERA40". Clim. Dyn., 33, 769-776.

Beniston, M. (2003). "Climatic change in mountain regions: a review of possible impacts". Climatic Change, 59, 5-31.

Beniston, M. (2006). "Mountain weather and climate: a general overview and a focus on climatic change in the Alps". Hydrobiologia, 562, 3-16.

Benoit, R., Desgagne, M., Pellerin, P., Pellerin, S., Chartier, Y. and Desjardins, S. (1997). "The Canadian MC2: A semi-Lagrangian semi-implicit wide-band atmospheric model suited for mesoscale process studies and simulation". Mon. Wea. Rev., 125, 2382–2415

Beranova, R. and Huth, R. (2008). "Time variations of the effects of circulation variability modes on European temperature and precipitation in winter". Int. J. Climatol., 28,139-158.

BOE 26th June 2013. Ref: BOE-A-2013-6900, pp 47795-47852.

Böhm, R., Jones, P.D., Hiebl, J., Frank, D., Brunetti, M. and Maugeri, M. (2009). "The early instrumental warm-bias: a solution for long central European temperature series 1760–2007". Climatic Change, 101, 41–67.

Bosch, J. and Martínez-Solano, I. (2006). "Chytrid fungus infection related to unusual mortalities of Salamandra salamandra and Bufo bufo in the Penalara Natural Park, Spain". Oryx, 40, 84-89.

Bosch J., Carrascal, L.M., Durán, L., Walker, S. and Fisher, M.C. (2007). "Climate change and outbreaks of amphibian chytridiomycosis in a montane area of Central Spain; is there a link?". Proc. Biol. Sci., 274, 253–260.

Bougeault, P., Binder, P., Buzzi, A., Dirks, R., Houze, R., Kuettner, J., Smith, R. B., Steinacker, R. and Volkert, H. (2001). "The MAP Special Observing Period". Bull. Amer. Met. Soc, 82, 433-462.

Bousquet, O. and Smull, B., (2006). "Observed mass transports accompanying upstream orographic blocking during MAP IOP8". Q. J. R. Met. Soc., 132, 2393-2413.

Broccoli, A. J. and Manabe, S. (1992). "The Effect of Orography on Midlatitude Northern Hemisphere Dry Climates", J. Clim., 5, 1181–1201.

Brock, F. V. and Richardson, S. J. (2001). "Meteorological Measurement Systems". Oxford University Press. ISBN-10: 0195134516, 290 pp.

Browning, K. A. (1986). "Conceptual models of precipitation systems". Weather and Forecasting, 1, 23-41.

Brugnara, Y., Brunetti, M., Maugeri, M., Nanni, T. and Simolo, C. (2012). "High-resolution analysis of daily precipitation trends in the central Alps over the last century". Int. J. Climatol., 32, 1406-1422.

Buytaert, W., Celleric, R. , Willemsc, P. , Bièvreb, B. and Wyseurea, G. (2006). "Spatial and temporal rainfall variability in mountainous areas: A case study from the south Ecuadorian Andes". J. Hydrology, 329, 413–421.

Buzzi, A. and Tibaldi, S. (1978). "Cyclogenesis in the lee of the Alps: A case study". Q. J. R. Met. Soc., 104, 271-287.

Cassou, C., Terray, L., Hurrell, J. W. and Deser, C. (2004). "North Atlantic winter climate regimes: Spatial asymmetry, stationarity with time, and oceanic forcing". J. Clim., 17, 1055–1068.

Castro, M., Gallardo, C., Jylha, K. and Tuomenvirta, H. (2007). "The use of a climate-type classification for assessing climate change effects in Europe from an ensemble of nine regional climate models". Climatic Change, 81, 329-341.

Chang, J. (ed.). (2012). "General circulation models of the atmosphere". Elsevier. 348 pp.

Cheval, S., Baciu, M., Dumitrescu, A., Breza, T., Legates, D. R., and Chendeş, V. (2011). "Climatologic adjustments to monthly precipitation in Romania". Int. J. Climatol., 31, 704-714.

Chvíla, B., Sevruk, B. and Ondrás, M. (2005). "The wind-induced loss of thunderstorm precipitation measurements". Atmos. Res., 77, 29-38.

Corte-Real, J., Qian, B. and Xu, H. (1998). "Regional climate change in Portugal: precipitation variability associated with large-scale atmospheric circulation". Int. J. Climatol., 18, 619–635.

Corte-Real, J., Xu, H. and Qian, B. (1999). "A weather generator for obtaining daily precipitation scenarios based on circulation patterns". Clim. Res. 13, 61–75.

Cortesi, N., Trigo, R. M., Gonzalez-Hidalgo, J. C. and Ramos, A. M. (2013). "Modelling monthly precipitation with circulation weather types for a dense network of stations over Iberia". Hydrol. Earth Sys. Sci., 17, 665-678.

Crochet, P., Jóhannesson, T., Jónsson, T., Sigurðsson, O., Björnsson, H., Pálsson, F. and Barstad, I. (2007). "Estimating the spatial distribution of precipitation in Iceland using a linear model of orographic precipitation". J. Hydrometeorol., 8, 1285-1306.

Daly, C., Neilson, R. P. and Phillips., D. L. (1994). "A statistical-topographic model for mapping climatological precipitation over mountainous terrain", J. Appl. Meteor., 33, 140-158.

Dominguez, M, Romera, R., Sanchez, E., Fita, L., Fernandez, J., Jimenez-Guerrero, P., Montavez, J. P., Cabos, W. D., Liguori, G. and Gaertner, M. A. (2013). "Present climate precipitation and temperature extremes over Spain from a set of high resolution RCMs", Clim. Res., 58, 149-164.

Durán, L. (2003). "Description and preliminary results of a Meteorological Network for High Altitudes". Geophys. Res. Abs., 5, 12466.

Durán, L. (2007). "Meteorología de montaña en el Parque Natural de Peñalara". Quintas Jornadas Científicas del Parque Natural de Peñalara y del Valle de El Paular, 1, 29-42.

Durán, L. and Sanchez, E. (2009). "Solar Radiation Calculation in a Mountain Region and its Relation with Other Environmental Parameters", Geophys. Res. Abs., 11, 9159.

Durán, L., Rodriguez-Fonseca, B., Sanchez-Sanchez, E. and Yagüe, C. (2012a): "Weather types and precipitation in the Iberian Central System", Geophys. Res. Abs., 14, 13428.

Durán, L., Sánchez, E. and Yagüe, C. (2012b): "Climatología pluviométrica de la Sierra de Guadarrama (1989-2010)", XXXII Jornadas Científicas de la Asociación Meteorológica Española: Meteorología y Calidad del Aire. ISBN: 978-84-695-6430-1.

Durán, L., Sánchez, E. and Yagüe, C. (2013). "Climatology of precipitation over the Iberian Central System mountain range". Int. J. Climatol., 33, 2260-2273.

Durán, L., Rodríguez, B., Yagüe, C. and Sánchez, E. (2014). "Patrones de flujo de vapor de agua, tipos de tiempo y precipitación en la Sierra de Guadarrama". XXXIII Jornadas Científicas de la AME, Oviedo.

Durán, L., Rodríguez-Fonseca, B., Yagüe, C. and Sánchez, E. (2015). "Water vapour flux patterns and precipitation at Sierra de Guadarrama mountain range (Spain)". Int. J. Climatol., 35, 1593-1610.

Durán, L. and Barstad, I. (2015). "Multi-scale validation of a Linear Model of Orographic Precipitation over Sierra de Guadarrama". To be submitted.

Durán, L. and Rodríguez-Muñoz, I. (2015a): "Developing a high resolution precipitation grid for Sierra de Guadarrama". International Symposium CLIMATE-ES 2015 - Progress on climate change detection and projections over Spain since the findings of the IPCC AR5 Report, Tortosa, Tarragona.

Durán, L. and Rodríguez-Muñoz, I. (2015b). "Automatic Monitoring of Weather and Climate at Mountain Areas. The Case of Peñalara Meteorological Network 1999-2014 ". To be submitted.

Esteban-Parra, M.J., Rodrigo, F.S. and Castro Díez, Y. (1998) "Spatial and temporal patterns of precipitation in Spain for the period 1880–1992". Int. J. Climatol., 18, 1557–1574.

Esteban, P., Jones, P. D., Martín-Vide, J. and Mases, M. (2005). "Atmospheric circulation patterns related to heavy snowfall days in Andorra, Pyrenees". Int. J. Climatol., 25, 319–329.

Fernandez-Mills, G. (2005) "Principal component analysis of precipitation and rainfall regionalization in Spain". Theor. Appl. Climatol., 50, 169-183.

Fernández-Montes S., Rodrigo, F. S., Seubert, S. and Sousa, P. M. (2013) "Spring and summer extreme temperatures in Iberia during las century in relation to circulation types". Atmos. Res., 127, 154-177.

Flato, G., J. Marotzke, B. Abiodun, P. Braconnot, S.C. Chou, W. Collins, P. Cox, F. Driouech, S. Emori, V. Eyring, C. Forest, P. Gleckler, E. Guilyardi, C. Jakob, V. Kattsov, C. Reason and Rummukainen, M. (2013). "Evaluation of Climate Models. In: Climate Change 2013: The Physical Science Basis". Contribution of Working Group I to the Fifth Assessment Report of the Intergovernmental Panel on Climate Change [Stocker, T.F., D. Qin, G.-K. Plattner, M. Tignor, S.K. Allen, J. Boschung, A. Nauels, Y. Xia, V. Bex and P.M. Midgley (eds.)]. Cambridge University Press, Cambridge, United Kingdom and New York, NY, USA.

Font-Tullot, I. (1983). "Climatología de España y Portugal". Madrid: Instituto Nacional de Meteorología. 296 pp.

Fortin, G., Perron, J. and Ilinca, A. (2005). "Behaviour and modeling of cup anemometers under Icing conditions". In 11th International Workshop on Atmospheric Icing of Structures, Montreal, Canada.

Frei, C. and Schär, C. (1998). "A precipitation climatology of the Alps from high-resolution rain-gauge observations", Int. J. Climatol., 18, 873-900.

Frei, C., Christensen, J. H., Déqué, M., Jacob, D., Jones, R. G. and Vidale, P. L. (2003). "Daily precipitation statistics in regional climate models: Evaluation and intercomparison for the European Alps". J. Geophys. Res.: Atmospheres, 108, 4124.

Gallego, M. C., J. A. García and J. M. Vaquero (2005). "The NAO signal in daily rainfall series over the Iberian Peninsula", Clim. Res., 29, 103-109.

García-Camacho, R., Albert, M. J. and Escudero, A. (2012). "Small-scale demographic compensation in a high-mountain endemic: the low edge stands still". Plant Ecology and Diversity, 5, 37-44.

García-Fernández, A., Iriondo, J. M., Bartels, D. and Escudero, A. (2013). "Response to artificial drying until drought-induced death in different elevation populations of a high-mountain plant". Plant Biology, 15, 93-100.

Garcia-Herrera, R., Hernández, E., Barriopedro, D., Paredes, D., Trigo, R. M., Trigo, I. F. and Mendes, M. A. (2007). "The outstanding 2004/05 drought in the Iberian Peninsula: associated atmospheric circulation". J. Hydrometeorol., 8, 483-498.

García-Romero, A., Muñoz, J., Andrés, N. and Palacios, D. (2010). "Relationship between climate change and vegetation distribution in the Mediterranean mountains: Manzanares Head valley, Sierra De Guadarrama (Central Spain)", Climatic Change, 100, 645-666.

García-Valero J. A, Montavez J. P., Jerez S., Gómez-Navarro J. J., Lorente-Plazas R. and Jiménez-Guerrero P. (2012). "A seasonal study of the atmospheric dynamics over the Iberian Peninsula based on circulation types". Theor. Appl. Climatol., 110, 291–310.

Gavilán, R., Fernández, F. and Blasi, C. (1998). "Climatic classification and ordination of the Spanish Sistema Central; relationships with potential vegetation". Plant Ecology 139, 1–11.

Geiger, R. (1965). "The climate near the ground". 5. edn., 1–611 p., Harvard University Press.

Génova, M. (2012). "Extreme pointer years in tree-ring records of Central Spain as evidence of climatic events and the eruption of the Huaynaputina Volcano (Peru, 1600 AD)". Clim. Past, 8, 751-764.

Gesch, D. B., Verdin, K. L. and Greenlee, S. K. (1999). "New land surface digital elevation model covers the Earth". EOS, Transactions American Geophysical Union, 80, 69-70.

Gimeno, L., Nieto, R., Trigo, R. M., Vicente-Serrano, S. M. and López-Moreno, J. I. (2010). "Where does the Iberian Peninsula moisture come from? An answer based on a Lagrangian approach". J. Hydrometeorol., 11, 421-436.

Giovannini, L., Zardi, D. and De Franceschi, M. (2011). "Analysis of the urban thermal fingerprint of the city of Trento in the Alps". J. Appl. Meteor. Climatol., 50, 1145-1162.

Giorgi, F. and Mearns, L. O. (1991). "Approaches to the simulation of regional climate change: A review". Rev. Geophys., 29, 191–216.

Gómez-González, C., Ruiz Zapata, M. B., García, G., José, M., López Saez, J. A., Santisteban, J. I., Mediavilla-López, R. M., Dominguez-Castro, F. and Vera López, S. (2009). "Evolución del paisaje vegetal durante los últimos 1.680 años BP en el Macizo de Peñalara (Sierra de Guadarrama, Madrid)". Revista española de micropaleontología, 41, 75-89.

Gonzalez-Rouco, J.F., Jimenez, J. L., Quesada, V. and Valero, F. (2001). "Quality Control and Homogeneity of Precipitation Data in the Southwest of Europe". J. Clim., 14, 964-978.

Goodess, C. M. and Jones, P. D. (2002). "Links between circulation and changes in the characteristics of Iberian rainfall", Int. J. Climatol., 22, 1593-1615.

Goodison, B. E., Sevruk, B., and Klemm, S. (1989). "WMO solid precipitation measurement intercomparison: Objectives, methodology, analysis". Atmospheric Deposition, 179, 57-64.

Goovaerts, P. (2000). "Geostatistical approaches for incorporating elevation into the spatial interpolation of rainfall", J. Hydrology, 228, 113-129.

Gottfried, M., Pauli, H., Futschik, A., Akhalkatsi, M., Barancok, P., Benito-Alonso, J.L., Coldea, G., Dick, J. Erschbamer, B., Fernandez-Calzado, M.R., Kazakis, G., Krajci, J., Larsson, P., Mallaun, M., Michelsen, O. Moiseev, D. Moiseev, P., Molau, U., Merzouki, A., Nagy, L., Nakhutsrishvili, G., Pedersen, B., Pelino, G., Puscas, M., Rossi, G., Stanisci, A., Theurillat, J.-P., Tomaselli, M., Villar, L. Vittoz, P., Vogiatzakis, I. and Grabherr, G. (2012). "Continent-wide response of mountain vegetation to climate change". Nature Climate Change, 2, 111-115

Granados, I., del Olmo, C. M., Robles, S. and Toro, M. (2006). "High mountain lakes of the Central Range (Iberian Peninsula): Regional limnology and environmental changes". Limnetica, 25, 217-252.

Granados, I. (2007). "¿Cómo cambiará la laguna Grande de Peñalara frente al cambio climático?". Actas de las Quintas Jornadas Científicas del Parque Natural de Peñalara y Valle de El Paular. Consejería de Medio Ambiente y Ordenación del Territorio. Comunidad de Madrid. Comunidad de Madrid, 1998-2009. Actas de las Jornadas Científicas del Parque Natural de Peñalara y el Valle de El Paular.

Granados, I. (2011). "¿Se puede medir el cambio global en Peñalara?". Foresta, 52, 28-29.

Grell, G. A., Dudhia, J. and Stauffer, D.R. (1995). "A description of the fifth generation Penn State/NCAR Mesoscale Model (MM5)". NCAR Tech. Note NCAR/TN-398

Groisman, P. Y. and Legates, D. R. (1994). "The accuracy of United States precipitation data". Bull. Amer. Meteor. Soc., 75, 215-227.

Guan, H., Wilson, J. L. and Makhnin, O. (2005). "Geostatistical Mapping of Mountain Precipitation Incorporating Autosearched Effects of Terrain and Climatic Characteristics". J. Hydrometeor., 6, 1018-1031.

Guemas, V., Salas-Mélia, D., Kageyama, M., Giordani, H., Voldoire, A. and Sanchez-Gomez, E. (2010). "Summer interactions between weather regimes and surface ocean in the North-Atlantic region". Clim. Dyn., 34, 527-546.

Gutiérrez-Girón, A. and Gavilán, R. G. (2010). "Spatial patterns and interspecific relations analysis help to better understand species distribution patterns in a Mediterranean high mountain grassland". Plant ecology, 210, 137-151.

Hartigan, J.A. and Wong, M. A. (1979). "Algorithm AS 136: A K-Means Clustering Algorithm", J. Roy. Statist. Soc. Series C (Applied Statistics), 28, 100-108.

Haylock, M. R., Hofstra, N., Klein-Tank, A. M. G., Klok, E. J., Jones, P. D. and New, M. (2008). "A European daily high-resolution gridded data set of surface temperature and precipitation for 1950–2006". J. Geophys. Res., 113, D20119.

Hazeu, G. W., Roupioz, L. F. S. and Perez-Soba, M. (2010). "Europe's ecological backbone: recognising the true value of our mountains" (No. 6, p. 225). Schutlz Grafisk.

Hedberg, O. (1964). "The phytogeographical position of the afroalpine flora". Recent Advances in Botany, 1, 914–919.

Henn, B., Raleigh, M. S., Fisher, A. and Lundquist, J.D. (2013). "A Comparison of Methods for Filling Gaps in Hourly Near-Surface Air Temperature Data". J. Hydrometeor, 14, 929–945.

Herrera, S., Fita, L., Fernández, J. and Gutiérrez, J.M. (2010). "Evaluation of the mean and extreme precipitation regimes from the ENSEMBLES regional climate multimodel simulations over Spain", J. Geophys. Res., 115, D21117.

Herrera, S., Gutiérrez, J.M., Ancell, R., Pons, M. R., Frías, M. D. and Fernández, J. (2012). "Development and analysis of a 50-year high-resolution daily gridded precipitation dataset over Spain (Spain02)". Int. J. Climatol., 32, 74-85.

Hodur, R. M. (1997). "The Naval Research Laboratory's Coupled Ocean/Atmosphere Mesoscale Prediction System (COAMPS)". Mon. Wea. Rev., 125, 1414–1430

Horcajada, F. (2011). "Genética de las poblaciones de corzo en el Parque Natural de Peñalara". Foresta, 52, 368-371.

Huber, U.M., Bugmann, H.K.M. and Reasoner, M. A. (2005). "Global Change and Mountain Regions: An Overview of Current Knowledge". Springer, Dordrecht. 650 pp.

Hughes, M., Hall, A. and Fovell, R. G. (2009). "Blocking in areas of complex topography, and its influence on rainfall distribution". J. Atmos. Sci., 66, 508-518.

Hurrell, J. W., Kushnir, Y., Ottersen, G. and Visbeck, M. (2003). "An overview of the North Atlantic oscillation". Geophysical Monograph-American Geophysical Union, 134, 1-36.

Inclán, R. M., De la Torre, D., Benito, M. and Rubio, A. (2007). "Soil CO2 efflux in a mixed pine-oak forest in Valsaín (Central, Spain)". The Scientific World, 7, 166-174.

Inclán, R.M., Uribe, C., De La Torre, D., Sánchez, M.D., Clavero, M.A., Fernández, A., Morante, R., Cardeña, A., Fernández, M. and Rubio, A. (2010). "Carbon dioxide fluxes across the Sierra de Guadarrama, Spain". European Journal of Forest Research, 129 , 93-100.

Inclán R.M, Gimeno, B.S., Peñuelas, J., Gerant, D. and Quejido, A. (2011). "Carbon Isotope Composition, Macronutrient Concentrations, and Carboxylating Enzymes in Relation to the Growth of Pinus halepensis Mill. When Subject to Ozone Stress". Water Air and Soil Pollution, 214, 587-598.

IPCC (2013). "*Climate Change 2013: The Physical Science Basis. Contribution of Working Group I to the Fifth Assessment Report of the Intergovernmental Panel on Climate Change".* [Stocker, T.F., D. Qin, G.-K. Plattner, M. Tignor, S.K. Allen, J. Boschung, A. Nauels, Y. Xia, V. Bex and P.M. Midgley (eds.)]. Cambridge University Press, Cambridge, United Kingdom and New York, NY, USA, 1535 pp.

Isotta, F. A., Vogel, R. and Frei, C. (2015). "Evaluation of European regional reanalyses and downscalings for precipitation in the Alpine region". Meteorologische Zeitschrift, 24, 15-37.

Iturrioz, I., Hernández, E., Ribera, P., and Queralt, S. (2007). "Instability and its relation to precipitation over the Eastern Iberian Peninsula". Adv. Geos., 10, 45-50.

Jacob, D., Bärring, L., Christensen, O.B., Christensen, J.H., de Castro, M., Deque, M., Giorgi, F., Hagemann, S., Hirschi, M., Jones, R., Kjellström, E., Lenderink, G., Rockel, B., Sanchez, E., Schär, C., Seneviratne, S.I., Somot, S., van Ulden, A. and van den Hurk B.(2007). "An inter-comparison of regional climate models for Europe: Model performance in Present-Day Climate". Climatic Change, 81, 31-52.

James, P. E. (1922). "Köppen's Classification of Climates: a Review". Mon. Wea. Rev., 50, 69-72.

Jiménez-Guerrero, P., Montávez, J.P., Domínguez, M., Romera, R., Fita, L., Fernández, J., Cabos, W.D., Liguori, G. and Gaertner, M.A. (2013). "Description of mean fields and interannual variability in an ensemble of RCM evaluation simulations over Spain: results from the ESCENA project", Clim. Res., 57, 201-220.

de Jong, C., Lawler, D. and Essery, R. (2009). "Mountain Hydroclimatology and Snow Seasonality– Perspectives on climate impacts, snow seasonality and hydrological change in mountain environments", Hydrol. Proc., 23, 955-961.

Juez, J. V. (2011). "El buitre negro en el Parque Natural de Peñalara". Foresta, 52, 363-365.

Jungo, P. and Beniston, M. (2001). "Changes in the anomalies of extreme temperature anomalies in the 20th century at Swiss climatological stations located at different latitudes and altitudes". Theor. Appl. Climatol., 69, 1-12.

Knight, J. R., Folland, C. K. and Scaife, A. A. (2006). "Climate impacts of the Atlantic multidecadal oscillation". Geophys. Res. Lett., 33, L17706.

Kunz, M. and Kottmeier, C. (2006). "Orographic Enhancement of Precipitation over Low Mountain Ranges. Part II: Simulations of Heavy Precipitation Events over Southwest Germany", J. Appl. Meteor. Climatol., 45, 1041–1055.

Kyriakidis, P. C., Kim, J. and Miller, N. L. (2001). "Geostatistical Mapping of Precipitation from Rain Gauge Data Using Atmospheric and Terrain Characteristics", J. Appl. Meteor., 40, 1855-1877.

Lavers, D. A. and Villarini, G. (2013). "The nexus between atmospheric rivers and extreme precipitation across Europe". Geophys. Res. Lett., 40, 3259–3264.

Leroy, M., Tammelin, B., Hyvönen, R., Rast, J. and Musa, M. (2002). "Temperature and humidity measurements during icing conditions". WMO Technical Conference on Meteorological and Environmental Instruments and Methods of Observation.

Lopez-Franca, N., Sanchez, E., Losada, T., Dominguez, M., Romera, R. and Gaertner, M. A. (2015). "Markovian characteristics of dry spells over the Iberian Peninsula under present and future conditions using regional climate models" Clim. Dyn., 45, 661-677.

Lo, Y-H.., Blanco, J.A., Seely, B., Welham, C. and Kimmins, J.P. (2011). "Generating reliable meteorological data in mountainous areas with scarce presence of weather records: The performance of MTCLIM in interior

British Columbia, Canada", Environmental Modelling and Software, 26, 5, 644-657.

López, R. and Justribó, C. (2010). "The hydrological significance of mountains: a regional case study, the Ebro River basin, northeast Iberian Peninsula", Hydrol. Sci., 55, 223-233.

López-Moreno, J.I. and García-Ruiz, J.M. (2004). "Influence of snow accumulation and snowmelt on streamflow in the Central Spanish Pyrenees". Hydrol. Sci. J., 49, 787-802.

López-Moreno, J. I., Beniston, M. and García-Ruiz, J.M. (2008). "Environmental change and water management in the Pyrenees: Facts and future perspectives for Mediterranean mountains", Glob. Pla. Change, 61, 300-312.

López-Moreno, J. I., Goyette, S. and Beniston, M. (2009). "Impact of climate change on snowpack in the Pyrenees: Horizontal spatial variability and vertical gradients". J. Hydrol., 374, 384-396.

Losada, T., Rodríguez-Fonseca, B., Mechoso, C. R. and Ma, H. Y. (2007). "Impacts of SST anomalies on the North Atlantic atmospheric circulation: a case study for the northern winter 1995/1996". Clim. Dyn., 29, 807-819.

Lurgi, M., López, B. C. and Montoya, J. M. (2012). "Climate change impacts on body size and food web structure on mountain ecosystems". Philosophical Transactions of the Royal Society of London B: Biological Sciences, 367, 3050-3057.

Makkonen, L., Lehtonen, P. and Helle, L. (2001). "Anemometry in icing conditions". J. Atmos. Oc.eanic Technology, 18, 1457-1469.

Marquínez, J., Lastra, J. and García, P. (2003) "Estimation models for precipitation in mountainous regions: the use of GIS and multivariate analysis", J. Hydrology, 270, 1-11.

Martínez de Pisón, E. (2006). "En torno al Guadarrama". Madrid : La Librería, 266 pp.

Martín-Vide, J. (2004). "Spatial distribution of a daily precipitation concentration index in peninsular Spain". Int. J. Climatol., 24, 959-971.

McGill, R., Tukey, J. W. and Larse, W. A. (1978). "Variations of Boxplots". The American Statistician., 32, 1, 12–16.

Medina, S., Smull, B. F., Houze Jr, R. A. and Steiner, M. (2005). "Cross-barrier flow during orographic precipitation events: Results from MAP and IMPROVE". J. Atmos. Sci., 62, 3580-3598.

Mera, A. G. D., Perea, E. L. and Orellana, J. A. V. (2012). "Taraxacum penyalarense (Asteraceae), a new species from the Central Mountains of Spain". Annales Botanici Fennici, 49, 91-94.

Merrill, R. M., Gutiérrez, D., Lewis, O. T., Gutiérrez, J., Díez, S. B. and Wilson, R. J. (2008). "Combined effects of climate and biotic interactions on the elevational range of a phytophagous insect". J. Animal Ecology, 77, 145-155.

Michalakes, J., Chen, S., Dudhia, J., Hart, L., Klemp, J., Middlecoff, J. and Skamarock, W. (2001). "Development of a next generation regional weather research and forecast model". In Developments in Teracomputing: Proceedings of the Ninth ECMWF Workshop on the use of high performance computing in meteorology, 1, 269-276.

Michelangeli, P., Vautard, R. and Legras, B. (1995). "Weather regime recurrence and quasi stationarity". J. Atmos. Sci., 52, 1237–1256.

Mo, K. and Ghil, M. (1988). "Cluster analysis of multiple planetary flow regimes, J. Geophys. Res., 93, 10927–10952.

Moeslund, J. E., Arge, L., Bøcher, P. K., Dalgaard, T. and Svenning, J. C. (2013). "Topography as a driver of local terrestrial vascular plant diversity patterns". Nordic Journal of Botany, 31, 129-144.

Momjian, B. (2001). "PostgreSQL: introduction and concepts". (Vol. 192). New York: Addison-Wesley. 365 pp.

Montouto-González O. (2000). "La flora vascular rara, endémica y amenazada del Parque Natural de Peñalara y su entorno. Amenazas y necesidades de conservación en la Finca de los Cotos". Segundas Jornadas Científicas del Parque Natural de Peñalara y Valle de El Paular. Comunidad de Madrid. Consejería de Medio Ambiente. D.G. del Medio Rural.

Moreno, J. L. I. (2011). "La flora protegida de Peñalara". Foresta, 52, 350-354.

Moron, V., Robertson, A. W., Ward, M. N. and Ndiaye, O. (2008). "Weather types and rainfall over Senegal. Part I: Observational analysis", J. Clim., 21, 266-287.

Muñoz-Díaz, D. and Rodrigo, F. S. (2004). "Impacts of the North Atlantic Oscillation on the probability of dry and wet winters in Spain". Clim. Res., 27, 33-43.

Neiman, P.J., Ralph, F. M., Wick, G. A., Lundqist, J. D. and Dettinger, M. D. (2008). "Meteorological Characteristics and Overland Precipitation Impacts of Atmospheric Rivers Affecting the West Coast of North America Based on Eight Years of SSM/I Satellite Observations". J. Hydrometeor., 9, 22–47.

New, M., Hulme, M. and Jones, P. D. (1999). "Representing twentieth century space-time climate variability, 1, Development of a 1961–90 mean monthly terrestrial climatology". J. Clim., 12, 829–856.

Nitu, R., Rasmussen, R., Hendrikx, J., Baker, B., Joe, P., Yang, D., Smith, C., Earle, M. E., Lanzinger, E., Kochendorfer, J., Roulet, Y., Wolff, M., Goodison, B. E., Liang, H., Vuglinsky, V., Timofeev, A., Koldaev, A., Sabarini, F., Mrozinski, L., Bilish, S., MacDonell, S., Aulamo, O., Harper, A., (2012). "WMO Intercomparison of Instruments and methods for the measurement of Solid Precipitation and Snow on the Ground: Organization of the formal experiment". WMO, IOM No. 109, TECO-2012.

North, G. R., Bell, T. L. and Cahalan, R.F. (1982). "Sampling errors in the estimation of empirical orthogonal functions". Mon. Wea. Rev., 110, 699 – 706.

Ortiz-Beviá, M. J., Sánchez-Gómez, E. and Alvarez-García, F. J. (2011). "North Atlantic atmospheric regimes and winter extremes in the Iberian peninsula". Nat. Hazards Earth Sys. Sci., 11, 971-980.

Ortiz-Santaliestra, M. E., Fisher, M. C., Fernández-Beaskoetxea, S. A. I. O. A., Fernández-Benéitez, M. J. and Bosch, J. (2011). "Ambient ultraviolet B radiation and prevalence of infection by Batrachochytrium dendrobatidis in two amphibian species". Conservation Biology, 25, 975-982.

Palacios, D. and Sánchez-Colomer, M. G. (1997). "The influence of geomorphologic heritage on present nival erosion: Peñalara, Spain". Geografiska Annaler: Series A, Physical Geography, 79, 25-40.

Palacios, D., de Andrés, N. and Luengo, E. (2003). "Distribution and effectiveness of nivation in Mediterranean mountains: Peñalara (Spain)".Geomorphology, 54, 157-178.

Palacios, D., de Andrés, N., de Marcos, J., and Vázquez-Selem, L. (2012). "Glacial landforms and their paleoclimatic significance in Sierra de Guadarrama, Central Iberian Peninsula". Geomorphology, 139, 67-78.

Panziera, L., Giovannini, L., Laiti, L. and Zardi, D. (2015). "The relation between circulation types and regional Alpine climate. Part I: synoptic climatology of Trentino". Int. J. Climatol., doi: 10.1002/joc.4314.

Paredes, D., Trigo, R. M., Garcia-Herrera, R. and Trigo, I. F. (2006). "Understanding precipitation changes in Iberia in early spring: weather typing and storm-tracking approaches". J. Hydrometeor., 7, 101-113.

Paulat, M., Frei, C. and Hagen, M. (2008). "A gridded dataset of hourly precipitation in Germany: Its construction, climatology and application". Met. Zeitschrift, 17, 719-732.

Pedraza, J.; Carrasco, R.M.; Martín-Duque, J.F. and Sanz Santos, M.A. (2004). "El Macizo de Peñalara (Sistema Central Español). Morfoestructura y modelado". Boletín de la Real Sociedad Española de Historia Natural Sección Geológica, 99, 185-196.

Pérez, J. B. (2011). "Los anfibios de Peñalara vuelven al paraíso". Foresta, 52, 366-367.

Peixoto, J.P and Oort, A.H. (1992). Physics of Climate. American Institute of Physics, 520 pp.

Pepin, N.C. and Seidel, D.J. (2005). "A global comparison of surface and free-air temperatures at high elevations". J. Geophys. Res., 110, D03104.

Pielke, R. A., Cotton, W. R., Walko, R. E. A., Tremback, C. J., Lyons, W. A., Grasso, L. D., Nichols, M. E., Moran, M. D.., Wesley D. A., Lee T. J. and Copeland, J. H. (1992). "A comprehensive meteorological modeling system– RAMS". Meteor. Atmos. Phys., 49, 69-91.

Polo, I., Ullmann ,A., Roucou, P. and Fontaine, B. (2011). "Weather Regimes in the Euro-Atlantic and Mediterranean Sector, and Relationship with West African Rainfall over the 1989–2008 Period from a Self-Organizing Maps Approach". J. Clim., 24, 3423–3432.

Queney, P., (1947). "Theory of perturbations in stratified currents with applications to airflow over mountain barriers". Dept. of Meteorology,Univ. of Chicago, Miscellaneous Rep. 23, 81 pp.

Rasmuson, E. M. (1968). "Atmospheric Water Vapor Transport and the Water Balance of North America". Mon. Wea. Rev., 96, 720–734.

Rasmussen, R., Baker, B. , Kochendorfer, J., Meyers, T., Landolt, S., Fischer, A. P., Black, J., Thériault, J. M., Kucera, P., Gochis, D., Smith, C., Nitu, R., Hall, M., Ikeda, K. and Gutmann, E. (2012). "How Well Are We Measuring Snow: The NOAA/FAA/NCAR Winter Precipitation Test Bed". Bull. Amer. Meteor. Soc., 93, 811-829.

Rath, V. (2012). "GUMNET-A new subsurface observatory in the Guadarrama Mountains, Spain". Geophys. Res. Abs., 14, 6475.

Rath, V., Fidel González Rouco, J., and Yagüe Anguis, C. (2014). "GUMNET-A new long-term monitoring initiative in the Guadarrama Mountains, Madrid, Spain". Geophys. Res. Abs., 16, 7124.

Rauscher, S. A., Coppola, E., Piani, C. and Giorgi, F. (2010). "Resolution effects on regional climate model simulations of seasonal precipitation over Europe". Clim. Dyn., 35, 685-711.

Richter, I. and Mechoso, C. R. (2006). "Orographic influences on subtropical stratocumulus". J. Atmos. Sci., 63, 2585-2601.

Riddle, E. E., Stoner, M. B., Johnson, N. C., L'Heureux, M. L., Collins, D. C. and Feldstein, S. B. (2012). "The impact of the MJO on clusters of wintertime circulation anomalies over the North American region". Clim. Dyn., 40, 1749-1766.

Rodó, X., Baert, E., and Comin, F. A. (1997). "Variations in seasonal rainfall in Southern Europe during the present century: relationships with the North Atlantic Oscillation and the El Niño-Southern Oscillation". Climate Dynamics, 13(4), 275-284.

Rodriguez-Fonseca, B. and de Castro, M. (2002). "On the connection between winter anomalous precipitation in the Iberian Peninsula and North West Africa and the summer subtropical Atlantic sea surface temperature". Geophys. Res. Lett., 29(18), 10-1.

Rodríguez-Fonseca, B. and Serrano, E. (2002). "Winter 10-Day Coupled Patterns between Geopotential Height and Iberian Peninsula Rainfall Using the ECMWF Precipitation Reanalysis". J. Clim., 15, 1309-1321.

Rodríguez-Fonseca, B., Polo, I., Serrano, E. and Castro, M. (2006). "Evaluation of the North Atlantic SST forcing on the European and Northern African winter climate". Int. J. Climatol., 26, 179-191.

Rodríguez-Puebla, C., Encinas, A. H., Nieto, S. and Garmendia, J. (1998) "Spatial and temporal patterns of annual precipitation variability over the Iberian Peninsula", Int. J. Climatol, 18, 299-316.

Rodríguez-Puebla, C., Encinas, A. H. and Saenz, J. (2001). "Winter precipitation over the Iberian peninsula and its relationship to circulation indices", Hydrology and Earth System Sciences, 5, 233-244.

Rojas, M., Li, L. Z. , Kanakidou, M., Hatzianastassiou, N., Seze, G. and Le Treut, H. (2013). "Winter weather regimes over the Mediterranean region: their role for the regional climate and projected changes in the twenty-first century", Clim. Dyn., 41, 551-571.

Rolland, C. (2003). "Spatial and seasonal variations of air temperature lapse rates in Alpine regions". J. Clim., 16, 1032-1046.

Romero R., Sumner, G., Ramis, C. and Genovés A. (1999a). "A classification of the atmospheric circulation patterns producing significant daily rainfall in the Spanish Mediterranean area", Int. J. Climatol., 19, 765–785.

Romero, R., Ramis, C., Guijarro, J. A. and Sumner, G. (1999b). "Daily rainfall affinity areas in the Mediterranean Spain". Int. J. Climatol. 19, 557-578.

Ruiz-Labourdette, D., Schmitz, M. F. and Pineda, F. D. (2013). "Changes in tree species composition in Mediterranean mountains under climate change: indicators for conservation planning". Ecological Indicators, 24, 310-323.

Ruíz Zapata, M. B., Gómez González, C., López Sáez, J. A. and Vera, M. S. (2009). "Reconstrucción de las condiciones paleoambientales del depósito Pñ (Macizo de Peñalara, Sierra de Guadarrama. Madrid), durante los últimos 2.000 años, a partir del contenido en microfósiles no polínicos (NPPs)". Geogaceta, 46, 135-138.

Salvati, M. and Brambilla, E. (2008). "Data Quality Control Procedures in Alpine Metereological Services". Università di Trento. Dipartimento di ingegneria civile e ambientale.

Sánchez-López, G., Hernández, A., Pla-Rabes, S., Toro, M., Granados, I., Sigró, J., Trigo, R.M., Rubio-Inglés, M.J., Camarero, L., Valero-Garcés, B. and Giralt, S. (2015). "The effects of the NAO on the ice phenology of Spanish alpine lakes". Climatic Change, 130, 1-13.

Sánchez, E., Domínguez, M., Romera, R., López de la Franca, N., Gaertner, M. A., Gallardo, C. and Castro, M. (2011). "Regional modeling of dry spells over the Iberian Peninsula for present climate and climate change conditions". Climatic Change, 107, 625-634.

Sancho, L. G., De la Torre, R., Horneck, G., Ascaso, C., de los Rios, A., Pintado, A., Wierzchos, J. and Schuster, M. (2007). "Lichens survive in space: results from the 2005 LICHENS experiment". Astrobiology, 7, 443-454.

Santolaria-Canales E. and the GuMNet Consortium Team (2015). "GuMNet - Guadarrama Monitoring Network. Installation and set up of a high altitude monitoring network, north of Madrid. Spain". Geophys. Res. Abs., 17, 13989.

Santos, J.A., Corte-Real, J. and Leite, S.M. (2005). "Weather regimes and their connection to the winter rainfall in Portugal", Int. J. Climatol., 25, 33-50.

Sanz-Elorza, M., Dana, E. D., González, A. and Sobrino, E. (2003). "Changes in the High-mountain Vegetation of the Central Iberian Peninsula as a Probable Sign of Global Warming". Annals of Botany, 92, 273-280.

Sawyer, J.S. (1962). "Gravity waves in the atmosphere as a threedimensional problem". Q. J. R. Meteor. Soc., 88, 412–425.

Schär, C. and Frei, C. (2005). "Orographic precipitation and climate change". In Global Change and Mountain Regions, 255-266. Springer Netherlands.

Schroeter, B., Sancho, L. G. and Valladares, F. (1999). "In situ comparison of daily photosynthetic activity patterns of saxicolous lichens and mosses in Sierra de Guadarrama, Central Spain". Bryologist, 102, 623-633.

Schotterer, U., Grosjean, M., Stichler, W., Ginot, P., Kull, C., Bonnaveira, H., Francou, B., Gäggeler, H.W., Gallaire, R., Hoffmann, G., Pouyaud, B., Ramirez, E., Schwikowski, M. and Taupin, J.D. (2003). "Glaciers and climate in the Andes between the Equator and 30° S: What is recorded under extreme environmental conditions?". In Climate Variability and Change in High Elevation Regions: Past, Present and Future, 157-175. Springer Netherlands.

Schuler, T. V., Crochet, P., Hock, R., Jackson, M., Barstad, I. and Johannesson, T. (2008). "Distribution of snow accumulation on the Svartisen ice cap, Norway, assessed by a model of orographic precipitation." Hydrological processes, 22, 3998-4008.

Schwaiger, H. P. and Bird, D. N. (2010). "Integration of albedo effects caused by land use change into the climate balance: Should we still account in greenhouse gas units?". Forest Ecology and Management, 260, 278-286.

Seidel, D. J. and Free, M. (2003). "Comparison of lower-tropospheric temperature climatologies and trends at low and high elevation radiosonde sites". Climatic Change 59, 53–74.

Serrano, A., García, J. A., Mateos, V. L., Cancillo, M. L. and Garrido, J. (1999). "Monthly Modes of Variation of Precipitation over the Iberian Peninsula". J. Clim., 12, 2894-2919.

Sevruk, B. (1996). "Adjustment of tipping-bucket precipitation gauge measurements". Atmos. Res., 42, 237-246.

Sevruk, B. and Klemm, S. (1989). "Catalogue of national standard precipitation gauges". World Meteorological Organization, 50 pp.

Shafer, M. A., Fiebrich, C. A., Arndt, D. S., Fredrickson, S. E. and Hughes, T. W. (2000). "Quality assurance procedures in the Oklahoma Mesonetwork". Journal of Atmospheric and Oceanic Technology, 17, 474-494.

Sieck, L. C., Burges, S. J. and Steiner, M. (2007). "Challenges in obtaining reliable measurements of point rainfall". Water Resources Research, 43. W01420.

Smiatek, G.H., Kunstmann, R., Knoche, R. and Marx, A. (2009). "Precipitation and temperature statistics in high-resolution regional climate models: evaluation for the European Alps". J. Geophys. Res., 114, D19107.

Smith, R. B. (1979). "The influence of mountains on the atmosphere". Adv. Ggeophys., 21, 87-230.

Smith, R. B. (2003). "A linear time-delay model of orographic precipitation". J. Hydrol., 282, 2–9.

Smith, R. B. and Grønas, S. (1993). "Stagnation points and bifurcation in 3-D mountain airflow". Tellus, 45A, 28–43.

Smith, R. B. and Barstad, I. (2004). "A linear theory of orographic precipitation". J. Atmos. Sci., 61, 1377-1391.

Smith, R. B, Barstad I. and Bonneau, L. (2005). "Orographic precipitation and Oregon's climate transition". J. Atmos. Sci., 62, 177–191.

Smith, R. B. and Evans, J. P. (2007). "Orographic precipitation and water vapor fractionation over the southern Andes". J. Hydromet., 8, 3-19.

Soares, P. M., Cardoso, R. M., Miranda, P. M., de Medeiros, J., Belo-Pereira, M. and Espirito-Santo, F. (2012). "WRF high resolution dynamical downscaling of ERA-Interim for Portugal". Clim. Dyn., 39, 2497-2522.

Toro, M., Granados, I., Robles, S. and Montes, C. (2006), "High mountain lakes of Central Range (Iberian Peninsula): regional limnology and environmental changes". Limnetica 25, 217–252.

Trigo, R. M. and DaCamara, C. C. (2000). "Circulation weather types and their influence on the precipitation regime in Portugal". Int. J. Climatol., 20, 1559-1581.

Trigo, R. M. and Palutikof, J. P. (2001). "Precipitation Scenarios over Iberia: A Comparison between Direct GCM Output and Different Downscaling Techniques". J. Clim., 14, 4422–4446.

Trigo, R.M., Pozo-Vázquez, D., Osborn, T. J., Castro-Díez, Y., Gámiz-Fortis, S. and Esteban-Parra, M. J. (2004) "North Atlantic oscillation influence on precipitation, river flow and water resources in the Iberian Peninsula", Int. J. Climatol., 24, 925-944.

Uppala, S., Dee, D., Kobayashi, S., Berrisford, P. and Simmons, A., (2008). "Towards a climate data assimilation system: status update of ERA Interim". ECMWF Newsletter, 115, 12-18.

Van Rossum, G. and Drake Jr, F. L. (1995). "Python reference manual". Amsterdam: Centrum voor Wiskunde en Informatica.

Vicente-Serrano, S. M., Trigo, R. M., López-Moreno, J. I., Liberato, M. L. R., Lorenzo-Lacruz, J., Beguería, S., Morán-Tejeda, E. and El Kenawy, A. (2011). "Extreme winter precipitation in the Iberian Peninsula in 2010: anomalies, driving mechanisms and future projections", Clim. Res., 46, 51–65.

Von Storch, H. and Zwiers, F. W. (2001). "Statistical analysis in climate research". Cambridge University Press, 484 pp.

Wang, F., Gonzalez, P., Notaro, M., Vimont, D. and Williams, J. W. (2013). "IPCC AR5 climate projections and exposure assessments for the US National Park System". In AGU Fall Meeting Abstracts, 1, 1059.

Warner, M. D., Mass, C. F. and Salathé Jr, E. P. (2012). "Wintertime Extreme Precipitation Events along the Pacific Northwest Coast: Climatology and Synoptic Evolution". Mon. Wea. Rev., 140, 2021-2043.

Whiteman, C. D. (2000). "Mountain meteorology: fundamentals and applications" (No. PNNL-12063). Pacific Northwest National Laboratory, Richland, WA (US). 376 pp.

Wilks, D. S. (2011). "Statistical methods in the atmospheric sciences". Academic press. 676 pp.

Wilson, R. J., Gutiérrez, D., Gutiérrez, J., Martínez, D., Agudo, R. and Monserrat, V. J. (2005). "Changes to the elevational limits and extent of species ranges associated with climate change". Ecol. Lett., 8, 1138-1146.

WMO World Meteorological Organization (2008). "Guide to Meteorological Instruments and Methods of Observation". WMO-No. 8. 7. Meteorological Organization, 978-92-63-100085, 681 pp.

Woodruff, S. D., Diaz, H. F., Elms, J. D. and Worley, S. J. (1998). "COADS Release 2 data and metadata enhancements for improvements of marine surface flux fields". Phys. Chem. Earth, 23, 517-526.

World Meteorological Organization. (2008). "Guide to Meteorological Instruments and Methods of Observation". WMO-No. 8, Seventh edition, 2008. 680 pp.

Wurtele, M. G., Sharman, R. D. and Datta, A. (1996). "Atmospheric lee waves". Annu. Rev. Fluid Mech., 28, 429–476.

Yasunari, T., Saito K. and Takata K. (2006). "Relative role of large-scale orography and land surface processes in the global hydroclimate. Part I: Impacts on monsoon systems and the tropics". J. Hydrometeor., 7, 626-641.

Zängl, G. (2007). "Interaction between dynamics and cloud microphysics in orographic precipitation enhancement: A high-resolution modeling study of two North Alpine heavy-precipitation events". Mon. Wea. Rev., 135, 2817-2840.

Zhang, Q., Xu, C. Y., Zhang, Z., Chen, Y. D., Liu, C. L. and Lin, H. (2008). "Spatial and temporal variability of precipitation maxima during 1960–2005 in the Yangtze River basin and possible association with large-scale circulation", J. Hydrol., 353, 215-227.

Zhang, X., Alexander, L., Hegerl, G. C., Jones, P., Klein Tank, A., Peterson, T. C., Trewin, B. and Zwiers, F. (2011). "Indices for monitoring changes in extremes based on daily temperature and precipitation data , WIREs". Climatic Change, 2, 851-870.

Zhu, Y. and Newell, R. E. (1994). "Atmospheric rivers and bombs". Geophys. Res. Lett., 21, 1999-2002.

Zhu, Y. and Newell, R. E, (1998). "A proposed algorithm for moisture fluxes from atmospheric rivers", Mon. Wea. Rev., 126, 725–735.

Zorita, E., Kharin, V. and von Storch, H. (1992). "The Atmospheric Circulation and Sea Surface Temperature in the North Atlantic Area in Winter: Their Interaction and Relevance for Iberian Precipitation". J. Clim., 5, 1097-1108.

Lenticular clouds along the valley are thrown towards Madrid due to a northwest wind that turns pure west at higher levels

APPENDIX I. Publications

Publications:

Bosch J., Carrascal, L.M., **Durán, L.**, Walker, S. and Fisher, M.C. (2007). "Climate change and outbreaks of amphibian chytridiomycosis in a montane area of Central Spain; is there a link?". Proc. Biol. Sci., 274, 253–260.

Durán, L., Sánchez, E. and Yagüe, C. (2013). "Climatology of precipitation over the Iberian Central System mountain range". Int. J. Climatol., 33, 2260-2273.

Durán, L., Rodríguez-Fonseca, B., Yagüe, C. and Sánchez, E. (2015). "Water vapour flux patterns and precipitation at Sierra de Guadarrama mountain range (Spain)". Int. J. Climatol., 35, 1593-1610.

Durán, L. and Barstad, I. (2015). "Multi-scale validation of a Linear Model of Orographic Precipitation over Sierra de Guadarrama". To be submitted.

Durán, L. and Rodríguez-Muñoz, I. (2015). "Automatic Monitoring of Weather and Climate at Mountain Areas. The Case of Peñalara Meteorological Network 1999-2014 ". Sumitted.

PROCEEDINGS OF THE ROYAL SOCIETY B

Proc. R. Soc. B (2007) **274**, 253–260
doi:10.1098/rspb.2006.3713
Published online 25 October 2006

Climate change and outbreaks of amphibian chytridiomycosis in a montane area of Central Spain; is there a link?

Jaime Bosch[1,*], Luís M. Carrascal[1], Luis Durán[2], Susan Walker[3] and Matthew C. Fisher[3]

[1]*Departamento de Biodiversidad y Biología Evolutiva, Museo Nacional de Ciencias Naturales, CSIC, José Gutiérrez Abascal, 2 28006 Madrid, Spain*
[2]*Departamento de Fisica y Matemática, Universidad Europea de Madrid, 28670 Villaviciosa de Odón, Madrid, Spain*
[3]*Department of Infectious Disease Epidemiology, Imperial College Faculty of Medicine, St Mary's Campus, Norfolk Place, London W2 1PG, UK*

Amphibian species are declining at an alarming rate on a global scale in large part owing to an infectious disease caused by the chytridiomycete fungus, *Batrachochytrium dendrobatidis*. This disease of amphibians has recently emerged within Europe, but knowledge of its effects on amphibian assemblages remains poor. Importantly, little is known about the environmental envelope that is associated with chytridiomycosis in Europe and the potential for climate change to drive future disease dynamics. Here, we use long-term observations on amphibian population dynamics in the Peñalara Natural Park, Spain, to investigate the link between climate change and chytridiomycosis. Our analysis shows a significant association between change in local climatic variables and the occurrence of chytridiomycosis within this region. Specifically, we show that rising temperature is linked to the occurrence of chytrid-related disease, consistent with the chytrid-thermal-optimum hypothesis. We show that these local variables are driven by general circulation patterns, principally the North Atlantic Oscillation. Given that *B. dendrobatidis* is known to be broadly distributed across Europe, there is now an urgent need to assess the generality of our finding and determine whether climate-driven epidemics may be expected to impact on amphibian species across the wider region.

Keywords: climate-change; chytridiomycosis; *Batrachochytrium dendrobatidis*; amphibian declines; epidemiology

1. INTRODUCTION

Recent and predicted future patterns of global climate change are a major concern for many conservational ecologists. In many regions, climate change has resulted in warming over the past 30 years (Thomas *et al.* 2004). However, this effect is not uniform and the complexity of global climatic patterns means that temperatures in some areas to date have not changed measurably or have even cooled. Amphibians have been shown to be undergoing precipitous declines and species extinction on a global basis, and the recent Global Amphibian Assessment has shown that out of 5743 species, 1856 (32.5%) are globally threatened (Stuart *et al.* 2004). While a large percentage of these declines are attributable to direct anthropogenic effects, such as habitat loss, a substantial amount (48%) are classed as 'enigmatic' declines with no identifiable cause (Stuart *et al.* 2004). The role of climate change in driving these declines has yet to be systematically addressed (Pounds 2001); however, several lines of evidence now suggest that climatic fluctuations may have a critical, and rapid, effect on amphibian populations by altering local densities (Carey & Alexander 2003) and species distributions (Araújo *et al.* 2006).

Recently, attention has been focused on the synergistic relationship between climate and infectious disease and their contribution to amphibian declines, known as the 'climate-linked epidemic hypothesis' (Harvell *et al.* 2002; Pounds *et al.* 2006). It has long been known that climate may play an indirect role in facilitating epidemics of amphibian infection disease (Kiesecker *et al.* 2001), and climatic fluctuations have been shown to encourage outbreaks of certain pathogens (Pounds & Crump 1994), such as the opportunistic fungus *Saprolegnia ferax* (Blaustein *et al.* 2003).

Chytridiomycosis is an emerging infectious disease of amphibians that is causing mass mortality and population declines worldwide (Berger *et al.* 1998; Daszak 2003). The causative agent, a non-hyphal zoosporic fungus, *Batrachochytrium dendrobatidis*, is a recently described species of the chytridiales (Longcore *et al.* 1999) which is known to infect over 93 species worldwide (www.jcu.edu.au/school/phtm/PHTM/frogs/chyglob.htm).

There are two major, non-mutually exclusive, hypotheses that attempt to explain the increasing impact of chytridiomycosis on global amphibian populations. The first hypothesis states that *B. dendrobatidis* is an introduced

* Author for correspondence (bosch@mncn.csic.es).

Electronic supplementary material is available at http://dx.doi.org/10.1098/rspb.2006.3713 or via http://www.journals.royalsoc.ac.uk.

Received 20 July 2006
Accepted 21 August 2006

INTERNATIONAL JOURNAL OF CLIMATOLOGY
Int. J. Climatol. (2012)
Published online in Wiley Online Library
(wileyonlinelibrary.com) DOI: 10.1002/joc.3602

RMetS
Royal Meteorological Society

Climatology of precipitation over the Iberian Central System mountain range

L. Durán,[a,b,c]* E. Sánchez[d] and C. Yagüe[e]

[a] *Dpto. Ciencias, Universidad Europea de Madrid, Madrid, Spain*
[b] *InterMet Sistemas y Redes S.L.U., Madrid, Spain*
[c] *Dpto. Astrofísica y Ciencias de la Atmósfera, Universidad Complutense de Madrid, Madrid, Spain*
[d] *Facultad de Ciencias Medioambientales, Universidad de Castilla la Mancha, Toledo, Spain*
[e] *Dpto. Geofísica y Meteorología, Universidad Complutense de Madrid, Madrid, Spain*

ABSTRACT: An analysis of the observed precipitation for the last 22 years (1989–2010) over *Sierra de Guadarrama* (centre of Iberian Central System) has been performed. Since this area has received less attention compared with other mountain ranges in Europe and the rest of the world, an exhaustive compilation of literature on precipitation main characteristics on Central Iberia (SW Europe) has been done. The analysis, based on both rain gauges and reanalysis, is focused on the search of the atmospheric mechanisms and moisture sources that lead to precipitation. Also, emphasis has been made in the role played by orography conditioning, the complex spatial patterns observed in the region. This work shows how it behaves as an orographic island that rises over an extensive plateau with a marked Atlantic forcing despite the distance these masses have to travel inlands, with mostly of wet days due to advection of moisture from the ocean and small amount of rain due to local sources of humidity and convective precipitation. It also shows the great enhancement of precipitation caused by the range due to orographic precipitation and the big differences found at the downwind and upwind side of the mountain leading to marked spatial patterns seasonal dependent, complex vertical gradients and high wind direction dependency. Finally, statistically significant mean conditions of variables related with orographic precipitation are given in order to be used as boundary conditions for orographic precipitation modelling exercises. This works gives a climatic framework for future precipitation assessments that could be conducted combining measurements and such models.

KEY WORDS moisture advection; orographic precipitation; alpine climate; Iberian Central System; Sierra de Guadarrama

Received 3 January 2012; Revised 22 June 2012; Accepted 9 August 2012

1. Introduction

The description of precipitation is a complex and challenging issue for meteorological scientists, due to its irregular nature in space and time, and the diversity of atmospheric scales and processes involved on its description. When the influence of the orography is included on the analysis of precipitation, the problem becomes even more complex. At the same time, precipitation over complex terrain is clearly one of the relevant research areas pointed by the main projects focused on water cycle studies, such as GEWEX (Global Energy and Water cycle Experiment) (Lawford *et al*., 2004). Complexity is both related to the observational description and the modelling issues. Thus, Lawford *et al*. (2007), for example, explicitly points to the 'lack of understanding the orographic processes and the best way to incorporate it into models' when dealing with hydrometeorological sciences. While many aspects of the basic mechanisms responsible for orographic precipitation have been understood, important issues remain unresolved (Roe, 2005). Mountainous environments have been described on the Agenda 21 document from United Nations Conference on Environment and Development as a major component of the global environment, being unique areas of the detection of climatic change and the assessment of climate-related impacts (Beniston, 2003).

Several precipitation databases (such as University of Delaware (Matsuura and Willmott, 2009) or CPC (Merged Analysis of Precipitation) (Chen *et al*., 2008) worldwide, among others), based on surface point observations, are available. For multiple purposes, precipitation has been interpolated into gridded observational databases, in order to be used for climate models validation, hydrology impact assessment, ecology studies and others. Climate Research Unit Database (CRU) (New *et al*., 1999) is one of the most widely used. They analysed with care what happens on mountainous areas and being cautious and more uncertain on mountainous areas, as they suffer from the complex terrain effect on spatial

* Correspondence to: L. Durán, Dpto. Astrofísica y Ciencias de la Atmósfera, Facultad de Ciencias Físicas, Universidad Complutense de Madrid, Avd. Complutense s/n, Madrid 28040, Spain.
E-mail: luis@intermet.es; luisduran@fis.ucm.es

INTERNATIONAL JOURNAL OF CLIMATOLOGY
Int. J. Climatol. **35**: 1593–1610 (2015)
Published online 20 June 2014 in Wiley Online Library
(wileyonlinelibrary.com) DOI: 10.1002/joc.4079

RMetS
Royal Meteorological Society

Water vapour flux patterns and precipitation at Sierra de Guadarrama mountain range (Spain)

L. Durán,[a,b]* B. Rodríguez-Fonseca,[c] C. Yagüe[c] and E. Sánchez[d]
[a] *Centro de Investigación, Seguimiento y Evaluación Sierra de Guadarrama, Madrid, Spain*
[b] *interMET Sistemas y Redes S.L.U., Madrid, Spain*
[c] *Dpto. Geofísica y Meteorología, Universidad Complutense de Madrid, Spain*
[d] *Facultad de Ciencias Medioambientales, Universidad de Castilla la Mancha, Toledo, Spain*

ABSTRACT: It is well known how mountains play a crucial role in the climate system and have very particular climate features compared to other regions. Sierra de Guadarrama is a part of the Iberian Peninsula Central System (Spain), a mountain range located in the center of an extensive plateau, dominated by a continental Mediterranean climate but under a strong Atlantic influence. This range provides fresh water to the different settlements in its vicinity, providing enough water resources to several millions of inhabitants, crop fields, industries and the city of Madrid, the capital of Spain. Nevertheless, there is no work studying the role of the synoptic scale in relation to the precipitation in this mountain range. To tackle this problem, this work calculates water vapour flux patterns (WVFPs) using total column water vapour flux as a predictor field due to the close relation between this parameter and the precipitation in mountainous areas. A clustering analysis on the first three principal components of the predictor field was performed and seven differentiated WVFPs were found using a cost function considering local precipitation data for optimum number of cluster determination. Then, an analysis is made for each component in terms of synoptic relation with other fields and well-known broader teleconnection patterns. Finally, an analysis in terms of their contribution to total precipitation, mean rain intensity and probability of precipitation is made. This work is expected to bring new light on the knowledge of precipitation climatology over this crucial and still not very well-known area, and it is a solid step for future precipitation modelling tools validation that combined with reliable measurements will allow to produce realistic precipitation assessments and forecasts in order to improve the hydrological management of this complex area.

KEY WORDS total column water vapour flux; orographic precipitation; Alpine climate; Iberian Central System; Sierra de Guadarrama

Received 22 November 2013; Revised 8 May 2014; Accepted 16 May 2014

1. Introduction

The Iberian Peninsula (IP hereafter) is a mid-latitude region limited by the Atlantic Ocean on the west and the Mediterranean Sea on the east. Its central part is dominated by a Mediterranean continental climate (Font, 1983) with a very marked summer drought (Durán *et al.*, 2013). The Iberian Central System mountain range is located in the middle of an extensive and high plateau with average heights of 650 m above sea level over the central part of the IP. It runs from southwest to northeast and has considerable elevations (*Pico Moro Almanzor*: 2592 m and *Pico Peñalara*: 2428 m). Although it is located at a relatively long distance from the Atlantic Ocean, most of the precipitation observed in that region is related to the advection of humid air masses from the Atlantic Ocean that are forced to go through the region (Muñoz-Díaz and Rodrigo, 2004; Durán *et al.*, 2013). This mountain range has been crucial for the survival of the different civilizations that have settled down on its southern side since centuries, and now is providing fresh water to millions of inhabitants and industries in the region. In particular, Madrid, the capital of Spain is located in that area. The mountain range Sierra de Guadarrama (SdG hereafter) is a medullar part of the Iberian Central System, located in the middle of the range (Figure 1) and has become part of the National Parks Network since 2013.

Several authors (Zorita *et al.*, 1992; Trigo *et al.*, 2001; Rodríguez-Fonseca and Serrano, 2002; Trigo *et al.*, 2004; Rodríguez-Fonseca *et al.*, 2006; Durán *et al.*, 2013) have shown the strong influence of the Atlantic Ocean on precipitation over this region. Humid air masses from the Atlantic are advected into the Peninsula and transported by storms, fronts and the general synoptic western circulation. These air masses are forced to ascend by the orography, leaving precipitation on their way. Many times orography plays a crucial role in the enhancement of precipitation (Smith and Barstad, 2004; Roe, 2005; Kunz and Kottmeier, 2006; Gottardi *et al.*, 2012; Stoelinga *et al.*, 2013). In winter, spring and fall, most of the precipitation in this area comes in the form of solid precipitation, due to the low temperatures reached at the higher elevations.

* Correspondence to: L. Durán, Centro de Investigación, Seguimiento y Evaluación Sierra de Guadarrama, Rascafría, Madrid, Spain. E-mail: luis@intermet.es

AUTOMATIC MONITORING OF WEATHER AND CLIMATE AT MOUNTAIN AREAS. THE CASE OF PEÑALARA METEOROLOGICAL NETWORK

L. DURÁN [a,b]* and I. RODRÍGUEZ-MUÑOZ [a]

[a] interMET Sistemas y Redes S.L.U., Madrid, Spain

[b] Centro de Investigación, Seguimiento y Evaluación Sierra de Guadarrama, Madrid, Spain

ABSTRACT

Mountains have a very peculiar climate, are an essential factor in the climate system and are excellent locations for monitoring weather and climate. Nevertheless there is still a lack of long term observations at these areas, mainly due to the harsh conditions for instruments and humans. This work describes the results obtained in the operation during the last decade of a mountain meteorological network installed and operated at Sierra de Guadarrama (Iberian Central System, Spain). This work includes very valuable information for the numerous scientists that are using its data, specially in the comprehension of the representativeness of the data. Also some technical and operational thoughts are shared, that will help other existing or future mountain meteorological networks operators in the design of a proper measuring strategy, ad-hoc station sitting criteria and a optimum selection of measuring techniques in terms of reliability. General statistics of the main variables are shown along with a set of conclusions about future improvements.

Multi-Scale Evaluation of a Linear Model of Orographic Precipitation Over Sierra de Guadarrama (Iberian Central System)

LUIS DURÁN[a,b*] & IDAR BARSTAD[c]

[a] *interMET Sistemas y Redes S.L.U. Madrid Spain*

[b] *Centro de Investigación, Seguimiento y Evaluación. Parque Nacional de la Sierra de Guadarrama. Rascafría. Madrid. Spain*

[c] *Uni Research, Bergen, Norway;*

ABSTRACT

A linear model of orographic precipitation has been validated trough the comparison of a set of simulations against observed precipitation at Sierra de Guadarrama (Iberian Central System). This mountain range is immersed in a Mediterranean Continentalized climate in a semi-arid region of Southern Europe. Long time series observations of three good quality observatories located at south, north and top of the mountain range has been selected for this evaluation. A multi scale approach is made according to daily, monthly and annual precipitation totals. For this case, some new phenomena are included to the original version of the model like a subsaturated condition and a topographic mesoscale flow blocking. Results show a good agreement with observations at all scales. Monthly scale shows the best behavior. The model is able to simulate accurately the summer drought. Some disagreement is found for winter months and also in May and October. While the winter over estimation has been might be attributable to under catching in the measuring process, the May and October under estimation has been related with convective origin precipitation. Some improvements have been pointed out to be necessary for having better results during long droughts. Now the first daily high resolution assessment of precipitation at this complex mountainous area is now available with reasonable accuracy covering from 1990 to 2013 with a 200 m horizontal resolution